Russian Chemical Reviews **81** (10) 875 – 917 (2012) © 2012 Russian Academy of Sciences and Turpion Ltd

DOI 10.1070/RC2012v081n10ABEH004313

Nonequilibrium thermodynamics of colloidal systems

V I Roldughin

Contents

I.	Introduction	875
II.	Main relations of classical nonequilibrium thermodynamics and their generalizations	877
III.	Nonequilibrium thermodynamics of boundary conditions	882
IV.	Nonequilibrium thermodynamics of new phase formation	889
V.	Nonequilibrium thermodynamics of the motion of colloidal particles	892
VI.	The motion of colloidal particles in nonuniform temperature field and the cross effects	899
VII.	Membrane processes	907

Abstract. The review concerns various aspects of application of the classical nonequilibrium thermodynamics to the description of transfer processes in colloidal systems. Specific features of the use of nonequilibrium thermodynamics in setting the boundary conditions, deriving the equations of motion of colloidal particles, and analyzing phase transformations and membrane processes are demonstrated. Considerable attention is paid to well-known phenomena in physical chemistry of colloidal systems that have been the subject of recent interest and study. The bibliography includes 367 references.

I. Introduction

Nonequilibrium thermodynamics, whose foundations were laid in the classical studies by Onsager more than eight decades ago,[1,2] was readily accepted by all researchers who study irreversible processes. Wide use of methods of nonequilibrium thermodynamics is due to versatility of its basic principles and to a relatively simple scheme of deriving phenomenological equations relating thermodynamic fluxes to forces and used for heuristic prediction of new effects. The Onsager symmetry relations for the kinetic coefficients present in the phenomenological equations allow one to simultaneously establish interrelations between various effects. It is important that substantiation of the symmetry of the matrix of kinetic coefficients does not require new arguments; it is sufficient to refer to the fundamental Onsager studies where this symmetry was established for some generalized system. When considering particular systems, researchers should only perform corresponding entropy production calculations serving as a basis for the derivation of phenomenological equations.

Admittedly, correct entropy production calculations were sometimes non-trivial, although at first glance they only required a correct use of universal conservation laws, namely, the mass, momentum and energy conservation laws. An illustration is provided by a classical monograph [3] where a variety of systems were analyzed from unified positions and which demonstrates repetitive character of the entropy production calculations; however, in each case, the authors use non-trivial arguments in choosing the computational scheme.

The thermodynamic forces used in the seminal works by Onsager [1,2] included scalar quantities, namely, deviations from the equilibrium values of temperature, pressure, concentration, *etc*. The thermodynamic fluxes included the derivatives of these parameters with respect to time (also scalar quantities). Casimir [4] substantiated the possibility of using vector quantities (the temperature and concentration gradients, the heat and matter flux densities, *etc*.) as thermodynamic fluxes and forces. This significantly extended the range of nonequilibrium processes that can be described by methods of nonequilibrium thermodynamics.

Also, there is a study by Prigogine,[5] who attempted to establish the applicability limits of nonequilibrium thermodynamics based on the kinetic theory of gases (see a monograph [6]). It was shown [5] that nonequilibrium thermodynamics can be used only if the flow of a gas can be described using a conventional hydrodynamic approximation. This communication was taken very seriously, as indicated by, *e.g*., the fact that a Section in the monograph [3] was devoted to analysis of its results. However, unlike Casimir, Prigogine narrowed the applicability limits of nonequilibrium thermodynamics. Based on his study, the authors of monographs [7,8] reported that nonequilibrium thermodynamics cannot be used to describe the flows of rarefied gases because the hydrodynamic approximation is

V I Roldughin A N Frumkin Institute of Physical Chemistry and Electrochemistry, Russian Academy of Sciences, Leninsky prosp. 31, 119991 Moscow, Russian Federation. Fax (7-495) 952 53 08, tel. (7-495) 955 46 47, e-mail: roldugin@phyche.ac.ru

Received 13 March 2012
Uspekhi Khimii **81** (10) 875 – 917 (2012); translated by A M Raevskiy

obviously insufficient in this case. In fact, this excluded a broad range of nonequilibrium processes that could seemingly be described within the framework of nonequilibrium thermodynamics. The case in point is nonequilibrium processes in gases interacting with the condensed phase; main effects in such systems occur in the kinetic boundary layers where the hydrodynamic approximation is inapplicable at all.

In the field of colloid chemistry, aerosols whose properties are also mainly determined by the kinetic boundary layers seemed to be unsuitable for the description by methods of nonequilibrium thermodynamics. Based on the results reported by Prigogine [5] (see a substantiating comment in Ref. 9 and conclusions drawn in Ref. 10), it was accepted that investigations of transfer processes in such systems using methods of nonequilibrium thermodynamics are impossible. It should be noted that, initially, attempts to apply methods of nonequilibrium thermodynamics to nonequilibrium aerosols led to results that violated the Onsager symmetry relations (see Refs 11–15; here we deliberately do not mention a variety of erroneous studies in order not to increase their citation indexes). Seemingly, the conclusions made by Prigogine [5] were thus substantiated. In essence, the study [5] precluded the possibility to apply methods of nonequilibrium thermodynamics to all nonequilibrium colloidal systems because most effects in them are associated with processes occurring within nonequilibrium boundary layers and conventional hydrodynamic approach to the description of these processes is not always obvious.

In fact, the conclusions based on the study [5] appeared to be greatly exaggerated; however, their confutation required considerable efforts, all the more so, there were compelling (not based on any models) reasons [16] of 'loss' of the Onsager symmetry on going to higher-order hydrodynamic equations (so-called Burnett equations which include the second derivatives of temperature, velocity, *etc*.). Studies [5, 16] have a common drawback, *viz*., their authors tried to find symmetry relations in conventional hydrodynamic equations augmented with additional terms associated with going beyond the scope of the hydrodynamic approximation. But they had to derive some additional equations to augment the hydrodynamic ones, because otherwise it is impossible to even formally introduce the cross kinetic coefficients for which the Onsager symmetry relations should be established. In other words, formally correct reasoning did not include a crucially important moment, namely, additional thermodynamic forces (the second and higher derivatives of thermodynamic parameters with respect to spatial coordinates) were introduced without new thermodynamic fluxes. Therefore, the problem was again reduced to correct entropy production calculations.

Erroneous character of the conclusions drawn based on the data of Ref. 5 was rigorously substantiated in Refs 17–19. In particular, it was shown [17] that nonequilibrium gas flows near solid surfaces should be considered taking into account the entropy production due to molecular collisions with surfaces. Such a kind of entropy production is impossible in the hydrodynamic approximation because this is a purely kinetic effect. As this kind of entropy production was included, the results obtained based on the molecular-kinetic approach appeared to be consistent with those obtained using nonequilibrium thermodynamics for a particular class of gas flows.

The problem in question was finalized in Refs 18 and 19 where it was shown that, if the entropy production calculations are carried out correctly, nonequilibrium thermodynamics can be used to describe arbitrary flows of rarefied gases and other fluids including studies of transfer processes only within the boundary layers where the hydrodynamic approximation cannot be used even as the starting point. The symmetry of the kinetic coefficients for generalized higher-order hydrodynamic equations upon introduction of additional (so-called non-physical) thermodynamic fluxes arising in the entropy production calculations was demonstrated for a general case.[18] In some cases, these additional thermodynamic fluxes can be interpreted physically, *e.g*., they include such components as the pressure flux density (vector flux), the heat flux density flux density (tensor flux), *etc*., while the conjugate thermodynamic forces are, *e.g*., $\Delta\mathbf{u}$ (vector quantity), $\nabla\nabla T$ (tensor quantity), *etc*., where $\mathbf{u}$ is the fluid velocity, T is the temperature, Δ is the Laplace operator, and ∇ is the gradient operator.

The results obtained in Ref. 18 were more recently reproduced for a particular case.[20] Also, the applicability of nonequilibrium thermodynamics to the description of arbitrary gas flows in terms of nonequilibrium distribution functions was demonstrated.[19] It was proposed to use the nonequilibrium part of the molecular velocity distribution function as the nonequilibrium 'thermodynamic' variable. In this case, 'phenomenological equations of nonequilibrium thermodynamics' are reduced to the kinetic equation for the distribution function and the Onsager symmetry relations in fact represent known symmetry relations for the Boltzmann collision integral (see monographs [6, 7]). It was thus shown that a correct methodological approach makes nonequilibrium thermodynamics applicable to studies of nonequilibrium processes irrespective of the approximation used to describe the nonequilibrium system. Indeed, further progress in nonequilibrium thermodynamics was made using the distribution functions as 'thermodynamic variables'. Detailed analysis of interrelations between nonequilibrium thermodynamics and kinetic theory can be found in the literature.[21–24] Note that kinetic models are also often used to determine the generalized thermodynamic parameters of nonequilibrium systems.[25]

Symmetry violation on going to higher-order hydrodynamics (see above) is similar in nature to the 'loss' of the Onsager symmetry on exclusion of the so-called fast variables from consideration.[26, 27] The presence of significantly different relaxation times is characteristic of colloidal, polymeric and glassy systems. In addition to the 'loss' of the Onsager symmetry such systems are characterized by violation of the fluctuation-dissipation theorem.[28, 29] It was shown [30] that violation of the Onsager symmetry is due to incorrect form of phenomenological equations provided that fast variables are excluded. If the entropy production and phenomenological equations including no fast variables are represented correctly, the Onsager symmetry relations are preserved. As in the case of passage to higher-order hydrodynamics, here one deals with additional thermodynamic fluxes introduced to ensure conservation of the Onsager symmetry. The aforesaid indicates the need for correct approach to the description of colloidal systems by methods of nonequilibrium thermodynamics.

Following de Groot and Mazur,[3] studies [17–20] in fact completed the statistical substantiation of classical non-

equilibrium thermodynamics and significantly extended the scope of its application. At nearly the same time, the development of so-called extended irreversible thermodynamics began.[31] The main idea in this field is to increase the number of variables describing the nonequilibrium state. Initially, the 'additional' variables included two physical quantities, *viz*., the heat and momentum fluxes and then their derivatives with respect to time were included (see, *e.g*., Refs 32–34). The addition of the fluxes of physical quantities to the set of variables determining the nonequilibrium state can be substantiated within the framework of the kinetic theory,[35] but the appearance of the derivatives with respect to time is still due to phenomenological considerations while the corresponding molecular-kinetic theory is still in the stage of development. Nevertheless, there is rapid progress in extended irreversible thermodynamics and its methods are successfully used in various fields.[36]

Recently, there have been systematic attempts to extend the applicability of nonequilibrium thermodynamics. It was shown[37] that the symmetry relations for the kinetic coefficients are also valid if the system relaxes under external restrictions, which implies a wider field of application of the Onsager theory. Attempts have been made[38,39] to extend the scope of nonequilibrium thermodynamics by including nonequilibrium characteristics to the set of variables appeared in the Gibbs equation and by using generalized transport equations for nonuniform fluids. The fundamentals are being developed[40] of passage from microscopic to macroscopic description (also using methods of nonequilibrium thermodynamics), which disclose the nature of the onset of irreversibility in this case. It was proposed[41] to generalize the Clausius inequality, which serves as a basis for nonequilibrium thermodynamics, by including the work of friction forces.

Methods of nonequilibrium thermodynamics are suitable for the description of fluctuations considered as internal variables.[42–44] There results serve as a basis for the so-called mesoscopic nonequilibrium thermodynamics. Note that the inclusion of internal variables in nonequilibrium thermodynamics is of fundamental importance in studies of colloidal systems, where the role of internal variables is played by characteristics of colloidal particles. Attempts to establish new variational principles[45] generalizing the known Prigogine theorem (see Ref. 3) of minimum entropy production in the steady state have been undertaken. Of particular interest is the maximum entropy production principle;[46–50] it is not related to the Prigogine theorem describing the steady state, and allows one to predict an optimum trajectory for the system moving towards this state.

Yet another investigation line in nonequilibrium thermodynamics is associated with the so-called second entropy.[51] Unlike conventional (first) entropy whose deviation from the equilibrium value is determined by the values of thermodynamic parameters at a given instant, the second entropy is a bilinear combination of nonequilibrium thermodynamic parameters whose values are measured at different instants. It is assumed that such a choice of the second entropy makes it possible to obtain more detailed information on the dynamics of the nonequilibrium system. The introduction of the second entropy allows one to establish relations generalizing the relations derived earlier within the framework of conventional statistical mechanics; in particular, this also concerns the Onsager symmetry relations. Detailed consideration of this approach goes beyond the scope of this review. Generalized nonequilibrium thermodynamics will also be left out of consideration because, with rare exception, colloidal systems can be described within the framework of classical nonequilibrium thermodynamics and even the problems whose solution requires the use of extended irreversible thermodynamics can be reduced to the classical problems. Note that at present, there has been a new tide of interest in nonequilibrium thermodynamics of colloidal systems, namely, a large number of studies on the title topic were reported in the last decade. This is due to strong effects manifested in nonequilibrium colloidal systems. Some effects still require unambiguous explanation; therefore, there is a need for the development of theoretical models, which will be presented in this review.

A single review seems to be too short to cover all aspects of nonequilibrium thermodynamics of colloidal systems. In particular, problems related to nonlinear effects, *e.g*., oscillatory phenomena on the surface of fluids in the presence of nonuniform adsorption layers composed of surfactants or nanoparticles will be left out of consideration. This is a subject of a featured review. Here we will restrict ourselves to the classical linear nonequilibrium thermodynamics of colloidal systems. We will also not consider problems concerning chemical reactions involving particles because they to a greater extent belong to problems in catalysis. Note that comprehensive reviews on the nonequilibrium thermodynamics of catalytic systems are available.[52–54]

II. Main relations of classical nonequilibrium thermodynamics and their generalizations

1. Main relations of nonequilibrium thermodynamics

Methodologically, nonequilibrium thermodynamics is as follows. Any physical quantity characterizing a subsystem varies with time owing to uncontrolled interaction with other parts of a system, *i.e*., one deals with random oscillations about a mean value. This is referred to as fluctuations of corresponding physical quantities. Determination of a fluctuation and establishment of the regularities of its temporal behaviour requires a microscopic description of the behaviour of the nonequilibrium system. This problem is still to be solved; therefore, the regularities of fluctuations of thermodynamic quantities and their temporal evolution are established using the Gibbs approach. To this end, a relation is used between the entropy of the system (S) as function of physicochemical characteristics

$$\mathbf{W} = (W_1, W_2, ..., W_n)$$

of the subsystem and the probability for the subsystem to be in a specified state

$$P_r(\mathbf{W}) \propto \exp\left[\frac{S(\mathbf{W})}{k}\right], \quad (1)$$

where k is the Boltzmann constant. This expression, in particular, shows that the most probable state of the system is characterized by the highest entropy S_0. This state is usually associated with the state of thermodynamic equilibrium in which the physical characteristics takes the values $\mathbf{W}_0$ that ensure the maximum value S_0 under preset initial

conditions. Relation (1) represents the second law of thermodynamics, according to which a nonequilibrium system evolves towards an increase in the entropy of a closed system.

Using expression (1), one can determine the probability for a physical quantity **W** to deviate to a predetermined extent from its equilibrium value. This is done as follows. Assume that the entropy of the system is a function of the deviations of the parameters **W** from their equilibrium values

$$a_i = W_i - W_{i0},$$

where W_{i0} is the value of the physical quantity W_i in thermodynamic equilibrium. Having expanded the entropy S in a series in terms of the deviations a_i and taking account of the maximum entropy value in the thermodynamic equilibrium, one gets

$$S = S_0 - \frac{1}{2}\sum_{i,j=1}^{n} g_{ij}\, a_i\, a_j, \tag{2}$$

where g_{ij} is the positively semidefinite matrix of the second derivatives; obviously, one has $g_{ij} = g_{ji}$.

Substituting the series (2) into expression (1) gives the expression for the probability of fluctuations of thermodynamic quantities:

$$P_{\mathrm{r}} = P_{\mathrm{r}0}\exp\left(-\frac{1}{2}\sum_{i,j=1}^{n} g_{ij}a_i a_j\right), \tag{3}$$

where $P_{\mathrm{r}0}$ is the normalizing constant that ensures the validity of the obvious equality

$$\int P_{\mathrm{r}}\mathrm{d}a_1\mathrm{d}a_2 \ldots \mathrm{d}a_n = 1.$$

The normalizing constant can be determined with ease and the final expression for the probability of fluctuations takes the form

$$P_{\mathrm{r}} = \frac{\sqrt{g}}{(2\pi)^{n/2}}\exp\left(-\frac{1}{2}\sum_{i,j=1}^{n} g_{ij}a_i a_j\right), \tag{4}$$

where g is the determinant of the g_{ij} matrix.

Usually, it is accepted that relaxation of fluctuations obeys the same laws as relaxation of macroscopic quantities. Assuming that for small deviations of the system from its equilibrium state, the changes in the macroscopic quantities with time (t) are described by linear equations

$$\frac{\mathrm{d}a_i}{\mathrm{d}t} = \sum_j \widehat{M}_{ij}a_j \tag{5}$$

($\widehat{M}_{ij}$ are coefficients of proportionality), Onsager[1,2] proposed to write these equations in another manner. He introduced new variables

$$\widehat{X}_i = -\frac{\partial S}{\partial a_i} = \sum_j g_{ij}a_j \tag{6}$$

called thermodynamic forces and the derivatives $\mathrm{d}a_i/\mathrm{d}t$ representing thermodynamic fluxes. As a result, Eqn (5) is transformed to

$$\frac{\mathrm{d}a_i}{\mathrm{d}t} = \sum_j L_{ij}\widehat{X}_j. \tag{7}$$

Equations (7) are called the phenomenological equations of nonequilibrium thermodynamics. Onsager showed that the advantage of Eqn (7) over Eqn (5) consists in that the kinetic coefficients L_{ij} in the former case obey the symmetry relations

$$L_{ij} = L_{ji}. \tag{8}$$

The relaxation equations (7) and the symmetry relations (8) serve as complete basis for thermodynamics of irreversible processes.

Note that relations (8) are valid both in the case of slow monotonic relaxation of the system to the state of thermodynamic equilibrium and in the case where this relaxation is accompanied by small fluctuations of thermodynamic quantities.[55]

To describe nonequilibrium processes from unified positions, the phenomenological equations of nonequilibrium thermodynamics are defined in somewhat different manner, namely, the so-called entropy production

$$\Delta S = \frac{\mathrm{d}S}{\mathrm{d}t} = -\frac{\mathrm{d}}{\mathrm{d}t}\sum_{i,j}\frac{1}{2}g_{ij}a_i a_j = -\sum_i \frac{\mathrm{d}a_i}{\mathrm{d}t}\sum_j g_{ij}a_j = \tag{9}$$

$$-\sum_i \frac{\mathrm{d}a_i}{\mathrm{d}t}\widehat{X}_i = -\sum_i \widehat{J}_i\widehat{X}_i,$$

is considered instead of the nonequilibrium entropy (2), or it is said that the entropy production is represented as bilinear combination of thermodynamic forces $\widehat{X}_i$ and fluxes

$$\widehat{J}_i = \frac{\mathrm{d}a_i}{\mathrm{d}t}.$$

Generally, not only the derivative of a thermodynamic variable with respect to time and the deviation of the variable from the equilibrium value, but also other physical quantities, *i.e.*, the heat flux, matter flux, temperature gradient, concentration gradient, *etc.* can appear in Eqn (9) as thermodynamic fluxes and forces. One should only represent the entropy production as a bilinear combination of parameters characterizing the nonequilibrium state of the system. Then, a unified scheme for construction of phenomenological equations is used, namely, based on the entropy production (9) one writes the equations

$$\widehat{J}_i = \sum_j L_{ij}\,\widehat{X}_j, \tag{10}$$

in which the kinetic coefficients meet the symmetry relations (8).

It should be noted that (i) thermodynamic fluxes (and forces) can have different tensor dimensionalities, *i.e.*, they can be scalar, vector or tensor quantities. Then, in the isotropic case, in accordance with the Curie principle, the system (10) is divided into a number of subsystems including quantities of the same dimensionality.

Then, if the thermodynamic characteristics $\widehat{X}_i$ and $\widehat{X}_k$ behave in different manner on time reversal (*e.g.*, one of them remains unchanged while the other changes its sign),

the symmetry relation for the kinetic coefficients takes the form

$$L_{ik} = -L_{ki}\,. \tag{11}$$

Expression (11) is called the Onsager–Casimir symmetry relation.

Entropy production (9) in the steady state is minimum. This fact was substantiated by Prigogine [3] and it is referred to as corresponding theorem. As mentioned above, there are a number of fundamental principles in nonequilibrium thermodynamics. We will formulate only one of them, the maximum entropy production principle, which will be used in the text below. This principle is less known than the Prigogine theorem; however, recently it has attracted increasing attention of researchers.

The maximum entropy production principle was formulated by Ziegler [56] and is as follows. Assume that we describe a nonequilibrium state of a system in the space of fluxes $\widehat{J}_i$ provided that the expression for the entropy production in this space is known. We have to express the fluxes $\widehat{J}_i$ through thermodynamic forces $\widehat{X}_i$ assuming a local equilibrium in the system. In our case, the expression for the entropy production (9) should be written as

$$\Delta S(\widehat{J}_i) = -\sum_k \widehat{X}_k(\widehat{J}_i)\widehat{J}_k\,. \tag{12}$$

Ziegler assumed that the expression for the thermodynamic forces can be derived using the following theorem: at a specified kind of the thermodynamic force $\widehat{X}_k$, the thermodynamic flux $\widehat{J}_k$ established in the system provides the maximum entropy production (12). In some cases, the maximum entropy production principle is formulated as follows: if the amplitude of fluctuations in the system is large enough, the state characterized by the maximum local entropy production is realized.

Mathematically, the maximum entropy production principle is given by

$$\delta_{\widehat{J}_k}\left[\Delta S(\widehat{J}_i) - \lambda_{\mathrm{L}}\left(\Delta S(\widehat{J}_i) + \sum_k \widehat{X}_k(\widehat{J}_i)\widehat{J}_k\right)\right]_{\widehat{X}_j} = 0,$$

where δ_J denotes the variational derivative with respect to J, $[\,]_X$ indicates that the variational derivative is taken at constant value of the parameter X and λ_{L} is the Lagrange multiplier.

Examples of application of this principle are given below. Now we will consider some examples related to the entropy production in unrestricted systems. Assume a flow of a one-component incompressible fluid at the velocity $\mathbf{u}$ accompanied by heat transfer under the action of a temperature gradient ∇T. The corresponding expression for the entropy production has the form [3]

$$\Delta S = -\frac{\mathbf{q}\nabla T}{T^2} - \frac{1}{T}\sum_{\alpha,\beta}\Pi_{\alpha\beta}\frac{\partial u_\alpha}{\partial x_\beta},$$

where $\mathbf{q}$ is the heat flux density, Π is the viscous stress tensor and x_β are the spatial coordinates. Since the fluxes ($\mathbf{q}$ and Π) and force (∇T and $\partial u_\alpha/\partial x_\beta$) present in the first and second terms in the right side have different tensor dimensionalities, following the Curie principle, we have to write two types of phenomenological equations

$$\mathbf{q} = -\lambda_{\mathrm{f}}\nabla \ln T, \tag{13a}$$

$$\Pi_{\alpha\beta} = -\eta_{\mathrm{f}}\left(\frac{\partial u_\alpha}{\partial x_\beta} + \frac{\partial u_\beta}{\partial x_\alpha}\right), \tag{13b}$$

where λ_{f} and η_{f} are respectively the thermal conductivity and viscosity of the fluid. Equation (13a) is the Fourier thermal conductivity law while Eqn (13b) represents the Newton law for viscous flow of fluids (it is written in the symmetric form because the stress tensor is symmetrical with respect to its variables).

It should be noted that a flowing fluid is usually characterized by a pressure gradient (∇p) defined by the Stokes equation

$$\eta_{\mathrm{f}}\Delta\mathbf{u} = \nabla p, \tag{14}$$

where Δ is the Laplacian. In principle, one can assume that the heat flux can also appear as a response to the pressure gradient. At least, the Curie principle does not rule this out. Landau and Lifshitz [57] reported a proof of impossibility for such a heat flux to appear, based on thermodynamics of irreversible processes. They believe that in the presence of the heat flux induced by the pressure gradient, the entropy production determined by the term containing the temperature gradient can have different sign, whereas it should be positive according to the second law of thermodynamics. In the text below we will show, based on the results,[18,19] that the heat flux can also appear as a response to the pressure gradient and it does not contradict the second law of thermodynamics. The generalization [18,19] of the equations of nonequilibrium thermodynamics is based on the kinetic theory. At present, attempts to derive more general transport equations based on the nonlinear response theory [58] and phenomenological considerations [59–61] are undertaken.

Yet another channel of entropy production appears in the case of flow of mixtures. This is interdiffusion of mixture components. Since the entropy production should not depend on the choice of the coordinate system, the corresponding expression should include those components of fluxes where the motion of the entire system is excluded. Then one gets

$$\Delta S = -\frac{\left(\mathbf{q} - \sum_i h_i\mathbf{J}_i\right)\nabla T}{T^2} - \frac{\sum_i \mathbf{J}_i\nabla\mu_i}{T} - \frac{1}{T}\sum_{\alpha,\beta}\Pi_{\alpha\beta}\frac{\partial u_\alpha}{\partial x_\beta}, \tag{15}$$

where h_i and μ_i are the specific enthalpy and chemical potential of the ith component, respectively,

$$\mathbf{J}_i = n_i(\mathbf{u}_i - \mathbf{u})$$

is the diffusion flux density, n_i is the number of the molecules of the kind i in the unit volume, $\mathbf{u}_i$ is the average velocity of the molecules of the kind i, $\mathbf{u}$ is the mass-average velocity of the mixture; the combination of parameters in front of the temperature gradient is the heat flux density in the mixture; and the chemical potential gradient is determined at constant temperature. If the components are influenced by external forces, the latter can be included in the chemical potential gradient.

The tensor equation of nonequilibrium thermodynamics remains unchanged and for the vector fluxes and forces one gets the system

$$\mathbf{q} - \sum_i h_i \mathbf{J}_i = L_{qq} \nabla \ln T + \sum_i L_{qi} \nabla \mu_i , \tag{16}$$

$$\mathbf{J}_i = L_{iq} \nabla \ln T + \sum_k L_{ik} \mu_k ,$$

where the coefficient L_{qq} is associated with the thermal conductivity of the mixture, the coefficient L_{ik} is associated with the diffusion coefficients, the coefficients L_{iq} describe thermal diffusion or the Soret effect, and the cross coefficients are associated with the diffusion thermoeffect, or the Dufour effect.

2. Generalizations of transport equations

The transport equations (16) correspond to classical nonequilibrium thermodynamics.[3] Passage to extended, or generalized, nonequilibrium thermodynamics is accompanied by the appearance of additional fluxes and forces. Without dwelling on details, note that in this case the phenomenological equations of the vector fluxes for, *e.g.,* one-component gas have the form [21]

$$\mathbf{q} = -\Lambda_{11} \nabla \ln T - \Lambda_{12} \Delta \mathbf{u}, \tag{17}$$

$$\mathbf{J}^v = -\Lambda_{21} \nabla \ln T - \Lambda_{22} \Delta \mathbf{u},$$

where Λ_{ik} are the kinetic coefficients.

Since the quantity $\Delta \mathbf{u}$ coincides with the pressure gradient up to a constant, the heat flux may also appear as a response to the pressure gradient. This does not contradict the second law of thermodynamics because an additional flux $\mathbf{J}^v$ is considered. It is hard to assign a physical sense to this flux because it is a complex function of the molecular velocity. However, there is no question about its existence because the heat flux induced by the pressure gradient was measured experimentally.

The approximation corresponding to the system of equations (17) also requires transformation of the tensor equations to the form

$$\mathbf{\Pi} = -\lambda_{11} \overline{\nabla \mathbf{u}} - \lambda_{12} \frac{\overline{\nabla \nabla} T}{T}, \tag{18a}$$

$$\mathbf{J}^T = -\lambda_{21} \overline{\nabla \mathbf{u}} - \lambda_{22} \frac{\overline{\nabla \nabla} T}{T}, \tag{18b}$$

where the bar denotes a symmetrical combination of the vector components

$$\overline{\nabla \mathbf{u}} = \left(\frac{\partial u_\alpha}{\partial x_\beta} + \frac{\partial u_\beta}{\partial x_\alpha} \right). \tag{19}$$

Note that the second term in Eqn (18a) characterizes thermal stresses which were considered as early as by Maxwell. But their inclusion in nonequilibrium thermodynamics required the introduction of yet another non-physical flux $\mathbf{J}^T$ conjugate to the thermal stresses. This flux is a complex function of the flux of a combination of the molecular velocities. The introduction of this quantity ensures the positive sign of entropy production.

When considering the flow of a mixture, taking account of additional terms, *e.g.*, similar to those included in expressions (17) and (18) also leads to new effects, namely, the appearance of (i) diffusion under the action of pressure gradient (pressure diffusion) and (ii) concentration stresses similar to thermal stresses if the double gradient $\nabla\nabla$ acts on the component concentrations. Detailed analysis of these equations of nonequilibrium thermodynamics can be found in the literature.[21,22]

The modified transport Eqns (17) and (18) can be transformed to a more symmetrical form. This is the case for the so-called thirteen moments approximation of the Grad method in the kinetic theory of gases [7,21] and underlies the extended irreversible thermodynamics.[31,36] These equations are as follows:

$$\mathbf{q} = -\Lambda_{11} \left(\nabla \ln T + \frac{2}{5p} \nabla \mathbf{\Pi} \right), \tag{20}$$

$$\mathbf{\Pi} = -\lambda_{11} \left(\overline{\nabla u} + \frac{2}{5p} \overline{\nabla q} \right). \tag{21}$$

As can be seen, the expressions for the heat flux and stress tensor specified by Eqns (17), (18), (20) and (21) almost coincide if for the coefficients Λ_{12} and λ_{12} one uses some particular values appropriately normalized to Λ_{11} and λ_{11}. The normalizing constant $2/5p$ was determined for gases. Liquids should be characterized by some other value of this coefficient; moreover, these values for Eqns (20) and (21) can differ from each other. The coefficients Λ_{11} and λ_{11} can be associated with the thermal conductivity and viscosity of the fluid, respectively.

As will be shown below, the additional terms introduced above play an important role in nonequilibrium thermodynamics of colloidal systems. If they are ignored, no correct boundary conditions and description of transfer processes in membrane systems (at least for gases) is obtained.

Yet another generalization of transport equations is due to investigation of transport processes in confined systems where the transport of matter is strongly affected by steric hindrances (Fig. 1) and there is no specific interaction. The use of mesoscopic nonequilibrium thermodynamics [62] allows one to derive the transport equations with a new structure, *viz*., they include not only the diffusion, but also the entropy contribution. In particular, for the particle flux one gets the expression

$$J_\mathrm{p} = -D_\mathrm{p} \frac{\mathrm{d}P_\mathrm{p}}{\mathrm{d}z} + P_\mathrm{p} \frac{D_\mathrm{p}}{k} \frac{\mathrm{d}S_\mathrm{p}}{\mathrm{d}z}, \tag{22}$$

where D_p is the diffusion coefficient of particles, P_p is the probability for particles to be at the point z (analogue of concentration) and S_p is the entropy of particles. The

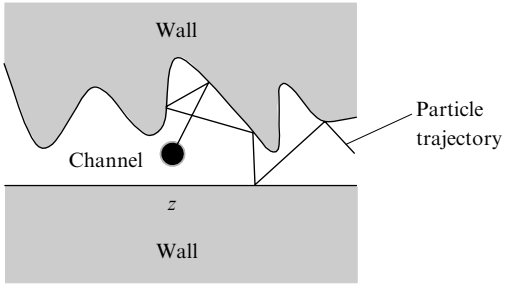


Figure 1. How the entropy factor influences the diffusion transport of particles.

entropy is a function of the coordinate z because for a freely moving particle the equilibrium probability (P_{pe}) varies from one point to another (see Fig. 1) and the equilibrium entropy is related to the equilibrium probability as follows:

$$P_{pe} = P_{p0} \exp\left(\frac{S_p}{k}\right),$$

where P_{p0} is the normalizing constant.

According to Eqn (22), particles are displaced from narrow gaps to wider regions; this should be taken into account when considering transport in membranes with narrow channels of variable cross-section, in particular, in zeolites. Note that in Eqn (22) the nature of the change in the entropy is insignificant, *viz*., these can be limitations in either the coordinate or phase space, which occurs in, *e.g*., diffusion of polymers in narrow pores.

Consider the Soret and the Dufour effects mentioned above. Thermal diffusion in gases was discovered in the mid-20th century. It should be noted that both effects have purely kinetic nature and depend rather strongly on the intermolecular interactions (*e.g*., both effects vanish for a particular type of interactions). Since it was these interactions that were used in the pioneering calculations by Maxwell, the coefficient of thermal diffusion in gases was found to be zero; this delayed the experimental detection of this effect by about five decades.[63] Then, thermal diffusion separation of gases became a main method of uranium enrichment.

Some authors state [64] that thermal diffusion separation and the cross heat effect are not observed in low-molecular-mass liquids; however, thermal diffusion in liquids does exist and is used in practice,[65] although the effect is weak. Probably, it is the kinetic nature of the effect that determines small values of the thermal diffusion coefficients in low-molecular-mass liquids. Note also that the published experimental data differ appreciably.[66, 67] As a consequence, the existing models for thermal diffusion are based on a large number of empirical arguments.[64, 68] Thermal diffusion in low-molecular-mass liquids can also be governed by co-operative fluctuations rather than features of intermolecular interactions, as was assumed in Ref. 69.

Recently, there has been a considerable interest in thermal diffusion phenomena and cross heat effects in colloidal dispersions and solutions of high-molecular-mass compounds. In particular, thermal diffusion is used for separation of macromolecules. In colloidal systems, these effects are due to a specific structure of boundary layers, thus becoming (to some extent) thermodynamic in nature. Note that there is no unified mechanism of transport processes for different systems. The nature of noticeable thermal diffusion in solutions of high-molecular-mass compounds is still a moot question [64, 70] and therefore we leave such systems out of consideration.

3. Transport equations for colloidal dispersions

Transport processes in colloidal systems are sometimes described by equations of type (16). Clearly, these equations work in the case of highly disperse aerosols where solid particles are treated as components of a gas mixture (so-called dusty-gas model [71–73]). However, studies of colloidal particles in liquids require modification of these equations because in this case one should use a large number of variables; *e.g*., a dispersion can be characterized by an order parameter related to the local orientation of anisotropic particles. Particles can be involved in Brownian motion and in macroscopic motions relative to the dispersion medium; this leads to additional hydrodynamic interaction (in addition to the force interaction) between them. A detailed description of transport processes in disperse systems is available in a monograph.[74]

Consider specific features of transfer processes in colloidal systems from the standpoint of Lhuillier.[75] The main features of transport equations are as follows. First, the expression for the stress tensor now includes new terms with the so-called elastic component

$$\Pi_{\alpha\beta} = -\eta_f\left(\frac{\partial u_\alpha}{\partial x_\beta} + \frac{\partial u_\beta}{\partial x_\alpha}\right) - N_p kT + \int \frac{\partial[\widehat{U}_{pp} + kT\ln P_d(r)]}{\partial \mathbf{r}} \mathbf{r} P_d(r)\mathrm{d}r, \tag{23}$$

where N_p is the concentration of particles, $P_d(r)$ are the probability density for the particle to be at the distance r from the pre-specified particle and $\widehat{U}_{pp}(r)$ is the potential of inter-particle interaction. Clearly, the second term is the osmotic pressure in the colloidal systems. Expression (23) was derived for spherical particles. For rod-like colloidal particles, the last two terms are replaced by

$$N_p kT \int (3\mathrm{e}_\alpha \mathrm{e}_\beta - 2\delta_{\alpha\beta})\psi(\mathbf{e})\mathrm{d}\mathbf{e} + N_p \int \left[\mathrm{e}_\alpha \frac{\partial \widehat{U}_{pp}}{\partial \mathrm{e}_\beta} + \mathrm{e}_\beta \frac{\partial \widehat{U}_{pp}}{\partial e_\alpha} - \mathrm{e}_\alpha \mathrm{e}_\beta \left(\mathrm{e}_\gamma \frac{\partial \widehat{U}_{pp}}{\partial \mathrm{e}_\gamma}\right)\right]\psi(\mathbf{e})\mathrm{d}\mathbf{e}, \tag{24}$$

where $\psi(\mathbf{e})$ is the orientation distribution function of particles; $\mathbf{e}$ is the vector specifying the orientation of rod-like particles; and $\delta_{\alpha\beta}$ is the Kronecker symbol.

Expressions (23) and (24) take into account only pair interactions of particles. The effect of three-particle interactions on the transport equations was also studied.[76] However, it should be noted that the description of concentrated colloidal dispersions requires the inclusion of both three-particle interactions and higher-order interactions; therefore, the results obtained in Ref. 76 are of purely theoretical interest.

Assuming a relative motion of particles and the disperse medium, new contributions will appear in the expression for the energy flux.[75] Rotational relaxation of rod-like particles can also be considered. Corresponding equations have the form [77]

$$\Pi_{\alpha\beta} = -\eta_f\left(\frac{\partial u_\alpha}{\partial x_\beta} + \frac{\partial u_\beta}{\partial x_\alpha}\right) - l_{\Pi w} w_{\alpha\beta}, \tag{25}$$

$$\frac{\mathrm{d}Q_{\alpha\beta}}{\mathrm{d}t} = -l_{w\Pi}\left(\frac{\partial u_\alpha}{\partial x_\beta} + \frac{\partial u_\beta}{\partial x_\alpha}\right) - l_{ww} w_{\alpha\beta}.$$

Here $l_{\Pi w}$, $l_{w\Pi}$ and l_{ww} are the kinetic coefficients, $\mathbf{Q}$ is the ensemble-average of the tensor $\mathbf{ee} - (1/3)\mathbf{I}$, where $\mathbf{I}$ is the unit tensor; $\mathbf{w}$ is the conjugate thermodynamic variable which is also expressed through the tensor $\mathbf{Q}$ provided that the system slightly deviated from its equilibrium state,

$$\mathbf{w} = A_w(T, N_p)\mathbf{Q} + B_w(T, N_p)\overline{\overline{\mathbf{Q}\,\mathbf{Q}}} + \ldots, \tag{26}$$

where double bar denotes the symmetrical traceless tensor and the dot denotes a convolution of two components. The coefficient $A_w(T,N_p)$ is of the order of the osmotic pressure.

A crucially important fact is that using Eqns (25) and thus working within the framework of linear transport equations, one can reveal the dependence of the viscosity of dispersion on the shear rate $\dot{\gamma}$. Rather simple reasoning leads to the following expression for the intrinsic viscosity [77]

$$[\eta]_{ef} = [\eta]_0 + \dot{\gamma}^2 \frac{\eta\varphi}{36 A_w D_r} C(r_e), \tag{27}$$

where $[\eta]_0$ is the intrinsic viscosity independent of the shear rate, η is the viscosity of pure solvent, φ is the volume fraction of particles, D_r is the rotational diffusion coefficient, $C(r_e)$ is a function of the semi-axis ratio r_e of ellipsoidal particles [the $C(r_e)$ values are of the order of unity].

It should be noted that the linear approximation allows one to describe the nonlinear effect, namely, the dependence of viscosity on the shear rate: the shear motion influences the statistical distribution function characterizing the orientation of particles. The kinetic coefficients also depend on the orientation of particles, which leads to a nonlinear influence of shear flow on the viscosity. From Eqns (25) it also follows that a colloidal dispersion exhibits some elasticity.[77] Experimental data on the rheological properties of colloidal systems are sufficiently covered in a review.[78]

Relaxation processes were described [79] within the framework of mesoscopic nonequilibrium thermodynamics as applied to the dielectric relaxation of a medium represented by a system of noninteracting polar molecules. There is no basic difference between dielectric relaxation of the molecular medium and relaxation of anisotropic colloidal particles because one can pass from one physical system to another by appropriately changing variables. A fundamentally important feature of Ref. 79 is the introduction and inclusion of memory effects, so in the simplest case the phenomenological equations are as follows:

$$J_\alpha = \int_{-\infty}^{0} L_{\alpha\beta}(t-t')\nabla_\beta \mu(t')\mathrm{d}t', \tag{28}$$

$$J_\alpha^\Omega = \int_{-\infty}^{0} l_{\alpha\beta}(t-t')\nabla_\beta^\Omega \mu(t')\mathrm{d}t',$$

where J_α^Ω is the flux density in the space of particle orientations and ∇_β^Ω is the corresponding gradient operator. Note that nonlocal (with respect to time and space) effects (the kinetic coefficients $L_{\alpha\beta}$ and $l_{\alpha\beta}$ represent integral operators) have long been used in nonequilibrium thermodynamics (see, *e.g.*, Ref. 30). The inclusion of the memory effects provides a more correct description of relaxation processes in, *e.g.*, polymeric systems.[79] Clearly, this is also of importance for colloidal dispersions whose relaxation times are rather long, especially in the case of glass-like colloidal systems.

Relaxation processes can be accompanied by large fluctuations, in particular, because of their long duration. The concentration fluctuation dynamics of colloidal particles was described within the framework of the Onsager theory.[80] A one-component colloidal system was studied. Transport of particles in the system was described by conventional diffusion-type equation with inclusion of memory effects, spatial nonlocal effects and thermodynamic fluctuations. This approach can be used to describe the dynamics of colloidal systems in the glassy state; here the relaxation times may fall on a macroscopic time scale. The dynamics of glassy colloidal systems was also described [81] within the framework of mesoscopic nonequilibrium thermodynamics and based on the Focker–Planck equation.[82]

Equations determining the overall dynamics of colloidal particles in fluids with temperature gradients were derived [83] based on the Bogolubov–Born–Green–Kirkwood–Yvon chain closed using the maximum information entropy principle. The authors [83] demonstrated the possibility of constructing a closed system of equations describing a nonequilibrium colloidal dispersion. In the equilibrium case, these equations are transformed to known relations. Brownian dynamics of particles in alternating external fields was analyzed using methods of nonequilibrium thermodynamics.[84] It was shown that the action of external factors can be reduced to renormalization of the temperature of particles involved in Brownian motion. This simplifies the description of various physicochemical processes with participation of such particles.

III. Nonequilibrium thermodynamics of boundary conditions

1. The slip boundary conditions

The behaviour of nonequilibrium colloidal systems is to a great extent determined by the boundary conditions relating macroscopic characteristics at interfaces. Usually, the so-called stick boundary conditions are applied to colloidal systems with liquid dispersion media. In this case, it is required that the corresponding parameters of the contacting media at interfaces be equal. In particular, for unmoveable solids the velocity of the liquid on their surface is set to be zero (hence the name 'stick boundary conditions'). For gaseous dispersion media, the situation is somewhat different: more than 100 years ago, Maxwell developed a theory of thermal slip of gases (this effect was discovered by Reynolds) and proposed the expression for the slip velocity

$$u_{ts} = K_{ts}\frac{\eta_g}{\rho}\frac{\nabla T}{T}, \tag{29}$$

where K_{ts} is the thermal slip coefficient (according to Maxwell, $K_{ts} = 0.75$), η_g is the dynamic viscosity of the gas, ρ is the density of the gas and ∇T is the temperature gradient (this vector lies in the surface plane).

Thermal slip in liquids is due to the existence of boundary layers with modified structure.[85,86] It was shown [87] that thermal slip in gases and liquids with necessity follows from the Le Chatelier–Braun principle in the presence of thermal stresses. Preservation of the thermal slip effect on going from a gas to a continuous medium was also reported.[88] At present, this effect is considered in detail when studying the motion of particles in media with temperature gradients.

Some other slip effects, *viz.*, viscous slip, diffusion slip, *etc.*, were predicted theoretically and observed experimentally. For colloidal systems with liquid dispersion media, the most important phenomenon was electroosmotic slip,[86,89,90] because effects associated with this phenomenon

are strong enough and can be detected with ease. Recently, in connection with the development of microfluidics, increasing attention has been paid to the so-called hydrophobic slip.[91–93] This phenomenon is analogous to viscous slip in gases; it was observed experimentally long ago and theoretically substantiated by Churaev.[94] Of course, more recent studies gave new data, but a great body of experimental data obtained earlier were reproduced again.† Studies of the flow of fluids in thin channels marked the tide of interest in the boundary conditions for fluids. It was necessary to introduce new models (see, *e.g.*, Ref. 59 and references in the text below), because the stick conditions or the inclusion of hydrophobic slip alone do not allow one to completely describe all features of the effects observed. For instance, studies of the motion across the surface of polymer melts require that relaxation processes in the melts also be taken into account;[95] however, this was usually ignored in the conventional choice of boundary conditions.

In carrying out chemical reactions the problem of boundary conditions also poses in the case of contact between condensed phases[96] because application of classical boundary conditions to non-steady-state processes can lead to divergence of physical quantities. The generalized boundary conditions reported in a monograph[96] (see also Ref. 97), which can in particular cases be reduced to various types of boundary conditions including those taking into account the jumpwise behaviour of the effects under study, make it possible to exclude divergence and significantly affect transport of components through gas-separation and ion-exchange membranes.[98] They also may appear to be useful in the studies of coagulation in colloidal systems; however, this issue goes beyond the scope of this review because we consider only steady-state processes.

The slip effects and jumps not always can be related to the actual value of the fluid velocity on the surface of a solid body. For instance, the slip velocity specified by expression (29) differs from the gas velocity at the rigid wall. This is due to the presence of boundary layers where the properties of the fluid change abruptly. The boundary layers can be of different nature. In gases, they are kinetic in character, being determined by the mean free path (l_f). In liquids, they are governed by the structural changes in the near-surface regions. As applied to electrokinetic phenomena, a boundary layer is an (extended) electrical double layer. The presence of boundary layers causes abrupt changes in different parameters including the velocity, temperature, concentration, *etc.*, in the near-surface region. On the macroscopic level, this is interpreted as jumps and slip (Fig. 2).

As in the case of transport phenomena in the bulk phase, the totality of transfer processes occurring at interfaces can be best described within the framework of thermodynamics of irreversible processes. Therefore, in this Section we will consider a general approach to specification of boundary conditions based on nonequilibrium thermodynamics.

Derjaguin[99–101] was the first who employed methods of thermodynamics of irreversible processes to determine the kinetic coefficient K_{ts} using a rather simple procedure. He considered[99] the Poiseuille flow in a cylindrical channel and calculated the isothermal heat flux arising as a response to

† In the text below, we will repeatedly point to the results obtained earlier and reproduced in modern studies.

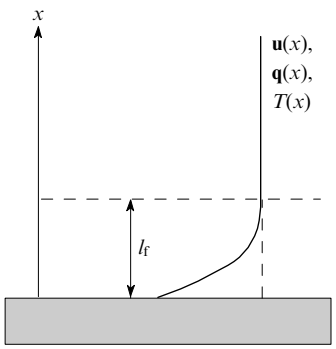


Figure 2. Changes in the main parameters within the boundary layers in nonequilibrium media.

pressure gradient within the framework of kinetic theory of gases in the second Chapman–Enskog approximation. Then, using relations of nonequilibrium thermodynamics derived for discontinuous systems[3] and the Onsager symmetry relations, the coefficient responsible for the gas flow caused by the temperature gradient was determined for this isothermal heat flux. However, the result of calculations ($K_{ts} = 1.5$) differed from the value calculated by the direct method. This, in particular, underlies the skepticism about the potential of nonequilibrium thermodynamics in the description of boundary effects. However, the discrepancy, which was due to neglect of heat transfer in the kinetic boundary layers, was then eliminated.[102]

Waldmann[103] proposed a procedure for specification of the boundary conditions for using methods of thermodynamics of irreversible processes. He derived an expression for the entropy production at the interface (ΔS_σ). The quantity ΔS_σ was defined as the total entropy difference between the fluxes in the gas and in the condensed phase integrated over the interface. Taking into account the mass, momentum and energy conservation laws on going through the interface and the invariance of ΔS_σ with respect to the Galilean transformation, Waldmann reduced the expression for ΔS_σ to a bilinear combination of thermodynamic fluxes and forces. The set of fluxes included the temperature jump, slip velocity and singular heat flux in the surface layer, the forces included the off-diagonal part of the stress tensor as well as the tangential and normal (to the surface) temperature gradients. More recently, it was shown that the Waldmann system of phenomenological equations of boundary conditions does not fulfill the symmetry relations. It was found that the Onsager symmetry relations are valid if the contributions of additional factors (in particular, the heat flux included by Derjaguin) to the entropy flux and to the surface entropy production are taken into account.[102] It should be noted that the somewhat incorrect result obtained by Waldmann is repeatedly reproduced in monographs.[104]

Yet another significant drawback of Waldmann's approach consists in that the boundary conditions are formulated ignoring the finite thickness of the boundary layer and the mass flux localized within this layer. This leads to the loss of some terms in the boundary conditions of the same order of magnitude as those obtained within the framework of the method *per se*.[11,14] The algorithm of deriving the boundary conditions with inclusion of finite layer thickness can be developed with ease; the structure of the expressions will change to some extent and a number of

new relations between the kinetic coefficients will appear.[105–109] The boundary conditions can also be specified by the joint approach using phenomenological considerations and the kinetic theory.[21, 22, 106, 107, 110] Progress in nonequilibrium thermodynamics of boundary conditions combined with kinetic methods for solution of boundary problems provides an explanation for some phenomena accompanying the flow of gases and liquids in channels and around solid bodies. However, here we will not dwell on these aspects in order to make the results presented below applicable to the widest range of problems. The readers who are interested only in the transfer processes in gases can find the corresponding results in the literature cited above and in Refs 111 and 112.

2. The balance equations at interfaces

Imagine that a fluid (liquid or gas) with nonuniform temperature and concentration distribution flows around a solid body. For simplicity, we will restrict ourselves to this case, although a situation with two immiscible fluids can also be considered.[108, 109] There is a near-surface boundary layer, such that the fluid viscosity and flow velocity can abruptly change within this layer (see Fig. 2). At long distances from the surface, the fluid flow is described by conventional hydrodynamic equations (*e.g.*, the Navier–Stokes equations). Let the conventional hydrodynamic equations be valid up to the interface. Let these equations have a solution in the form of some bulk velocity **u**. The difference between the true fluid flow velocity in the boundary layer and **u** will be taken into account using the boundary conditions, namely, let the boundary conditions for **u** be formulated in such a manner that the true solution be coincided with **u** outside the boundary layer.

Let the true mass flux density of the fluid ($\mathbf{J}_t$) be

$$\mathbf{J}_t = \rho\mathbf{u} + \mathbf{j}_b, \tag{30}$$

where ρ is the fluid density far from the interface. The boundary flux $\mathbf{j}_b$ vanishes at long distances from the interface because the true flux density should coincide with the 'bulk' hydrodynamic density, *i.e.*

$$\mathbf{J}_t \to \rho\mathbf{u}$$

on moving away from the surface. From the continuity equations (in the steady-state case) for the true flux density and the bulk hydrodynamic flux it follows

$$\mathrm{div}(\mathbf{J}_t) = 0, \mathrm{div}(\rho\mathbf{u}) = 0 \Rightarrow \mathrm{div}(\mathbf{j}_b) = 0. \tag{31}$$

Assume that the surface of the solid body is impermeable to the fluid; then, the normal component of the flux should be equal to zero,

$$\mathbf{J}_{tx}\big|_\Sigma = 0,$$

where x is the coordinate normal to the surface; the symbol Σ denotes that the corresponding quantity is taken at the surface of the solid. Taking into account this fact, integration of Eqns (31) along the normal to the surface and vanishing of $\mathbf{j}_b$ far from the interface leads to

$$u_x\big|_\Sigma = -\frac{1}{\rho}\mathrm{div}_\tau\hat{\mathbf{j}}_{b\tau}, \tag{32}$$

where div_τ denotes two-dimensional divergence in the coordinates lying in the surface plane and $\hat{\mathbf{j}}_{b\tau}$ is the tangential mass flux density integrated along the normal to the surface

$$\hat{\mathbf{j}}_{b\tau} = \int_0^\infty \mathbf{j}_{b\tau}\mathrm{d}x. \tag{33}$$

The balance equation for the energy flux is derived analogously

$$\left(J^e_{ex} - J^e_{ix}\right)\Big|_\Sigma = -\mathrm{div}_\tau\hat{\mathbf{j}}^e_{b\tau}, \tag{34}$$

where the superscript denotes that we deal with the energy fluxes; $\mathbf{J}^e_e$, $\mathbf{J}^e_i$ are the energy flux densities in the fluid and in the solid, respectively.

If the fluid flows around a solid body, the balance equation for the momentum is not necessary. The corresponding equation for two contacting liqiud media has the form[109]

$$\left(\Pi^{te}_{xx} - \Pi^{ti}_{xx}\right)\Big|_\Sigma = -\mathrm{div}_\tau\widehat{\Pi}_{x\tau} + \widehat{\Pi}_{\tau\tau'}K_{\tau\tau'}\delta_{\tau\tau'}, \tag{35}$$

$$\left(\Pi^{te}_{x\tau} - \Pi^{ti}_{x\tau}\right)\Big|_\Sigma = -\mathrm{div}_{\tau'}\widehat{\Pi}_{x\tau'} + \widehat{\Pi}_{x\mu}K_{\mu\mu}\delta_{\mu\tau},$$

where $\Pi^{te}_{\mu\nu}$, $\Pi^{ti}_{\mu\nu}$ are the momentum flux density tensors in the 'external' and internal fluids (with inclusion of pressure), respectively; $\delta_{\mu\nu}$ is the Kronecker symbol, $K_{\tau\tau'}$ is the interface curvature tensor and it is assumed that summation is performed over the $\tau = x, y$ values if the two indexes are equal to each other.

The equality (35) extends the Laplace equation to the case of nonequilibrium systems. In equilibrium, the quantities Π^{te}_{xx} and Π^{ti}_{xx} coincide with the pressure in the contacting phases and

$$\widehat{\Pi}_{\tau\tau'} = -\sigma\delta_{\tau\tau'},$$

where σ is the surface tension at the interface.

From the balance Eqns (32) and (34) it follows that apparent flux discontinuities due to the changes in the fluid characteristics in the near-boundary regions are observed at the interface in the nonequilibrium case.

By introducing specific surface fluxes one can derive phenomenological equations for the interfacial characteristics.[102, 110, 113, 114] Of course, they also include nonequilibrium parameters characterizing the bulk phase, because contact of two equilibrium bulk phases does not produce a nonequilibrium surface. Note that the boundary conditions for the surface phases were obtained not only within the framework of conventional thermodynamics, but also within the framework of generalized nonequilibrium thermodynamics[115] and so-called GENERIC (General Equation for the Nonequilibrium Reversible–Irreversible Coupling) formalism[116] which includes joint interaction between equilibrium and nonequilibrium processes. Nonequilibrium surfaces of neat liquids are also described using surface characteristics,[117, 118] *e.g.*, the surface viscosity; microscopic treatment also involves the introduction of a correction to the surface tension and some other characteristics. The equations thus derived provide a better description of processes occurring at the interface. An example is provided by Ref. 119 where phenomenological equations

for the liquid crystal/isotropic phase interface were derived. These equations include not only conventional thermodynamic characteristics (see below), but also the surface parameters, such as the order parameter, elastic moduli, *etc*.

3. Equations of nonequilibrium thermodynamics for interfaces

As mentioned above, the balance equations are part of boundary conditions. One should also have the expression for fluxes in the boundary layer and the boundary conditions for tangential components. The latter can be established using methods of nonequilibrium thermodynamics. Consider a one-component fluid flowing around a solid body (for more complex systems, we will present a number of final results as examples).

Our starting point is the following expression for the entropy production at the interface:

$$\Delta S_\sigma = J_n^S - J_{in}^S, \tag{36}$$

where

$$J_n^S = (\mathbf{J}^S \mathbf{n}),$$

$$J_{in}^S = (\mathbf{J}_\mathrm{i}^S \mathbf{n}),$$

$\mathbf{n}$ is the external normal to the surface; $\mathbf{J}^S$, $\mathbf{J}_\mathrm{i}^S$ are the entropy flux densities in the fluid and in the solid. Assuming no mass transfer through the interface, for the density of the entropy flux directed outward of the solid body one has

$$\mathbf{J}_\mathrm{i}^S = \frac{\mathbf{q}^\mathrm{s}}{T_0}, \tag{37}$$

where $\mathbf{q}^\mathrm{s}$ is the heat flux density in the solid body and T_0 is the surface temperature.

The form of the expression for the entropy flux in the gas phase and the balance equations at the interface eventually determines the structure of the boundary conditions. Based on the results of numerous studies, it was proposed to calculate the entropy flux using the so-called Burnett transport equations.[21] The corresponding entropy flux density is given by

$$\mathbf{J}^S = \frac{\mathbf{q}}{T} - \frac{2}{5}\frac{\mathbf{q}\,\mathbf{\Pi}}{pT}$$

(we will not analyze more complex expressions for the entropy flux, *e.g*., those considered in Ref. 120, because this will go beyond the approximation used in the surface entropy production calculations). Using this expression and the balance equations, the entropy production at the interface can be transformed to

$$\begin{aligned}\Delta S_\sigma = {} & \frac{1}{2}\left(q_n^\mathrm{s} + q_n\right)\left(\frac{1}{T_0} - \frac{1}{T(0)} + \frac{2}{5pT_0}\Pi_{nn}\right) + \\ & + \frac{\mathbf{\Pi}_{\tau n}}{T_0}\left(\mathbf{u}_\tau(0) + \frac{2}{5p}\mathbf{q}_\tau\right) + \frac{\hat{\mathbf{j}}_\tau^n}{n}\,\frac{1}{T_0}\,\frac{\partial(p+\Pi_{nn})}{\partial\boldsymbol{\tau}} - \\ & - \frac{1}{2}\,\hat{\mathbf{j}}_\tau^q\,\frac{\partial}{\partial\boldsymbol{\tau}}\left(\frac{1}{T_0} + \frac{1}{T(0)} - \frac{2}{5pT_0}\Pi_{nn}\right),\end{aligned} \tag{38}$$

where p is the pressure; $\mathbf{u}_\tau(0)$ and $T(0)$ are respectively the apparent velocity and the temperature of the fluid on the surface of the solid body; and $\boldsymbol{\tau}$ is the two-dimensional vector lying in the surface plane.

Let us choose the expressions for fluxes in the form

$$I_0 = \frac{1}{T_0} - \frac{1}{T(0)} + \frac{2}{5pT_0}\Pi_{nn}, \tag{39}$$

$$\mathbf{I}_1 = \frac{1}{T_0}\left(\mathbf{u}_\tau(0) + \frac{2}{5p}\mathbf{q}_\tau\right),$$

$$\mathbf{I}_2 = \hat{\mathbf{j}}_{\mathrm{b}\tau}^q = \hat{\mathbf{j}}_{\mathrm{b}\tau}^\varrho - \frac{5}{2}\frac{p}{\rho}\hat{\mathbf{j}}_{\mathrm{b}\tau},$$

$$\mathbf{I}_3 = \frac{\hat{\mathbf{j}}_{\mathrm{b}\tau}}{\rho}.$$

The corresponding forces are given by

$$X_0 = \frac{1}{2}\left(q_n^\mathrm{s} + q_n\right), \tag{40}$$

$$\mathbf{X}_1 = \frac{\mathbf{\Pi}_{\tau n}}{T_0},$$

$$\mathbf{X}_2 = \frac{\partial(p+\Pi_{nn})}{\partial\boldsymbol{\tau}},$$

$$\mathbf{X}_3 = \frac{\partial}{\partial\boldsymbol{\tau}}\left(\frac{1}{T_0} + \frac{1}{T(0)} - \frac{2}{5pT_0}\Pi_{nn}\right).$$

Then, the phenomenological equations (boundary conditions) are as follows:

$$I_0 = L_{00}X_0, \tag{41}$$

$$\mathbf{I}_k = \sum_{j=1}^{3} L_{kj}\mathbf{X}_j.$$

They fulfill the Curie principle and, according to the Onsager theorem, $L_{ik} = L_{ki}$.

In most practically important cases, normal stresses are insignificant and one can restrict himself to representation of heat flux only through the temperature gradient. As a result, the phenomenological equations (41) are simplified and take the form

$$\frac{T(0) - T_0}{T_0} = L_{00}\frac{q_n}{T_0}, \tag{42}$$

$$\mathbf{u}_\tau(0) + \frac{2}{5}\frac{\mathbf{q}_\tau}{p} = L_{11}\mathbf{\Pi}_{n\tau} + L_{12}\frac{1}{T^2}\frac{\partial T}{\partial\boldsymbol{\tau}} + L_{13}\frac{1}{T}\frac{\partial p}{\partial\boldsymbol{\tau}}, \tag{43a}$$

$$\hat{\mathbf{j}}_{\mathrm{b}\tau}^q = L_{21}\mathbf{\Pi}_{n\tau} + L_{22}\frac{1}{T^2}\frac{\partial T}{\partial\boldsymbol{\tau}} + L_{23}\frac{1}{T}\frac{\partial p}{\partial\boldsymbol{\tau}}, \tag{43b}$$

$$\hat{\mathbf{j}}_{\mathrm{b}\tau} = L_{31}\mathbf{\Pi}_{n\tau} + L_{32}\frac{1}{T^2}\frac{\partial T}{\partial\boldsymbol{\tau}} + L_{33}\frac{1}{T}\frac{\partial p}{\partial\boldsymbol{\tau}}. \tag{43c}$$

Solution of hydrodynamic problems requires Eqn (43a), which specifies the boundary condition for the tangential velocity. Equations (43b) and (43c) are necessary because they appear in the boundary conditions (33) and (34) for the normal fluxes. The first term on the right side of Eqns (43a)

determines the slip of the fluid under the action of tangential stresses,

$$\Pi_{x\tau} = -\eta_f \frac{d\mathbf{u}_\tau}{dx}.$$

This kind of slip is known as isothermal slip; in microfluidics, it is usually called hydrophobic slip

$$\mathbf{u}_\tau(0) = -L_{11}\eta_f \frac{d\mathbf{u}_\tau(x)}{dx} = b_h \frac{d\mathbf{u}_\tau(x)}{dx}, \quad (44)$$

where b_h is the slip length.

The second term on the right side of Eqns (43a) along with the term $(2/5p)\mathbf{q}_\tau$ characterizes the thermal slip described by Eqn (29). Recall that

$$\mathbf{q}_\tau = -\lambda_f \frac{\partial T}{\partial \tau},$$

and, hence,

$$L_{12} + \frac{2\lambda_f}{5p} = \frac{\eta_f}{\rho} K_{ts}.$$

The third term characterizes the so-called baroslip which usually makes a little contribution to transport processes.

The L_{21} coefficient in Eqn (43b) determines heat transfer in the boundary layer under the action of tangential stresses. This effect is characterized by the so-called heat of transfer when fluids flow through porous bodies. The heat of transfer causes, in particular, thermal polarization of membranes (see below).

Equation (42) describes the temperature jump at the interface due to the presence of heat flux along the normal to the surface. It is determined by the mean free path of molecules in the case of gas flows and by changes in the structure and thermal conductivity within the boundary layer in the case of fluid flows. This effect plays an important role in the determination of the thermophoresis velocity of aerosol particles. It is also significant if evaporation and condensation occur at the interface.

Initially, Waldmann's boundary conditions did not include the third thermodynamic force or the term $(2/5p)\mathbf{q}_\tau$ in the first flux, and the mass flux in the boundary layer was assumed to be zero. It was accepted that only a singular heat flux can be transferred across the surface. The Onsager relations are not fulfilled for these truncated equations because the term $(2/5p)\mathbf{q}_\tau$ makes the predominant contribution to the thermal slip coefficient K_{ts} (*cf.* its value equal to 3/2 *vs.* about -0.33 for the L_{12} term). The boundary conditions can also be obtained for the flow of mixtures including electrolytes. Below we will present the corresponding equations for a binary gas mixture to demonstrate a pattern for constructing boundary conditions for any systems (simplified equations will also be considered).

In this case, Eqn (42) remains unchanged and the system of three vector Eqns (43) is replaced by the system of four vector equations

$$\mathbf{u}_\tau(0) + \frac{2}{5}\frac{\mathbf{q}_\tau}{p} = L_{11}\mathbf{\Pi}_{n\tau} + L_{12}\frac{1}{T^2}\frac{\partial T}{\partial \boldsymbol{\tau}} + L_{13}\frac{1}{T}\frac{\partial p}{\partial \boldsymbol{\tau}} + \quad (45)$$

$$+ L_{14}\frac{p}{T}\left(\frac{\partial c}{\partial \boldsymbol{\tau}} + \frac{m_2 - m_1}{\rho n}\frac{\partial \ln p}{\partial \boldsymbol{\tau}}\right),$$

$$-\hat{\mathbf{j}}^q_{b\tau} = L_{21}\mathbf{\Pi}_{n\tau} + L_{22}\frac{1}{T^2}\frac{\partial T}{\partial \boldsymbol{\tau}} + L_{23}\frac{1}{T}\frac{\partial p}{\partial \boldsymbol{\tau}} +$$

$$+ L_{14}\frac{p}{T}\left(\frac{\partial c}{\partial \boldsymbol{\tau}} + \frac{m_2 - m_1}{\rho n}\frac{\partial \ln p}{\partial \boldsymbol{\tau}}\right),$$

$$\hat{\mathbf{j}}_{b\tau} = L_{31}\mathbf{\Pi}_{n\tau} + L_{32}\frac{1}{T^2}\frac{\partial T}{\partial \boldsymbol{\tau}} + L_{33}\frac{1}{T}\frac{\partial p}{\partial \boldsymbol{\tau}} +$$

$$+ L_{34}\frac{p}{T}\left(\frac{\partial c}{\partial \boldsymbol{\tau}} + \frac{m_2 - m_1}{\rho n}\frac{\partial \ln p}{\partial \boldsymbol{\tau}}\right),$$

$$\hat{\mathbf{j}}^v_{b\tau} = L_{21}\mathbf{\Pi}_{n\tau} + L_{42}\frac{1}{T^2}\frac{\partial T}{\partial \boldsymbol{\tau}} + L_{43}\frac{1}{T}\frac{\partial p}{\partial \boldsymbol{\tau}} +$$

$$+ L_{44}\frac{p}{T}\left(\frac{\partial c}{\partial \boldsymbol{\tau}} + \frac{m_2 - m_1}{\rho n}\frac{\partial \ln p}{\partial \boldsymbol{\tau}}\right),$$

where $c = n_1/n$ is the concentration of the first component, $n = n_1 + n_2$ is the total number of molecules per unit volume, m_1 and m_2 are molecular masses of the components; ρ_1 and ρ_2 are the densities of the components,

$$\hat{\mathbf{j}}^v_{b\tau} = \frac{\hat{\mathbf{j}}^{(1)}_{b\tau}}{\rho_1} - \frac{\hat{\mathbf{j}}^{(2)}_{b\tau}}{\rho_2}$$

is the average velocity difference between the components in the boundary layer, $\hat{\mathbf{j}}^{(i)}_{b\tau}$ are the component mass fluxes in the boundary layer,

$$\hat{\mathbf{j}}_{b\tau} = \hat{\mathbf{j}}^{(1)}_{b\tau} + \hat{\mathbf{j}}^{(2)}_{b\tau}$$

is the total mass flux in the boundary layer; in this case,

$$\hat{\mathbf{j}}^q_{b\tau} = \hat{\mathbf{j}}^e_{b\tau} - \frac{5}{2}\frac{p}{\rho}\left(\frac{m_2 - m_1}{n} n_1 n_2 \hat{\mathbf{j}}^v_{b\tau} + \hat{\mathbf{j}}_{b\tau}\right).$$

The L_{14} coefficient determines the so-called diffusion slip, *i.e.*, the slip of the mixture under the action of the concentration gradient

$$\mathbf{u}_{ds}(0) = K_{ds} D_{12} \frac{\partial c}{\partial \boldsymbol{\tau}}, \quad (46)$$

where K_{ds} is the diffusion slip coefficient and D_{12} is the interdiffusion coefficient of the mixture components.

Diffusion slip is related to osmotic motion of mixtures in porous bodies, diffusiophoresis of colloidal particles and many other effects. The role of diffusion slip in various physicochemical processes was thoroughly considered by Mills.[121] The L_{14} cross coefficient governs the relative motion of mixture components within the boundary layer due to tangential hydrodynamic stresses. This effect is related to reverse osmotic separation of components in membranes and determines the concentration polarization.

The boundary conditions can be extended by including, *e.g.*, charge transfer. Then, one should write equations and kinetic coefficients determining electroosmotic slip and the cross effect (transfer of electric current in the boundary layer) called the flow current (see below).

4. Boundary conditions at the evaporation/condensation surface

As mentioned above, the boundary conditions derived by methods of nonequilibrium thermodynamics are written using some simplifying assumptions. In particular, they do not include the normal component of the fluid velocity, which differs from zero [see Eqns (32)] and is responsible for additional scalar fluxes and forces.[22, 110] Usually, the normal component on the surface of a solid body is small (of the order of the ratio of the boundary layer thickness to the particle size or capillary size). However, in some cases, it can significantly differ from zero. The cases in point are evaporation/condensation processes. The boundary conditions for this situation were thoroughly analyzed [108, 109] and it was shown that nonequilibrium thermodynamics makes it possible to predict a number of unusual effects.

Compared to the surface of a solid body, the surface of a liquid has additional degrees of freedom associated with its complex motion. Because of this, calculations of the entropy production on the surface of a liquid should take into account additional fluxes and forces having scalar, vector and tensor dimensionalities. Additional thermodynamic forces are formed by combinations of the ∇ operator and the velocity of motion of the liquid surface. The appearance of such forces has a particular physical meaning. In the case of inelastic scattering (or escape) by a nonuniformly moving surface, the distribution of molecules becomes different from the Maxwell distribution. This difference should affect the transfer of mass, momentum and energy in the boundary layers (eventually, the hydrodynamic boundary conditions). The effects were studied in detail elsewhere;[108, 109] here mention may be made of an interesting consequence due to the temperature jump and the vapour pressure drops on the evaporating surface.

The case in point is inversion of temperature profile predicted by Pao,[122] *viz*., in the vapour phase, the slope of the temperature profile between the surfaces of two liquids can be inverse to that specified by the temperature difference between the liquids. The effect has been studied in detail within the framework of the kinetic theory [123, 124] and nonequilibrium thermodynamics.[125–127] It was shown that the effect is consistent with the second law of thermodynamics.

Phenomenological equations on an evaporating surface have the form [126, 128]

$$T(0) - T_s = -l_{11}q_n - l_{12}n_s u_n(0), \tag{47}$$

$$\frac{T_s(p(0) - p_s)}{n_s} = -l_{21}q_n - l_{22}n_s u_n(0),$$

where T_s is the temperature at the surface of the liquid, $T(0)$ and $p(0)$ are respectively the extrapolated temperature and pressure on the surface of the liquid, $n_s u_n(0)$ is the evaporation rate, q_n is the heat flux through the surface, p_s is the equilibrium vapour pressure over the flat liquid surface, and n_s is the equilibrium concentration of vapour molecules. The minus signs on the right side emphasize positive values of the l_{ij} coefficients. The Onsager symmetry for the coefficients appeared in Eqs (47) was confirmed by various methods including numerical experiments.[129–131]

It is convenient to introduce the temperature T_p corresponding to the equilibrium between the liquid and vapour at the pressure $p(0)$. Then, using the Clapeyron–Clausius equation, one can write

$$\frac{T_s\big(p(0) - p_s\big)}{n_s} = (T_p - T_s)L_e, \tag{48}$$

where L_e is the heat of evaporation.

Assume that two liquid volumes are separated by a flat gap of width H, filled with a vapour. The liquid temperatures are T_1 and T_2 (Fig. 3). Let us determine the temperature profile of vapour in the gap. Let the temperatures T_1 and T_2 be maintained at some distance from interfaces and the surface temperatures T_{s1} and T_{s2} be determined from the self-consistent solution to the problem. Let $T_1 > T_2$; then, the liquid evaporates from surface 1 and condenses on surface 2. Let evaporation be slow and the mean free path be small compared to H. To a first approximation, the vapour pressure in the gap is constant. This means that T_e is a constant too and the heat flux is zero. Using Eqns (47) and (48), one gets the temperatures of the liquid surfaces:

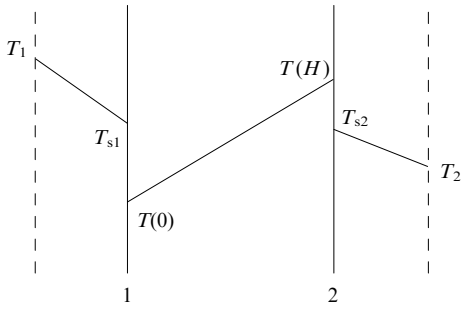


Figure 3. Temperature profile between the evaporation surfaces (T_1) and condensation surfaces (T_2) at $T_1 > T_2$.

$$T_{s1} = T_p + \frac{l_{22}}{L_e}n_s u_n, \tag{49}$$

$$T_{s2} = T_p - \frac{l_{22}}{L_e}n_s u_n.$$

Applying the first equation in (47) to the surfaces at $x = 0$ and $x = H$ leads to

$$T(0) = -\left(l_{12} - \frac{l_{22}}{L_e}\right)n_s u_n + T_p, \tag{50}$$

$$T(H) = \left(l_{12} - \frac{l_{22}}{L_e}\right)n_s u_n + T_p.$$

At $L_e > l_{22}/l_{12}$, the slope of the temperature profile in the vapour phase is opposite to that specified by the external temperature jump.

The kinetic coefficients l_{ij} were calculated by different authors. For instance, in the case of complete accommodation, one has [132]

$$l_{12} = \frac{T_s}{n_s}\sqrt{\frac{m}{2kT}}\frac{\sqrt{\pi}}{8}\left(1 + \frac{16}{5\pi}\right), \tag{51}$$

$$l_{22} = \frac{kT_s^2}{n_s}\sqrt{\frac{m}{2kT}}\frac{\sqrt{\pi}}{2}\sqrt{\pi}\left(\frac{9}{8}+\frac{4}{\pi}\right).$$

For a number of systems, these coefficients were determined experimentally.[133–138]

The inverse profile is obtained at $L_e > 4.73\,kT_s$. Since one always has $L_e > 10\,kT_s$, the temperature profile should be inverted for all fluids.

This effect attracts considerable attention of researchers. Attempts to detect it experimentally have been made. The temperature jump at the interface was demonstrated,[139–141] but its magnitude and even sign were different from the theoretical predictions. The reasons for these discrepancies are still unknown. A strange feature of the experiments[139–141] consists in a nonlinear temperature profile beyond the Knudsen layer. This is hard to explain from the standpoint of the kinetic theory. Various attempts to explain the results did not clarify the situation.

The following remarks concerning these experiments may be made. First, the temperature of the gas was measured with a thermocouple. The technique requires that special care be taken; in particular, the heat transfer coefficient between vapour and thermocouple should be known, whereas this parameter was left out of consideration by the authors of Refs 139–141. Second, the thermocouple is placed in the moving vapour with temperature gradients rather than in steady-state vapour; this also should to some extent influence the measured temperature. This fact was not discussed at all in Refs 139–141. Third, condensation of saturated vapour on the thermocouple having a lower temperature can skew the results of measurements. Fourth, the authors admitted the presence of nitrogen impurity (about 2%) in the vapour; this may affect the experimental results (even at low concentrations, the non-condensed component influences the effect in question). For instance, it was reported[142] that the effect is almost completely suppressed at impurity concentrations of the order of the Knudsen number (this parameter is small in the experiments under study). Also evaporation processes in gas mixtures should be considered taking into account the viscosity effects,[143] which complicates analysis of the phenomenon under study. Eventually, one can show that the energy flux transferred by thermal radiation exceeds the heat transfer in the vapour through thermal conductivity by several orders of magnitude, being also considerably higher than convective transfer of enthalpy vapour; this flux can also significantly skew the results of measurements.

A molecular dynamics study[144] showed that the local equilibrium approximation satisfactorily works near the evaporation/condensation surface, thus justifying the use of methods of nonequilibrium thermodynamics. Also, formally, the experimental data[139–141] were described in Ref. 145 assuming a possible dependence of the condensation (evaporation) coefficient on the molecular velocity; however, the simplest kinetic theory used in Ref. 145 was inappropriate for the description of boundary layers. Recently, this model was again used[146] to describe condensation/evaporation processes. A comparison of the results obtained in the study and in molecular dynamics calculations showed that the phenomenological equations (47) and the Onsager symmetry relations are fulfilled if the dependence of the accommodation coefficient on the molecular velocity is taken into account and that the observed deviations from the symmetry relations can be due to nonlinear effects which by default lie beyond the applicability range of linear nonequilibrium thermodynamics.

It should be noted that the dependences of the condensation coefficient on energy in the description of evaporation processes were also considered earlier[147] within the framework of mesoscopic nonequilibrium thermodynamics which uses not only macroscopic variables, but also some internal variables. In some sense, the use of the mesoscopic approach is similar to treatment of the boundary layers as an individual system described y specific equations on the local rather than integral level. Of course, Eqns (50) also follow from mesoscopic nonequilibrium thermodynamics. This confirms their validity equations under the conditions when evaporation requires the overcoming of a potential barrier.

The aforesaid concerned evaporation and condensation in one-component systems. The situation in multicomponent mixtures is much more complicated. Phase transitions in multicomponent systems were described within the framework of nonequilibrium thermodynamics and using dynamic simulation methods in, *e.g.*, Refs 148 and 149. We will not analyze this situation because a formally complicated description leads actually to predictable results.

5. Nonequilibrium thermodynamics of three-phase contact line

Using nonequilibrium thermodynamics, one can also describe the motion of the three-phase contact line.[150–152] The pattern used to derive equations is similar to that presented above; there is also an analogy between the final equations for both cases, except that the thermodynamic fluxes and forces now refer to the three-phase contact line rather than the boundary layer. We will not dwell on these equations because they give no basically new results, being at the same time cumbersome. The simplest example of description of the dynamics of the three-phase contact line using nonequilibrium thermodynamics is as follows.[86, 153] The entropy production is determined from the work produced in the motion of the three-phase contact line and the phenomenological equations have the form

$$u_l = L_{ll}[\sigma_{sv} - \sigma_{sl} - \sigma_{lv}\cos(\theta)], \tag{52}$$

where L_{ll} is the phenomenological coefficient; u_l is the velocity of the three-phase contact line; σ_{sv}, σ_{sl}, σ_{lv} are the energies for the solid/vapour interfaces, solid/liquid and liquid/vapour interfaces, respectively; θ is the equilibrium contact angle. Experiments with the 'silicon oil–steel support' system[153] confirmed the validity of relation (52). These experiments were carried out at different roughness of the support. A larger array of experimental data was reported in a study[154] where a number of some nonlinear models for drop spreading were considered. The dynamics of the three-phase contact line is strongly affected by evaporation and condensation processes accompanies by thermal effects. This significantly complicated the character of the motion of this line, namely, the effect of heat transfer was revealed by methods of nonequilibrium thermodynamics. A more complex description of the dynamics of the three-phase contact line, in particular, taking into account evaporation/condensation processes was reported recently.[155, 156]

IV. Nonequilibrium thermodynamics of new phase formation

The description of new phase formation using methods of nonequilibrium thermodynamics seems to be quite interesting. The overall problem is divided into two individual problems concerning (i) the kinetics of nucleation and (ii) the growth of new-phase nuclei.

1. Nonequilibrium thermodynamics of nucleation

The need for using methods of nonequilibrium thermodynamics in studies of nucleation processes is dictated by the following. First, there is a problem of deriving equations describing the dynamics of a new-phase nucleus.[157] As mentioned above, nonequilibrium thermodynamics gives the most general description of nonequilibrium processes. Second, nucleation is usually described as diffusion of a nucleus in the generalized multidimensional space.[86] The diffusion coefficient appearing in corresponding equations is a tensor quantity. The symmetry of this tensor is an important issue, while the Onsager symmetry relations allow one to unambiguously determine the symmetry of particular coefficients. Third, nonequilibrium thermodynamics makes it possible to modify the expression for the nucleation rate to bridge the gap between the theory and experiment. Fourth, using the principles of nonequilibrium thermodynamics, one can predict the morphology of the growing new-phase nuclei.

Note that direct application of nonequilibrium thermodynamics to nucleation studies faces some difficulties. Indeed, a critical nucleus is in the metastable state and a deviation from the equilibrium is followed by further deviation rather than relaxation to the metastable state so the Onsager theory is inapplicable for formal reasons. Based on this fact, erroneous conclusions about symmetry violation of the diffusion tensor appearing in the equation for the kinetics of nucleation are sometimes drawn. In the text below we will show that it is possible to describe nucleation in a manner consistent with the Onsager theory. Note that the Onsager idea of microscopic reversibility, which was employed to prove the symmetry of the kinetic coefficients, can be used to substantiate [158] the equations derived to describe the growth of supercritical nuclei based on the dynamics of subcritical fluctuations.

A nonequilibrium steady state can be established only in open systems by introducing appropriate boundary conditions.[3] Derjaguin was the first who proposed to describe nucleation within the framework of the steady-state approximation.[159] This approach was used to develop nonequilibrium thermodynamics of nucleation.[160] The pattern proposed [160] was used in more recent studies.[161, 162]

A steady state of nucleation is created using an ensemble of systems representing a volume $\widehat{V}_n$ filled with supersaturated vapour (for clarity, we will use the term 'vapour'). In a reservoir of the volume $\widehat{V}_n$, a small volume V_n is selected (or the entire reservoir volume $\widehat{V}_n$ is divided into cells of volume V_n) using a semi-permeable membrane through which only subcritical nuclei can pass. It is accepted that the volume of the critical nucleus is $v_c \ll V_n \ll \widehat{V}_n$ and the new phase formation is possible only in the volume V_n, whereas the remaining part of the volume $(\widehat{V}_n - V_n)$ is the source of monomers and plays the role of a thermostat. Three states are possible for the system (Fig. 4):

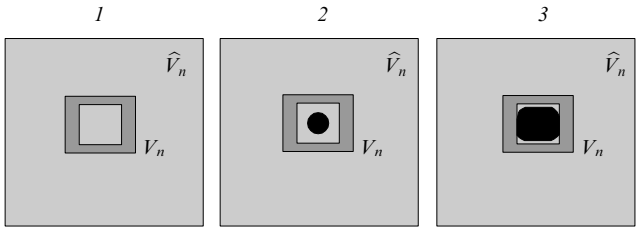


Figure 4. Scheme illustrating nucleation followed by the establishment of a steady state.
For notations *1–3*, see text.

1 — the V_n volume contains no near-critical and supercritical nuclei, being filled with supersaturated vapour only;

2 — the V_n volume contains a near-critical nucleus;

3 — the V_n volume contains a supercritical nucleus which, owing to the supersaturated state of vapour, fills the whole volume V_n with a probability close to unity (further growth of the nucleus is suppressed by the porous membrane).

Fluctuations may lead to both the formation of a new phase and a reverse transition from state *3* to state *1* (very rare event for this system).

Having a suffiently large number of such systems, one can determine the equilibrium distribution of nuclei $\Phi_e(\mathbf{x})$ along the generalized coordinate $\mathbf{x}$, when the flow of nuclei from state *1* to state *3* is exactly compensated by the reverse flux (the probability of evaporation of the nucleus in the V_n volume through fluctuation is low; however, transition $1 \to 3$ can be compensated by the large number of systems in the state *3*).

Note that recently, statistical systems with rarely occurring transitions between two states have been studied in detail using methods of nonequilibrium statistical mechanics. Interrelations between statistical description and the approach underlying the Onsager theory were studied.[163] Also, that study demonstrated the symmetry of kinetic coefficients (analogues of diffusion coefficients in the generalized space, see below). We will not use the methods [163] to prove symmetry; our approach to the solution of this problem will be simpler but no less rigorous.

Imagine that a particular number of systems containing supercritical nuclei are periodically removed from the ensemble and, simultaneously, systems in the state *1* are introduced into the ensemble. As a result, one gets a nonequilibrium distribution of nuclei along the generalized coordinates in the system and, consequently, the flux of nuclei towards the supercritical region. Let us calculate the entropy production due to such a flux. Note that an analogous procedure for creation of a steady nonequilibrium state was used [164] in statistical analysis of nucleation in the system described by the Ising model.

The entropy density (s_n) in the nonequilibrium system can be determined using the Gibbs postulate [3]

$$s_n = \Phi(\mathbf{x}) k \ln \frac{\Phi(\mathbf{x})}{\Phi_e(\mathbf{x})}, \tag{53}$$

where $\Phi(\mathbf{x})$ is the nonequilibrium distribution of nuclei along the generalized coordinate, which obeys the equation [86]

$$\frac{\partial \Phi(\mathbf{x},t)}{\partial t} = \sum_{i,j} \frac{\partial}{\partial x_i}\left[D_{ij}^n(\mathbf{x},t)\Phi_e(\mathbf{x}) \frac{\partial}{\partial \mathbf{x}_j}\left(\frac{\Phi(\mathbf{x},t)}{\Phi_e(\mathbf{x})}\right)\right], \tag{54}$$

where D_{ij}^n is the generalized diffusion coefficient. The expression for the flux density J_i^n of nuclei in the generalized space is presented in square brackets.

Using Eqn (54), the entropy balance equation is as follows:

$$\frac{\partial s_n}{\partial t} = \frac{\partial}{\partial x_i}\left[J_i^n k\left(\ln\frac{\Phi}{\Phi_e}+1\right)\right] + J_i^n \frac{\partial}{\partial x_i} k \ln\frac{\Phi}{\Phi_e}. \tag{55}$$

Here the last term on the right side represents the expression for the entropy production due to nucleation. Taking account of this expression and the general principles of nonequilibrium thermodynamics, one can write the following phenomenological equations:

$$J_i^n = \sum_j L_{ij}^n \frac{\partial}{\partial x_j} k \ln\frac{\Phi}{\Phi_e}, \tag{56}$$

where the coefficients L_{ij}^n should fulfill the Onsager symmetry relations $L_{ij}^n = L_{ji}^n$. In conventional notations, [see Eqn (54)], we get

$$L_{ij}^n = \frac{D_{ij}^n \Phi(\mathbf{x})}{k}, \tag{57}$$

and symmetry of the generalized diffusion coefficient follows from the Onsager symmetry relations.

Note that the symmetry of the generalized diffusion coefficient follows from not only postulates of nonequilibrium thermodynamics, but also from microscopic calculations. Computations [165] for the one-dimensional (1D) case can be extended to the multidimensional situation (see, *e.g.*, Ref. 166). The computational scheme is as follows. Consider the fluctuation dynamics in the generalized space. Assume that the overall flux of nuclei includes the steady flux J_{sti}^n and the fluctuation component

$$J_i^n = J_{sti}^n + \tilde{J}_i^n. \tag{58}$$

The fluctuation flux $\tilde{J}_i^n$ is characterized by a zero mean value and obeys the fluctuation-dissipation theorem

$$\left\langle \tilde{J}_i^n(\mathbf{x},t)\tilde{J}_i^n(\mathbf{x}',t')\right\rangle = 2kL_{ij}^n \delta(\mathbf{x}-\mathbf{x}')\delta(t-t'), \tag{59}$$

where the angle brackets $\langle ... \rangle$ denote the averaging over ensemble and $\delta(\mathbf{x})$ is the Dirac delta function. From Eqns (59), the Green–Kubo relation for the diffusion coefficient follows:

$$D_{ij}^n = \frac{1}{\Phi(\mathbf{x},t)} \int d\mathbf{x}' \int_0^\infty dt \langle \tilde{J}_i^n(\mathbf{x},0)\tilde{J}_i^n(\mathbf{x}',t)\rangle. \tag{60}$$

This relation clearly shows that the generalized diffusion coefficient is symmetrical.

Methods of nonequilibrium thermodynamics can also be applied to the integral relations. Determine the entropy production in a volume V_x of the generalized space. In the steady-state case, integration of the entropy production over the generalized volume can be reduced using the Ostrogradskii–Gauss theorem to integration over the hypersurface of the volume V_x. As a result, the expression for the total entropy production takes the form

$$\Delta s_t = \oint J_n^n \left(\ln\frac{\Phi}{\Phi_e}+1\right) d\Sigma, \tag{61}$$

where integration is performed over the hypersurface and J_n^n is the flux of nuclei normal to this surface.

Assuming small deviations of the system from equilibrium (supercritical nuclei are rarely removed from the system), the difference $1-\Phi(\mathbf{x})/\Phi_e(\mathbf{x})$ can also be considered small. Then, using principles of nonequilibrium thermodynamics, one can write the phenomenological equation

$$J_n^n(\mathbf{x}_\Sigma) = \oint \Lambda(\mathbf{x}_\Sigma, \mathbf{x}'_\Sigma)\left[1-\frac{\Phi(\mathbf{x}'_\Sigma)}{\Phi_e(\mathbf{x}'_\Sigma)}\right] d\Sigma', \tag{62}$$

where $\Lambda(\mathbf{x}_\Sigma, \mathbf{x}'_\Sigma)$ is a symmetrical operator

$$\Lambda(\mathbf{x}_\Sigma, \mathbf{x}'_\Sigma) = \Lambda(\mathbf{x}'_\Sigma, \mathbf{x}_\Sigma),$$

the Σ subscript at the variable x denotes that the corresponding expression is taken at the hypersurface. Clearly, for the steady state the total flux of nuclei

$$J_t^n = \oint J_n^n(\mathrm{x}_\Sigma) d\Sigma, \tag{63}$$

is a constant.

If the hypersurface is behing the saddle point in the space of the variables determining the state of nuclei, from Eqns (62) it follows that the flux of nuclei is proportional to $1-\Phi(\mathbf{x})/\Phi_e(\mathbf{x})$. Usually, this coefficient is set to be equal to unity because it is admitted that $\Phi(\mathbf{x})/\Phi_e(\mathbf{x}) = 0$ in the supercritical region. However, this is not always true. For instance, in the 1D case the nucleation rate is given by

$$J^n = J_{st}^n \left[1-\frac{\Phi(\mathbf{x}_{sc})}{\Phi_e(\mathbf{x}_{sc})}\right], \tag{64}$$

where $\mathbf{x}_{sc}$ is the a supercritical point in the nucleus size space. Note that in various theories of nucleation the expression in square brackets is usually ignored without any grounds.

From relation (64) it is seen that even for purely formal reasons the nucleation rate can be much lower than that predicted by the classical theory (J_{st}^n). Since the $\Phi(\mathbf{x})/\Phi_e(\mathbf{x})$ ratio cannot be evaluated experimentally, the nucleation rate in the classical theory is determined up to a constant. Experimental methods can significantly differ from one another in procedure for creation of supersaturation and removal of supercritical nuclei, so the value $1-\Phi(\mathbf{x})/\Phi_e(\mathbf{x})$, strictly speaking, can depend on the experimental conditions and vary over a wide range. This should be taken into account when comparing theoretical and experimental data.

Summing up, the approach to the determination of the entropy production in the nucleation proposed in Ref. 157 (see above) was in fact used in Ref. 167 in an attempt to describe the evolution of a nonequilibrium system with fluctuations.

2. Nonequilibrium thermodynamics of nucleation and growth of nuclei

The procedure for application of nonequilibrium thermodynamics to nucleation studies (see above) seems to be rather 'passive' because it is only used to establish the symmetry relations for kinetic coefficients. However, methods of nonequilibrium thermodynamics can also be used in the 'active' manner. For instance, it was shown [168] that nonequilibrium thermodynamics is suitable for deriving generalized equations describing not only nucleation, but also subsequent growth of nuclei. The approach is based on the expression for the entropy change (for simplicity, we will consider a 1D case)

$$\delta S = -\frac{1}{T}\int \mu(v,t)\delta\Phi(v,t)\mathrm{d}v, \tag{65}$$

where v is the volume of the nucleus, μ is the chemical potential, and $\Phi(v)$ is the size (volume) distribution function of the nuclei. From this the local entropy production and phenomenological equation are as follows:

$$\Delta S_{\mathrm{i}} = -\frac{1}{T} J \frac{\partial \mu}{\partial v}, \tag{66}$$

$$J = -L(v)\frac{\partial \mu}{\partial v},$$

where $L(v)$ is the Onsager coefficient.

Then, the chemical potential is represented as

$$\mu(v) = kT\ln[a_{\mathrm{c}}\Phi(v)],$$

where $a_{\mathrm{c}}(v)$ is the activity of nuclei;

$$a_{\mathrm{c}} = \exp\frac{\phi}{kT}, \tag{67}$$

and ϕ is some physical potential. The expression for the flux takes the form

$$J = -L(v)\frac{1}{\Phi}\left(kT\frac{\partial \Phi}{\partial v} + \Phi\frac{\partial \phi}{\partial v}\right). \tag{68}$$

Using the Onsager coefficient representation through the diffusion coefficient $D(v)$ in the generalized space

$$\frac{L(v)}{k\Phi} = D(v)v^{\alpha}, \tag{69}$$

and the expression

$$\phi = \frac{\phi_0}{v^{\varepsilon}} \tag{70}$$

for the potential ϕ, by appropriate choice of parameters one can obtain, *e.g.*, the equation for the flux

$$J = -\sigma v^{\chi}\Phi - Dv^{\varepsilon}\frac{\partial \Phi}{\partial v}, \tag{71}$$

which correctly describes nucleation and growth of crystals in melts.[169] The σ parameter is associates with the interface energy. Equations of type (70) for physical fluxes are also used [170] to describe vacancy formation processes by the nucleation mechanism and corresponding formation of voids.‡ Potentials[168] for the description of new phase formation can also be chosen in another manner.[171] This approach was extended to more complex situations.[172]

3. Nonequilibrium thermodynamics and morphological selection of crystal shape

The problem of formation of dendritic structures in the course of crystal growth has long been studied.[173] At present, the morphological stability of growing crystals is analyzed using the maximum entropy production principle.[174] The approach is essentially as follows. The entropy production is given by

$$\Delta S = -\frac{1}{T}J\nabla\mu,$$

where J is the flux of the crystallizing component and $\nabla\mu$ is the chemical potential gradient. The flux is related to the interface motion velocity by a linear relation $J \sim u_{\mathrm{s}}$. It is assumed that growth of both spherical particles and particles of more complex shape is possible. In the former case, the particle radius (R) changes with time in accordance with the diffusion law of growth (expressions for mixed kinetically controlled and diffusion-controlled growth can also be used). In the latter case, the model for spherical particles with distorted surface is used, *i.e.*, the particle radius is

$$r(\theta,\varphi,t) = R(t) + r_0(t)\cos(k_{\mathrm{p}}\varphi), \tag{72}$$

where k_{p} is the wave vector of perturbation, $r_0(t)$ is the perturbation amplitude and t is time.

One has to calculate the difference between the entropy productions corresponding to the growth of a spherical crystal and a crystal with distorted surface which depends on the wave vector k_{p} and the running radius R. At a particular value R_{b} of the radius of the spherical particle (it is also called the binodal radius), the growth of dendritic rather than spherical particles becomes more favourable from the standpoint of maximum entropy production. The expression for the binodal radius is [175]

$$R_{\mathrm{b}} = \frac{1}{2}\left(\Omega_{\mathrm{b}} + \sqrt{\Omega_{\mathrm{b}}^2 + \frac{4\alpha k_{\mathrm{p}}(2k_{\mathrm{p}}^2-1)}{2k_{\mathrm{p}}-1}}\right), \tag{73}$$

where

$$\Omega_{\mathrm{b}} = 1 - \frac{\alpha k_{\mathrm{p}}}{2k_{\mathrm{p}}-1} + \frac{2A_{\lambda}k_{\mathrm{p}}(k_{\mathrm{p}}^2-1)}{2k_{\mathrm{p}}-1}.$$

Here

$$\alpha = \frac{D}{\beta R_{\mathrm{c}}}$$

is the dimensionless parameter characterizing the growth regime (diffusion regime $\alpha \to 0$, kinetic regime $\alpha \to \infty$); D is the diffusion coefficient; β is the parameter determining transition from the kinetic to diffusion growth regime; R_{c} is the radius of the critical nucleus; and A_{λ} is the parameter characterizing the relative supersaturation in the system.

‡ The expression for the flux was also obtained [170] using methods of nonequilibrium thermodynamics.

A comparison of the data obtained using the maximum entropy production principle and by numerical solution of the equations nuclei growth from a supersaturated solution revealed good agreement between them.[175]

In particular, according to predictions based on the maximum entropy production principle, the number of growing new-phase structures with different morphologies should increase with the parameter α. Figure 5 presents the structures formed from spherical nuclei in the supersaturated solution at different instants.

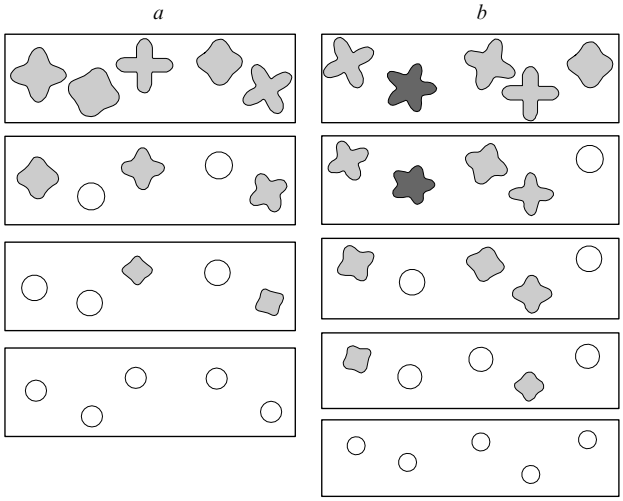


Figure 5. The evolution of nuclei in systems with different values of the supersaturation parameter α: 1 (*a*) and 100 (*b*).[179]

Note that selection of the structure morphologies also occurs during the growth of fractal systems.[176–178] A number of thermodynamic functions of fractal systems, such as the free energy, entropy and specific heat capacity were introduced long ago.[179–181] It is natural to expect that methods of nonequilibrium thermodynamics can be employed to describe the growth of fractal structures. They indeed were used by some authors who was based on the maximum entropy principle,[182, 183] according to which the system tends to adopt a configuration corresponding to the maximum entropy value. Here one can find an analogy with the maximum entropy production principle, although these approaches are not identical. Therefore, we leave the maximum entropy principle out of detailed consideration.

V. Nonequilibrium thermodynamics of the motion of colloidal particles

The first attempt to use thermodynamics of irreversible processes in studies of disperse systems was made[184] to establish a relation between electrophoresis and the Dorn effect. However, the approach appeared to be cumbersome and too complicated to be used for generalization to other nonequilibrium processes. A more convenient method[185] made it possible to apply the known phenomenological equations for discontinuous systems[3] to studies of thermophoresis of aerosol particles. More recently, it was used in studies of electrokinetic and diffusion phenomena.[90]

Phenomenological equations of nonequilibrium thermodynamics were derived not only for ensembles,[184, 185] but also for single particles.[11, 13, 186, 187] In this case, there is no need for integral phenomenological relations for discontinuous systems because local phenomenological equations establishing new relations between various nonequilibrium effects are used instead. In particular, this approach made it possible to predict[12] and then experimentally detect[188] the effect of thermal polarization of bodies in a rarefied gas flow. Detailed theory of the effect was analyzed.[189] Recently, this effect again has attracted the attention of researchers.[190–193]

1. The dynamics of particles in a homogeneous medium

Consider nonequilibrium thermodynamics of motion of single particles in a homogeneous fluid using the approach proposed in Ref. 194. Let us construct the corresponding phenomenological equations. This is not a challenge. The product of the force acting on the particle by the particle velocity gives the energy dissipation rate which can be associated with the entropy production. A real situation is more complicated because numerous issues appear. We will not dwell on them, but it should be noted that, *e.g.*, taking into account the slip of the fluid on the particle surface poses the problem how to take account the related dissipation energy. Therefore, in the text below we will use different approaches to the determination of the entropy production. They are convenient (if not the sole) in considering the dynamics of single colloidal particles.

Emphasize that we study a system characterized by a small deviation from equilibrium, when one can use linear relations between thermodynamic fluxes and forces; fluctuation effects responsible for the motion of the thermodynamic system towards a decrease in entropy are ignored. These effects have been a subject of recent interest including experiments with colloidal systems.[195–200] Note that taking account of nonlinear and fluctuation effects leads to violation of some fundamental relations; *e.g.*, the relation between the diffusion coefficient and the particle mobility described by the known Einstein relation is more complicated.[195]

A single colloidal particle placed in a homogeneous fluid executes Brownian motion. The particle velocities are distributed by the Maxwell law,[201] *i.e.*, the probability for a particle to have the velocity $\mathbf{U}$ is

$$P_{\mathrm{p}} \propto \exp\left(-\frac{M_{\mathrm{p}}\mathbf{U}^2}{2kT}\right), \tag{74}$$

where M_{p} is the particle mass. However, Brownian motion can be treated as a fluctuation process and the probability for a particle to be in the 'nonequilibrium' state characterized by the velocity $\mathbf{U}$ is determined by the corresponding change in the entropy δS on fluctuation; therefore, one can write

$$P_{\mathrm{p}} \propto \exp\left(-\frac{M_{\mathrm{p}}\mathbf{U}^2}{2kT}\right) = \exp\frac{\delta S}{k}. \tag{75}$$

As usually in constructing thermodynamics of irreversible processes,[3, 201] assume that the macroscopic velocity of the particle acquired as a result of a fluctuation decreases under the action of viscous friction forces. Then, the entropy production in this process can be written as follows:

$$\frac{\mathrm{d}(\delta S)}{\mathrm{d}t} = -\frac{M_\mathrm{p}\mathbf{U}}{T}\frac{\mathrm{d}\mathbf{U}}{\mathrm{d}t} = -\frac{\mathbf{F}_\mathrm{p}\,\mathbf{U}}{T}, \tag{76}$$

where $\mathbf{F}_\mathrm{p}$ is the viscous friction force acting on the particle moving at the velocity $\mathbf{U}$.

In accordance with the general principles of nonequilibrium thermodynamics, phenomenological equations can be written in the form

$$\mathbf{U} = -\mathbf{Z}\,\mathbf{F}_\mathrm{p}, \tag{77}$$

where the mobility tensor $\mathbf{Z}$ should be symmetrical, *i.e.*

$$Z_{ij} = Z_{ji}. \tag{78}$$

When considering a steady motion of the particle under the action of external force, the sign in equality (77) should be changed (friction force is directed opposite to the external force).

In fact, equalities (78) represent the Onsager symmetry relations for the mobility tensor. Note that a traditional proof of the symmetry of the mobility tensor [202] is nontrivial. In this review, it is substantiated based on the general principles of thermodynamics of irreversible processes.

Methods of nonequilibrium thermodynamics allow rotational motion of the particle to be taken into account with ease. Indeed, if the particle is characterized by the tensor of the moment of inertia $\mathbf{I}_\mathrm{p}$, the probability for a particle to have the velocity $\mathbf{U}$ and the angular velocity Ω is

$$w \propto \exp\left(-\frac{M_\mathrm{p}\mathbf{U}^2}{2kT} - \frac{\Omega\,\mathbf{I}_\mathrm{p}\,\Omega}{2kT}\right) \propto \exp\frac{\delta S}{k}. \tag{79}$$

If the velocities of translational and rotational motion of the particle acquired as a result of fluctuation relax involving viscous friction forces, the equation for the entropy production is

$$\frac{\mathrm{d}(\delta S)}{\mathrm{d}t} = -\frac{M_\mathrm{p}\mathbf{U}}{T}\frac{\mathrm{d}\mathbf{U}}{\mathrm{d}t} - \frac{\Omega}{T}\mathbf{I}_\mathrm{p}\frac{\mathrm{d}\Omega}{\mathrm{d}t} = -\frac{\mathbf{F}_\mathrm{p}\,\mathbf{U}}{T} - \frac{\Omega\,\mathbf{T}_\mathrm{p}}{T}, \tag{80}$$

where $\mathbf{T}_\mathrm{p}$ is the viscous torque exerted on the particle, and the symmetry of the tensor of the moment of inertia is taken into account.

The phenomenological equations of nonequilibrium thermodynamics are as follows:

$$\mathbf{U} = -\mathbf{Z}\,\mathbf{F}_\mathrm{p} - \mathbf{Y}\,\mathbf{T}_\mathrm{p}, \tag{81}$$

$$\Omega = -\mathbf{Y}^T\mathbf{F}_\mathrm{p} - \mathbf{G}\,\mathbf{T}_\mathrm{p},$$

where the rotational mobility tensor $\mathbf{G}$ is also symmetrical,

$$G_{ij} = G_{ji}, \tag{82}$$

and the symmetry of other coefficients is taken into account by introducing mutually transposed matrices $\mathbf{Y}$ and $\mathbf{Y}^T$.

When considering a steady motion and rotation under the action of external force and torque, the signs in Eqns (81) should be reversed.

Thus, within the framework of nonequilibrium thermodynamics one can readily prove the symmetry of the translational and rotational mobility tensors and to establish relations between the tensors relating the external force and torque to the angular velocity and velocity of translational motion of the particle, respectively.

However, this approach is unsuitable in studies of the motion of particles in inhomogeneous media because it is difficult to take into account the influence of particles on heat transfer, diffusion, *etc.* In this case, it is more appropriate to use another method of deriving equations of nonequilibrium thermodynamics for single particles.[11, 12, 186, 187]

2. Nonequilibrium thermodynamics of particles in inhomogeneous media

Consider motion of a particle of arbitrary shape in a multicomponent mixture with constant external temperature gradient ∇T, concentration gradient ∇c_i and the electrical potential gradient $\mathbf{E}$. Let the particle move at a constant velocity $\mathbf{U}_\infty$ relative to the system associated with the mass-average velocity of the mixture under the action of external force $\mathbf{F}$. Compute the entropy production ΔS_p due to the presence of an 'alien' particle in the inhomogeneous medium. For the steady-state case, the entropy balance equation valid for both the fluid and particle can be written as [3]

$$\mathrm{div}(\mathbf{u}s + \mathbf{J}^S) = \Delta S_\mathrm{l}. \tag{83}$$

Here $\mathbf{u}$ is the mass-average velocity of the mixture, s is the entropy density of the mixture, $\mathbf{J}^S$ is the entropy flux density in the system of coordinates related to the centre of mass of the moving fluid and ΔS_l is the local entropy production density.

The form of the equations for local entropy production is unknown. We also cannot use the equation for the local entropy production which was obtained for unbounded media (see, *e.g.*, Ref. 3). Transport phenomena within boundary layers should be described using relevant expressions for the entropy production density (see Section III). The local entropy production in inhomogeneous gases differs from the expression presented in monograph [3] and for unbounded media.[21, 22] However, an advantage of the approach considered in this review consists in that there is no need for the particular form of the local entropy production.

Integrate Eqn (83) over the volume containing the particle. On the right side, we thus get the total entropy production ΔS_V. The left side will be transformed following the Ostrogradskii–Gauss theorem to the integral over the boundary surface. It is convenient to use a cylinder of a rather large radius (Fig. 6), with the centre of symmetry at the centre of mass of the particle, and the axis directed along external temperature and concentration gradients (z axis). This will be our boundary surface. If the radius of the cylinder much exceeds the cylinder height, integration over the surface of the cylinder is reduced to integration over the end surfaces, *i.e.*

$$\Delta S_V = 2\pi\int_0^\infty (u_z s + J_z^S)l\,\mathrm{d}l\Big|_{z=-H}^{z=H}. \tag{84}$$

Two important aspects should be mentioned. First, expression (84) includes only the entropy flux in the inhomogeneous medium. It follows that, although the structures

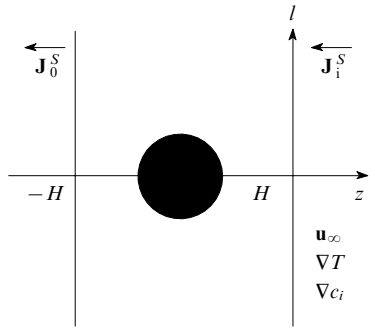


Figure 6. Schematic for calculations of the entropy production due to the presence of a particle in a nonuniform medium.

of the flux and entropy production near the particle surface are unknown, the entropy production due to the presence of the particle can be calculated using the asymptotics of the entropy flux in the inhomogeneous medium at a long distance from the particle. Second, if the lateral surfaces of the cylinder are at long distance from the particle, one can use the purely hydrodynamic expression for the entropy flux because various corrections and the boundary effects [21, 22] will contribute negligibly and can thus be ignored.

The total entropy flux in the mixture can be written as [3]

$$J_{lz}^S = u_z s + J_z^S = \frac{u_r(p\delta_{rz} - \Pi_{rz})}{T_0} + \frac{q_z}{T} + \tag{85}$$

$$+ \sum_{i=1}^{N} \frac{J_{iz}(\mu_i - \mu_N)}{T_0} - \frac{I_z \Psi}{T_0},$$

where $\mathbf{q}$ is the heat flux density, μ_i is the chemical potential of the ith component, N is the number of components,

$$\mathbf{J}_i = \rho_i(\mathbf{u}_i - \mathbf{u})$$

is the diffusion flux density of the ith component, ρ_i is the density of the ith component, $\mathbf{u}_i$ is the average velocity of the ith component, $\mathbf{I}$ is the electric current density and Ψ is the electrostatic potential.

The temperature, pressure and concentration distributions far from the particle can be determined using general solutions to the steady-state Navier–Stokes equations for the velocity and pressure and the Laplace equations for the temperature and concentrations.[202] At long distances from the particle (distance from the centre $r \to \infty$), these solutions are as follows:

$$p = p_0 + \frac{\mathbf{f}_\mathrm{p}\,\mathbf{r}}{r^3}, \tag{86}$$

$$T = T_0 + \frac{\mathbf{A}\,\mathbf{r}}{r^3} + \nabla T\,\mathbf{r},$$

$$c_j = c_{j0} + \frac{\mathbf{B}_j\,\mathbf{r}}{r^3} + \nabla c_j\,\mathbf{r},$$

$$\Psi = \Psi_0 + \frac{\mathbf{d}\,\mathbf{r}}{r^3} + \mathbf{E}\,\mathbf{r},$$

where $\mathbf{r}$ is the vector of spatial coordinates; $\mathbf{A}$ and $\mathbf{B}_j$ are the thermal and concentration dipole moments of the particle, respectively; and $\mathbf{d}$ is the electrostatic dipole moment. The quantity $\mathbf{f}_\mathrm{p}$ is related to the force acting on the particle [202]

$$\mathbf{F} = -4\pi\mathbf{f}_\mathrm{p}. \tag{87}$$

Using the distributions (86), the entropy production (84) can be calculated with ease and it is possible to select the vector fluxes and forces corresponding to the colloidal particle. Since the overall expression [187] for the entropy production is cumbersome, we will restrict ourselves to consideration of simplified pair equations of nonequilibrium thermodynamics, which describe the motion of colloidal particles in the temperature gradient, concentration gradient, *etc*. fields as well as the cross effects.

a. Thermophoresis and thermal polarization

Consider a one-component non-conducting medium with a nonzero temperature gradient. Having written the entropy flux (85) appropriately, the expression for entropy production due to the presence of a particle is as follows:

$$\Delta S_\mathrm{p} = \frac{\mathbf{F}\,\mathbf{U}_\infty}{T_0} + \frac{4\pi\lambda_\mathrm{e}\mathbf{A}\,\nabla T}{T_0}. \tag{88}$$

The phenomenological equations following from expression (88) have the form

$$\mathbf{U}_\infty = \lambda_{00}\mathbf{F} + \lambda_{0T}\nabla T, \tag{89}$$

$$\frac{4\pi\lambda_\mathrm{e}\mathbf{A}}{T_0} = \lambda_{T0}\mathbf{F} + \lambda_{TT}\nabla T,$$

where λ_e is the thermal conductivity of the medium.

In the case of an aspherical particle, the equations have the same form, but the kinetic coefficients are tensor quantities. The Onsager symmetry relations are the same as the coefficients in Eqns (81).

The coefficient λ_{00} defines the velocity of the particle motion in the fluid under the action of an external force. In fact, the same coefficient (its reciprocal) appears in Eqn (77). For a spherical particle of radius R, the λ_{00} coefficient determined from the Stokes law is

$$\lambda_{00} = \frac{1}{6\pi\eta_\mathrm{f}R}.$$

The λ_{0T} coefficient relates the particle velocity to the temperature gradient. This coefficient depends strongly on the nature of the medium, on the particle size and on the physicochemical characteristics of particles. The motion of a particle as a response to the force of the temperature gradient is called thermophoresis. This effect has been studied for more than a century,[12] but it still remains a subject of considerable attention of researchers.[203]

The λ_{TT} coefficient determining the thermal dipole moment of the particle placed in the medium with a nonzero temperature gradient is well known for particles whose size much exceeds the thickness of the boundary layers. Taking into account the continuity of the temperature and heat fluxes at the surface of a spherical particle (see, *e.g.*, monograph [57]), one gets

$$\lambda_{TT} = 4\pi\frac{\lambda_\mathrm{e} - \lambda_\mathrm{i}}{\lambda_\mathrm{i} + 2\lambda_\mathrm{e}}\frac{R^3}{T_0}, \tag{90}$$

where λ_i is the thermal conductivity of the particle.

The effect governed by the λ_{T0} coefficient specifying the thermal dipole moment of the particle moving under the action of external force in homogeneous medium is less known. It was predicted theoretically [12] and observed experimentally in a study of the motion of particles in gases.[188] The appearance of the thermal dipole moment is due to the presence of isothermal heat fluxes in the boundary layers. In the case of gases, there exists also the bulk isothermal heat flux proportional to the pressure gradient (for more detail, see Ref. 21). Since the flow of a gas around a particle is accompanied by the appearance of a nonuniform pressure field, isothermal heat fluxes also appear.

b. Diffusiophoresis and diffusion polarization

If a binary mixture of fluids flows around a particle (solid particle, a droplet, a bubble) at constant temperature with no electrical effects, the entropy production and phenomenological equations have the form

$$\Delta S_{\mathrm{p}} = \frac{\mathbf{F}\,\mathbf{U}_{\infty}}{T_0} + \frac{4\pi \mathbf{B}_1\, D_{12}(\partial\mu_1/\partial c_1)\nabla c_1}{c_2 T_0}, \tag{91}$$

$$\mathbf{U}_{\infty} = \lambda_{00}\mathbf{F} + \lambda_{01}\nabla c_1\,, \tag{92a}$$

$$\frac{4\pi D_{12}\mathbf{B}_1(\partial\mu_1/\partial c_1)}{c_2} = \lambda_{10}\mathbf{F} + \lambda_{11}\nabla c_1. \tag{92b}$$

Here c_1 and c_2 are the respective component concentrations. We also used the relation $D_{11} = -D_{12}$ taken from Ref. 3; it should be valid for the kinetic coefficients present in the phenomenological diffusion transport equations. At low concentrations, as well as for gases or ideal mixtures one has

$$\frac{\partial\mu}{\partial c_1} = \frac{kT}{c_1}.$$

Equation (92a) describes the motion of a particle in a binary mixture under the action of an external force and a concentration gradient. The motion of particles under the action of concentration gradient, or diffusiophoresis, is a well-known effect [85] used in practice. The velocity of diffusiophoresis is determined by solving the hydrodynamic equations with the diffusion slip condition (46) for particle surface. The slip coefficient depends on the nature of the moving medium. For gases, it was for the first time calculated by Kramers and Kistemaker,[204] who obtained the following expression for the diffusion slip velocity:

$$u_{\mathrm{ds}} = \frac{\sqrt{m_1} - \sqrt{m_2}}{c_1\sqrt{m_1} + c_2\sqrt{m_2}}\, D_{12}\nabla c_1 = K_{\mathrm{ds}} D_{12}\nabla c_1. \tag{93}$$

More recently, numerous attempts to calculate this coefficient for various models were undertaken.[22] It was found that the coefficient depends on not only the mass difference, but also on the differences between the diameters of molecules (d_i) and on their accommodation coefficients (b_i). An approximate expression has the form [22]

$$K_{\mathrm{ds}} = 1.07\,\frac{m_1 - m_2}{m_1 + m_2} - 0.75\,\frac{d_1 - d_2}{d_1 + d_2} - 2.0\,\frac{b_1 - b_2}{b_1 + b_2}. \tag{94}$$

The diffusiophoresis velocity of particles whose size exceeds the thickness of the boundary layers is [86]

$$\mathbf{U}_{\mathrm{df}} = -K_{\mathrm{ds}} D_{12}\nabla c_1. \tag{95}$$

If the particle size is much smaller than the mean free path, the diffusiophoresis velocity is given by

$$\mathbf{U}_{\mathrm{df}} = -\frac{\sqrt{m_1} - \sqrt{m_2}}{c_1\sqrt{m_1} + c_2\sqrt{m_2}}\, D_{12}\nabla c_1. \tag{96}$$

Noteworthy is the term with the combination of masses in relations (93) and (96). This accidental coincidence is due to the approximate character of computations by Kramers and Kistemaker and expression (96). Actually, the diffusiophoresis velocity of small particles is noticeably different from the diffusion slip velocity.

The diffusiophoresis velocity for intermediate values of the Knudsen number was also calculated.[205] Calculations and experiments [206] showed that the diffusiophoresis velocity depends slightly on the ratio of the particle size to the mean free path of molecules; therefore, we leave this dependence out of consideration.

The expression for the diffusiophoresis velocity of particles suspended in a binary nonelectrolyte mixture is [85]

$$\mathbf{U}_{\mathrm{df}} = \frac{kT}{\eta}\,\xi\nabla c_1\,, \tag{97}$$

$$\xi = \int_0^{\infty} \frac{c(x) - c_1}{c_1}\, x dx,$$

where c_1 is the concentration in the bulk solution and $c(x)$ is the concentration within the boundary layer.

The diffusiophoresis velocity of a particle in electrolyte is expressed in a more complicated manner because in this case, electrostatic interactions play some role.[90] An example of diffusiophoresis velocity calculations for electrolytes with nonuniform charge distribution is available in the literature.[207] For a thin electrical double layer, symmetrical electrolyte and a uniformly charged sphere one has [208]

$$\mathbf{U}_{\mathrm{df}} = \frac{\varepsilon_0\zeta}{4\pi}\,\frac{kT}{\eta z_i \mathrm{e}}\,\frac{\nabla c_0}{c_0}\left\{\frac{D_2 - D_1}{D_1 + D_2} + \frac{4kT}{Z\mathrm{e}\zeta}\ln\left[\mathrm{ch}\left(\frac{z_i \mathrm{e}\zeta}{4kT}\right)\right]\right\}, \tag{98}$$

where z_i is the ion charge; Z is the ion valence; e is the proton charge; ζ is the zeta-potential of the particle surface; D_1 and D_2 are the diffusion coefficients of anions and cations, respectively; c_0 is the electrolyte concentration; and ε_0 is the dielectric constant of the electrolyte. The authors of Ref. 208 also presented the expression for the diffusiophoresis velocity of particles in more complex situations and calculated the diffusiophoresis velocity of porous particles.[209]

Diffusiophoresis is traditionally used for coating. At present, attempts are made to apply it in microfluidics for control of colloidal particles. Schemes of concentration or 'dilution' of particles in microchannels are shown in Fig. 7. Studies on the design of nanodevices whose operation is based on the diffusiophoretic effect were reported. For instance, it was shown that nanotube-based diffusiophoretic 'nanomotors' can move at a velocity of 0.5 m s^{-1} while

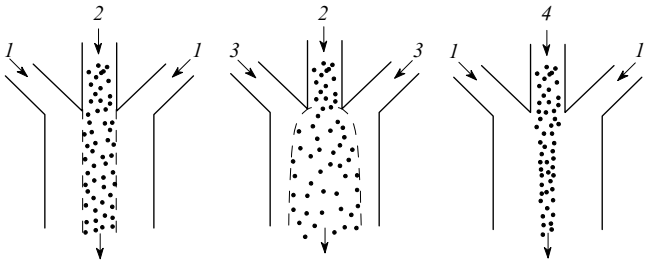


Figure 7. Concentration and dilution of a colloidal solution by diffusiophoresis of particles.
Dispersion medium (*1*), colloidal solution (*2*), medium + salt dispersion (*3*) and colloidal solution + salt (*4*).

nanotube-based nanorotors can have angular velocities to 30 rps.[210]

Diffusiophoresis also plays an important role in traditional areas of colloidal chemistry. For instance, it may have a strong effect on the motion of particles in channels in filtration of colloidal particles through thin-pore membranes.[211–213] Chen and Keh[211] studied the motion of a single particle in a flat channel, whereas the other two studies are devoted to diffusiophoresis in a cylindrical capillary. It is also believed that diffusiophoresis plays a significant role in scavenging processes.[214–216]

The λ_{11} coefficient in Eqn (92b) characterizes the concentration field appeared around an alien particle placed in a diffusing binary mixture. This coefficient is often encountered in the solution of diffusion problems. The λ_{10} coefficient determining the diffusion polarization of particles is less predictable because it appears only in considering the surface phenomena. The effect described by this coefficient influences many processes including electrokinetic and membrane ones and is well known.

In simulating a porous body or a membrane by an ensemble of particles (so-called cell model), the diffusion polarization particles will govern the reverse osmosis effect.[90]

c. Electrophoresis and the Dorn effect

Abstracting from the complex composition of electrolyte solutions, consider the purely electrokinetic effects. To this end, we leave only the terms determining the motion of the particle relative to the entire fluid and the electrokinetic phenomena in the expression for the flux (85). The entropy production and phenomenological equations take the form

$$\Delta S_{\mathrm{p}} = \frac{\mathbf{F}\,\mathbf{U}_{\infty}}{T_0} - \frac{4\pi\kappa\mathbf{d}\,\mathbf{E}}{T_0}, \tag{99}$$

$$\mathbf{U}_{\infty} = \lambda_{00}\mathbf{F} + \lambda_{0E}\mathbf{E} \tag{100}$$

$$-4\pi\kappa\mathbf{d} = \lambda_{E0}\mathbf{F} + \lambda_{EE}\mathbf{E},$$

where κ is the conductivity of the electrolyte.

Clearly, the λ_{0E} coefficient describes the velocity of electrophoresis. The classical relationship for the electrophoresis velocity of colloidal particles of the size R is as follows[90]:

$$U_{\mathrm{ef}} = \frac{\varepsilon_0\zeta\,\mathbf{E}}{6\pi\eta_{\mathrm{f}}}\left\{1 + \frac{\kappa-\kappa_{\mathrm{p}}}{2\kappa+\kappa_{\mathrm{p}}}\left[2f\left(\frac{R}{r_{\mathrm{D}}}\right)-2\right]\right\}, \tag{101}$$

where κ_{p} is the conductivity of the particle, r_{D} is the Debye radius and the function $f(R/r_{\mathrm{D}})$ tends to unity at $R/r_{\mathrm{D}} \ll 1$ and to 3/2 at $R/r_{\mathrm{D}} \gg 1$.

At $R/r_{\mathrm{D}} \gg 1$, the electrophoresis velocity can be found from the solution to the hydrodynamic problem provided slip on the particle surface:

$$u_{\mathrm{es}} = -\frac{\varepsilon_0\zeta\,\mathbf{E}}{4\pi\eta_{\mathrm{f}}}. \tag{102}$$

For an arbitrary ratio of the mean particle size to the Debye radius, the hydrodynamic problem is solved immediately for the boundary layer. Expression (101) is obtained assuming the stick boundary condition at the particle surface. These calculations usually work for the so-called primitive model for electrolyte which predicts a simple relation between the electrokinetic potential and the structure of the electrical double layer. Such models are tested using the results of electrophoresis velocity measurements.[217]

Real situations are much more complicated because the primitive models for hydrophobic surfaces also include an additional parameter associated with the hydrophobic slip.[218] In particular, the electroosmotic slip velocity becomes equal to

$$u_{\mathrm{es}} = -\frac{\varepsilon_0\zeta\,\mathbf{E}}{4\pi\eta_{\mathrm{f}}}\left(1 + \frac{b_h}{r_{\mathrm{D}}}\right). \tag{103}$$

Experiments and molecular simulation[219–221] showed that hydrophobic slip significantly influences the electrokinetic phenomena if electrolytes flow in porous bodies. Hydrophobic slip is also taken into account in the consideration of thermophoretic (also affected by the electroosmotic slip) and electrophoretic mobility of particles.[222, 223] If the Debye radius exceeds the particle size, the slip effect causes the electrophoresis velocity to increase because the viscous friction force decreases.[223]

The electrokinetic properties of particles and capillary-porous systems are usually 'tuned' by adsorption of surfactants or polyelectrolytes on their surfaces.[224] Colloidal particles can also be deposited on the surface.[225] The advantage of the last-mentioned method consists in the possibility of fine and controllable regulation of the electrokinetic parameters of the surface, because usually the particles deposited have well-characterized electrokinetic parameters. The electrokinetic potential can be varied by periodically varying the number of deposited layers of the particles bearing different charges; here, the shape of the modified surface is of no concern.[225]

Expression (97) was obtained assuming that external electric field does not influence the electrokinetic potential ζ. In fact, this means that the external field has no effect on the surface charge. Actually, the particle is always characterized by some extent of polarization; therefore, the external field always affects the electrokinetic potential. The role of polarization effects becomes much more important in considering the fluid flow in microchannels.[226–233] The electrophoresis velocity of spherical particles whose dielectric constant is higher than that of the dispersion medium (strong polarization conditions) was determined.[234] The dependence of particle mobility on the dielectric constant ratio of the particles and the dispersion medium and on the electric field magnitude was established for a thin electrical

double layer. It was shown that an increase in the polarizability of particles causes an n-fold decrease in their mobility. An increase in the field strength may lead to mobility reduction by some orders of magnitude.

The λ_{EE} coefficient characterizes the conventional polarizability of particles, *i.e.*, it is related to the dipole moment induced on the particle by the external field. It can be determined with ease from the solution of electrostatic problem for conductors

$$\lambda_{EE} = 4\pi \frac{\kappa - \kappa_{\rm p}}{\kappa_{\rm p} + 2\kappa} \kappa R^3. \tag{104}$$

The λ_{E0} coefficient is also well known, namely, it specifies magnitude of the dipole moment induced on the particle moving in a homogeneous electrolyte. The appearance of a dipole moment on the moving particle provided no external field is called the Dorn effect.[90] It is related through the Onsager symmetry relations to electrophoresis of particles and other phenomena observed in colloidal systems. For instance, the Dorn effect determines the so-called sedimentation potential, *viz.*, sedimentation of an ensemble (layer) of particles produces a potential difference between the upper and lower boundaries of the layer due to the appearance of a dipole moment on each particle (strictly speaking, this is just the way of constructing nonequilibrium thermodynamics of colloidal particles in the classical study [184]). It is also related to the flow potential in a porous body modelled by an ensemble of particles, namely, the flow potential appears as a consequence of induction of the dipole moment on each particle (here, on the contrary, the fluid moves through a layer of particles).

This approach to the determination of the flow potential was thoroughly analyzed, in particular, in a monograph.[90] Examples of related calculations for a concentrated dispersion of colloidal particles are available in Refs 235–237 whose author used the cell model and confirmed fulfillment of the Onsager symmetry relations for the coefficients characterizing the electrophoretic mobility and sedimentation potential. Note that the cell model is to some extent similar to the approach described above, but it unavoidably uses (in principle, undetermined) boundary conditions at the external surface of the cell. The uncertainty can be eliminated by using the pattern of constructing equations of nonequilibrium thermodynamics of colloidal particles (see above). The cell model still has an advantage, namely, it allows the velocity of electrophoretic motion in concentrated dispersions to be determined, which was actually done in Refs 235–237.

A study [238] on the effect of hydrophobic slip on the dipole moment induced on the moving particle showed that the slip changes the dipole moment magnitude in a complex manner, namely, at large Debye radii, the dipole moment increases as the slip coefficient increases; for thin double layers, the slip causes the dipole moment to increase at low and moderate ζ-potentials and has no effect at high ζ-potentials.

Pairs of equations (89), (92) and (100) define the 'main' cross effects related to the motion of colloidal particles in inhomogeneous media. In some cases, these cross phenomena can be complicated by other effects. In particular, the diffusion polarization is important when considering electrophoresis and the Dorn effect, while electric polarization of particles contributes largely to considering diffusiophoresis in electrolytes. Electrical phenomena are also observed in the presence of temperature gradient (thermoelectricity). For this reason, the pairs of equations mentioned above can be treated as particular cases of a more general system; its form is available in, *e.g.*, the monograph.[86]

Like diffusiophoresis, electrophoresis is widely used in microfluidics [239] and for separation of particles and macromolecules, creation of electrochemical sediments to stimulate the flow of fluids and dispersions in thin channels, sensors and fuel cells.[240] Therefore, the number of studies on the electrokinetic phenomena in increasingly more complicated systems also increases.[241–244]

3. Nonequilibrium thermodynamics of colloidal particles in the presence of photon gas

Now we will dwell in some more detail on yet another pair of phenomenological equations describing the dynamics of colloidal particles under nonequilibrium conditions. The case in point is photophoresis of particles and the cross effect. Photophoresis is the motion of particles under the action of light. Recently, progress in microfluidics gave an impetus to increasing interest in studies of the motion of bubbles in fluids under the action of laser radiation.[245] An experimental implementation of a Stirling engine with 2.94-μm melamine colloidal particle suspended in aqueous solution and periodically heated by laser radiation as the working substance was reported.[246] Some authors also describe the propagation of electromagnetic radiation in inhomogeneous media within the framework of thermodynamics of nonequilibrium processes.[247–249] Taking into account a high heuristic level of nonequilibrium thermodynamics, it is interesting to present the phenomenological equations for the motion particles and bubbles in the electromagnetic radiation field.[250]

Our starting point will be the following expression for the photon gas entropy density:[104]

$$S_{\rm ph} = k \sum_g \int \left[(N_k + 1) \ln(N_k + 1) - N_k \ln N_k \right] \frac{{\rm d}\mathbf{k}_{\rm ph}}{(2\pi)^3}, \tag{105}$$

where summation is performed over photon polarizations and integration is carried over the wave vector $\mathbf{k}_{\rm ph}$,

$$\mathbf{k}_{\rm ph} = \frac{\omega}{c},$$

ω is the electromagnetic radiation frequency, c is the speed of light, N_k is the number of photons with a given polarization and wave vector.

In the following, the photon polarization will not be specified explicitly. The equilibrium photon concentration is given by

$$N_{0k} = \frac{1}{\exp(\hbar\omega/kT) - 1}, \tag{106}$$

where $\hbar$ is the Planck constant.

The intensity of radiation is simply related to the number of photons N_k:

$$I_k = \frac{\hbar\omega^3}{2\pi^2 c^2} N_k. \tag{107}$$

The entropy flux of a photon gas is

$$\mathbf{J}^S = k\int \mathbf{c}\left[(N_k+1)\ln(N_k+1) - N_k\ln N_k\right]\mathrm{d}\mathbf{\Omega}_{\mathrm{ph}}\,, \tag{108}$$

where integration is performed over the solid angle, and for nonequilibrium photon gas one has

$$N_k = N_{0k}(1+\varphi_k), \tag{109}$$

φ_k is the correction to the equilibrium distribution. Having expanded the entropy flux in a series with respect to φ_k, in the linear approximation with respect to φ_k one gets:

$$\mathbf{J}^S = k\int \mathbf{c}N_{0k}\varphi_k \ln\left(\frac{N_{0k}+1}{N_{0k}}\right)\mathrm{d}\mathbf{\Omega}_{\mathrm{ph}}\,. \tag{110}$$

Consider a situation corresponding to photophoretic motion of a colloidal particle. Assume a colloidal particle of arbitrary shape placed in a homogeneous fluid flow in which directed transfer of photons along a specified direction occurs. One should determine the entropy production due to the presence of an alien particle in this inhomogeneous system.

As above, we will calculate the difference between the entropy fluxes through two planes between which the particle is localized. In calculating the flux and field N_{0k} we again restrict ourselves to the dipole approximation for the radiation field in the vicinity of the particle

$$N_{0k} = N^0_{0k} + \frac{\mathbf{P}\,\mathbf{r}}{r^3}\,, \tag{111}$$

where N^0_{0k} is the photon field in the absence of the particle, $\mathbf{P}$ is the corresponding coefficient in the photon field distribution; here, we ignore the possibility for the particle to have a higher temperature than that of the gas (this situation was taken into account in Ref. 250). For the entropy production one gets

$$\Delta S_{\mathrm{ph}} = \frac{\mathbf{F}\,\mathbf{U}_\infty}{T_0} + \frac{4\pi k\mathbf{P}\,\mathbf{J}_{0N}}{N_{0k}(N_{0k}+1)}\,, \tag{112}$$

where $\mathbf{J}_{0N}$ is the uniform photon flux in the absence of the particle.

The phenomenological equations are quite obvious:

$$\mathbf{U}_\infty = \lambda_{00}\mathbf{F} + \lambda_{0f}\frac{\mathbf{J}_{0N}}{N_{0k}(N_{0k}+1)}\,, \tag{113}$$

$$4\pi kT\,\mathbf{P} = \lambda_{f0}\mathbf{F} + L_{ff}\frac{\mathbf{J}_{0N}}{N_{0k}(N_{0k}+1)}.$$

The kinetic coefficients should fulfill the Onsager symmetry relations $\lambda_{0f} = \lambda_{f0}$.

Consider the simplest case for a photophoretic motion of a spherical particle, namely, a black body in a transparent medium. In this case, for the photophoresis velocity one has [250]

$$\mathbf{U}_{\mathrm{ph}} = \frac{1}{3}K_{\mathrm{ts}}\frac{\eta_{\mathrm{f}}}{\rho T_0}\frac{\hbar\omega\mathbf{J}_{0N}}{\lambda_{\mathrm{i}}+2\lambda_{\mathrm{e}}}\,, \tag{114}$$

where ρ is the particle density and λ_{i} and λ_{e} are the thermal conductivities of the particle and the environment, respectively.

From Eqn (114) one gets the expression for the λ_{0f} kinetic coefficient:

$$\lambda_{0f} = \frac{1}{3}K_{\mathrm{ts}}\frac{\eta_{\mathrm{f}}}{\rho T_0}\frac{\hbar\omega N_{0k}(N_{0k}+1)}{\lambda_{\mathrm{i}}+2\lambda_{\mathrm{e}}}\,. \tag{115}$$

To determine the λ_{f0} coefficient, one should consider the motion of a spherical particle in homogeneous medium under the action of an external force. In the vicinity of the particle moving in the homogeneous medium, a temperature field (thermal polarization) appears due to isothermal heat fluxes caused by the pressure gradients and boundary effects, *i.e.*, the particle acquires thermal dipole moment. A black body characterized by a nonuniform temperature distribution will emit anisotropic photon radiation, *i.e.*, a specific kind of a dipole moment of the radiation intensity distribution by the particle surface appears. The number of photons emitted from the unit surface particle per unit solid angle is:

$$J_{\mathrm{ph}} = \frac{c}{4\pi}\frac{1}{\exp[\hbar\omega/kT_i(\mathbf{R})]-1} \approx \tag{116}$$

$$\approx -\frac{c}{4\pi}\frac{\hbar\omega\exp(\hbar\omega/kT_0)}{[\exp(\hbar\omega/kT_0)-1]^2}\frac{K_{\mathrm{ts}}\eta_f}{2\pi R^3(\lambda_{\mathrm{i}}+2\lambda_{\mathrm{e}})}\frac{\mathbf{F}\,\mathbf{R}}{kT_0^2}\,,$$

where $\mathbf{R}$ is the radius-vector of a point on the particle surface.

The photon flux at a given point distant from the particle can be calculated with ease. The photon concentration at the given point is determined from the photon flux. The photon field (photons are emitted from the particle surface) obeys the distribution (111) and one has

$$\mathbf{P} = \frac{1}{3}\frac{1}{4\pi}N_{0k}(N_{0k}+1)\hbar\omega\frac{K_{\mathrm{ts}}}{kT_0^2}\frac{\eta_{\mathrm{f}}}{\rho}\frac{F}{\lambda_{\mathrm{i}}+2\lambda_{\mathrm{e}}}\,. \tag{117}$$

From this one gets expression (115) for the λ_{f0} coefficient, *i.e.*, the Onsager symmetry relations are fulfilled. Considering a total spectrum of radiation, instead of photons with a particular frequency, the symmetry relations will also be fulfilled for the integral coefficients.

Thus, nonequilibrium thermodynamics predicts a nontrivial effect, namely, a moving colloidal particle generates electromagnetic radiation. A feature of this situation consists in that one side of the particle emits photons while the other side absorbs them, *i.e.*, radiation formally occurs without energy expenditure. More exactly, the energy expenditure for radiation is compensated by the electromagnetic energy inflow from the thermal reservoir (the environment).

4. The dynamics of particles in nonuniform flux

The possibility to extend the system of phenomenological equations for the motion of particles is due to consideration of nonuniform temperature gradient, concentration gradient and variable in the gas velocity space (*i.e.*, taking into account thermodynamic forces of the types $\nabla\mathbf{u}$, $\nabla\nabla\mathbf{u}$, $\nabla\nabla T$, *etc.*).[187] We will analyze this possibility taking a nonuniform flow flowing around an immobile particle as an example.

Consider the simplest case of a flow corresponding to the need to take into account higher derivatives of macrocharacteristics of the medium in constructing phenomeno-

logical equations. Let the initial liquid (gas) flow velocity distribution in the vicinity of the point where the particle is placed be described by an arbitrary function $\mathbf{u}(\mathbf{r})$ which is sufficiently smooth to be expanded into a Taylor series

$$\mathbf{u}(\mathbf{r}) = \mathbf{u}(0) + \mathbf{r} \otimes \nabla\mathbf{u} + \frac{1}{2}\mathbf{r}\mathbf{r} \otimes \nabla\nabla\mathbf{u} + \ldots, \quad (118)$$

where $\otimes$ denotes the scalar product of tensors.

Let the origin be at the solid particle. As a result, the flow field becomes perturbed and takes the form

$$\tilde{\mathbf{u}}(\mathbf{r}) = \mathbf{u}(\mathbf{r}) + \mathbf{u}'(\mathbf{r}),$$

where $\mathbf{u}'(\mathbf{r})$ is the perturbation introduced by the particle, which decreases at long distance.

Clearly, the perturbed fluid will be characterized by an additional entropy production due to the presence of the particle, which can be calculated as described above. Without dwelling on computational details,[187] one finally gets

$$\Delta S_\mathrm{p} = u_\mu(0) \int\limits_{S_\mathrm{b}} \Pi^\mathrm{t}_{\mu\nu} n_\nu \mathrm{d}S_\mathrm{b} + \sum_{k=0}^{\infty} \frac{1}{k!} \nabla^k u_\mu \otimes \int\limits_{S_\mathrm{b}} r^k \Pi^\mathrm{t}_{\mu\nu} n_\nu \mathrm{d}S_\mathrm{b}, \quad (119)$$

where $\mathbf{n}$ is the vector normal to the particle surface used for integration; Π^t is the hydrodynamic stress tensor determined from the total velocity $\tilde{\mathbf{u}}(\mathbf{r})$.

Note that

$$\int\limits_{S_\mathrm{b}} \Pi^\mathrm{t}_{\mu\nu} n_\nu \mathrm{d}S_\mathrm{b}$$

is the component of the force F_μ acting on the particle from the gas. Having denoted the moments

$$F^k_\mu = \frac{1}{k!} \int\limits_{S_\mathrm{b}} r^k \Pi^\mathrm{t}_{\mu\nu} n_\nu \mathrm{d}S_\mathrm{b}, \quad (120)$$

as F^k_μ, we get the following system of phenomenological equations:

$$F_\mu = \tilde{\Lambda}_{00} u_\mu(0) + \sum_{n=1}^{\infty} \tilde{\Lambda}_{0n} \otimes \nabla^n u_\mu, \quad (121)$$

$$\ldots\ldots\ldots\ldots\ldots\ldots\ldots\ldots\ldots\ldots\ldots\ldots$$

$$F^k_\mu = \tilde{\Lambda}_{k0} u_\mu(0) + \sum_{n=1}^{\infty} \tilde{\Lambda}_{kn} \otimes \nabla^n u_\mu,$$

for which the Onsager symmetry relations have the form

$$\tilde{\Lambda}_{ml} = \tilde{\Lambda}^T_{lm}.$$

The first equation in the system (121) represents the extension of the Faxen relation[202] to the case for a fluid with arbitrary velocity field which flows around a solid particle. Such flows are not rare to occur, and solutions to particular problems require computations of the force acting on the particle from the fluid side. The force is determined by the coefficients $\tilde{\Lambda}_{0k}$. Direct calculations of these coefficients are difficult even for solid bodies with simple geometries; however, they can be computed using the Onsager symmetry relations

$$\tilde{\Lambda}_{0k} = \tilde{\Lambda}^T_{k0}.$$

To this end, using the system (121), one should determine the moments $\mathbf{F}^k$ for the motion of the particle in the uniform fluid (or flowing of a uniform flow around the particle). Simple calculations in the hydrodynamic approximation give for a spherical particle

$$\Lambda_{20} = \pi\eta_\mathrm{f} R^2,$$

which coincides with the Λ_{02} value determined for this case earlier by Faxen.[202] Therefore, the particle placed in the nonuniform flow is influenced by the force

$$\mathbf{F} = 6\pi\eta_\mathrm{f} R\mathbf{u} + \pi\eta_\mathrm{f} R^3 \Delta\mathbf{u}. \quad (122)$$

From this expression, in particular, it follows that, depending on the flow character, in the absence of external force the particles can be ahead of or behind the fluid flow.

Thus, using nonequilibrium thermodynamics methods, we readily determined the coefficient in the second term on the right side of Eqn (122), whereas direct calculations are labour- and time-consuming.[202]

The scheme presented above makes clear the character of generalization of the symmetry relations (122) to the case for arbitrary temperature and concentrations fields.

VI. The motion of colloidal particles in nonuniform temperature field and the cross effects

Recently, researchers have paid considerable attention to the motion of colloidal particles in media with temperature gradients and to the corresponding cross effects. Numerous models and a large array of experimental data are available.

Since the discovery of thermophoresis[12] it was accepted that it can be realized with ease only in gases in the presence of temperature gradients and that the velocity of thermophoresis in liquids is low (to 10 μm s^{-1} at temperature gradients to 300 deg cm^{-1}, see Refs 85 and 203). It was assumed that so low velocities are only of theoretical interest. The Soret effect in liquids was also considered weak; however, experiments[251] with colloidal nanosized systems revealed an unexpectedly strong Soret effect. This gave researchers an impetus to studies of thermophoresis in liquids. The phenomenon is used for separation of macromolecules in organic solvents,[64, 252] for control of colloidal particles in the formation of photonic crystals[253–255] and bubbles in microchannels.[256–258]

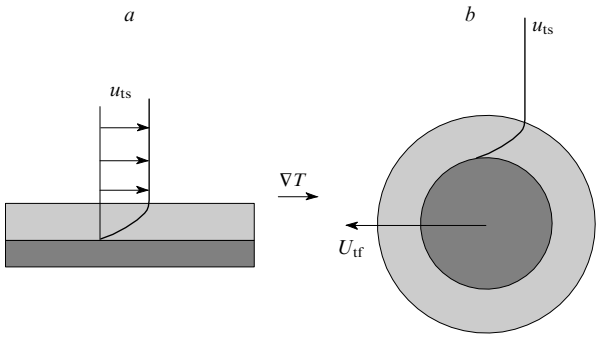


Figure 8. Definition of the thermal slip velocity of a fluid (*a*) and the thermophoresis velocity of particles (*b*).
U_tf is the thermophoresis velocity.

The mechanism of thermophoresis of colloidal particles in liquids is due to the existence of specific liquid boundary layers near the solid surface (Fig. 8).[85] The same mechanism also operates in the case of thermophoresis of macromolecules, although attempts to reveal an unusual mechanism are still carried out.[64] The slip in gases is due to the presence of kinetic boundary layers (see Section V).

1. Thermophoresis of solid particles

Specific boundary layers are due to the interaction of molecules with the solid, namely, solid particles exert some force on the fluid molecules. As a result, the pressure in the boundary layers differs from the pressure in the bulk by δp, which, naturally, depends on temperature because the concentration of molecules in the liquid obeys the Boltzmann distribution. Note that the temperature dependence of δp is of complex character.

In the presence of a temperature gradient in the surface plane, a δp gradient parallel to the temperature gradient is created provided that no pressure drops occur in the bulk fluid. The δp gradient causes motion of the liquid in the boundary layer, which also carries the bulk fluid. If there is no pressure gradient in the bulk fluid, in the steady-state case one deals with a uniform fluid flow and, because of the thin boundary layer, the situation is like the fluid 'slips' on the surface. The slip velocity is readily obtained from solution to the Navier–Stokes equations:

$$u_{ts} = -\frac{1}{\mu}\int_0^\infty x\nabla\delta p(x)\mathrm{d}x = -\frac{1}{\mu}\int_0^\infty x\frac{\partial\delta p(x)}{\partial T}\nabla T\mathrm{d}x = \tag{123}$$

$$= K_{ts}\frac{\eta_f}{\rho}\nabla\ln T.$$

Integration is performed along the normal to the surface with an infinite upper limit because $\delta p = 0$ outside the boundary layer. One can admit rapid establishment of thermodynamic equilibrium in the transverse direction because the boundary layer is thin; therefore, the boundary has no excess chemical potential and one gets from conventional thermodynamic relations

$$\frac{\partial\delta p}{\partial T} = \frac{\rho\delta h}{T},$$

where δh is the excess enthalpy of the fluid in the boundary layer. It follows that the thermal slip coefficient for fluids is

$$K_{ts} = -\frac{\rho^2}{T\eta_f^2}\int_0^\infty x\delta h(x)\mathrm{d}x. \tag{124}$$

This relation obtained[85] using principles of thermodynamics of irreversible processes makes it possible to calculate the thermophoresis and fluid thermoosmosis velocities for various systems through the change in the fluid enthalpy in the boundary layers. Recently, many results reported in Ref. 85 were reproduced again.[203] The slip velocity [see Eqn (123)] also determines thermoosmosis of fluids in capillaries.

From relations (123) and (124) it follows that for lyophilic interfaces characterized by stronger intermolecular bonds (and, therefore, lower enthalpy), thermoosmosis occurs towards warmer regions, whereas thermophoresis occurs towards colder regions. For lyophobic surfaces, these directions should be reversed. Bubbles in liquid move towards warmer regions because the gas phase is lyophobic with respect to liquids. Recent detailed studies showed that the direction of thermophoresis of particles depends strongly on their nature, on the surface state and on the type of the dispersion medium, so particles can move either along the direction of the temperature gradient and in the opposite direction.[203] If particles bear surface charges, the thermophoresis velocity abruptly increases due to an increase in the extension of boundary layers and to manifestation of mixed thermoelectric and thermal diffusion effects.

According to the Gouy–Chapman theory of the structure of the electrical double layer, the thermal slip coefficient is given by[85, 203, 259, 260]

$$K_{ts} = -\frac{\varepsilon_0\psi_0^2\rho}{32\pi\eta_f^2}\left(1 + \frac{T}{\varepsilon_0}\frac{\partial\varepsilon_0}{\partial T}\right), \tag{125}$$

where ψ_0 is the surface potential of particles. As can be seen, the velocity of thermophoresis is proportional to the squared surface potential.

Relation (125) describes only a few effects determining thermophoresis of particles. The so-called secondary effects also make some contribution. Changes in temperature cause the appearance of electric fields which also influence the motion of particles. For instance, the electric field created in electrolytes in the presence of a temperature gradient is

$$E_T = \Psi_0^T\frac{\nabla T}{T}, \tag{126}$$

where Ψ_0^T is -15 mV for NaCl solution and $+70$ mV for NaOH solution.

Thus, the thermophoretic and electrophoretic components of motion always coexist, the contribution of the latter to the slip coefficient being equal to

$$K_{ts}^E = \frac{\varepsilon_0\zeta\rho}{4\pi\eta_f^2}\Psi_0. \tag{127}$$

If particles move in a solution, the secondary effects appear. It is the effect of the temperature field that is responsible for redistribution of the concentration near the particle and the appearance of additional forces due to diffusiophoresis. The density can vary over a wide range with temperature and the fluid density determines the dispersion interaction forces, which are also temperature-dependent. As a result, additional driving forces appear in the fluids with temperature gradients.[203]

The velocity of thermophoresis of solid particles is calculated by solving the problem of uniform flow around a sphere with the slip boundary condition at the surface. The slip is assumed to be proportional to the local temperature gradient. The result for a spherical particle whose size much exceeds the thickness of the boundary layers is as follows:

$$\mathbf{U}_{tf} = -K_{ts}\frac{\eta_f}{\rho T}\frac{2\lambda_e}{\lambda_i + 2\lambda_e}\nabla T. \tag{128}$$

If the particle size is comparable with the thickness of the boundary layer, determination of the velocity of ther-

mophoresis requires knowledge of the pressure distribution within the boundary layer. Such a distribution can be determined using a number of models. If the particle size is small compared with the thickness of the boundary layer, the velocity of thermophoresis will be determined by the thermal slip coefficients with corresponding numerical factors.[203]

Thermal slip on the surface of colloidal particles was observed experimentally[261] using 10 μm polystyrene or silica particles suspended in a NaCl solution (*i.e.*, stabilized by electrostatic forces). Particles had different surface charges and, correspondingly, the directions of the slip velocity were also different. These experiments confirmed the concept of thermal slip complicated by the secondary effects as the main mechanism of the Soret effect in colloidal systems.

Thus, thermophoresis of particles in electrolyte solutions depends strongly on their compositions. As an example, Fig. 9 presents the data on the thermophoretic mobility (D_T) relating the particle velocity to the temperature gradient

$$\mathbf{U}_{tf} = D_T \nabla T,$$

for 13-nm spherical polystyrene particles suspended in NaCl and LiCl solutions at pH 10.3. Rather large values of the thermophoretic mobility coefficient at low salt concentrations can be explained by large thermal diffusion coefficient of HO^- anions whose motion creates the thermoelectric field responsible for the motion of negatively charged particles towards the warmer region.

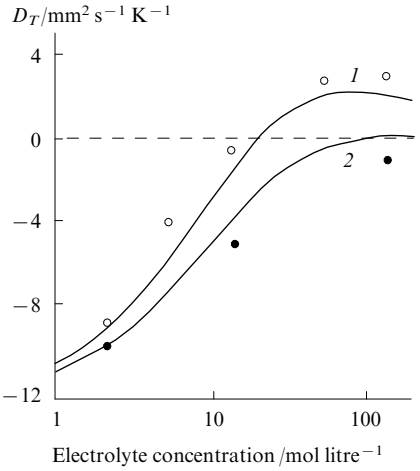


Figure 9. Thermal diffusion coefficient of polystyrene nanoparticles plotted *vs.* electrolyte concentration in NaCl (*1*) and LiCl (*2*) solutions.[262]
Solid lines denote the results of calculations using the contributions (125) and (127).

The role of the primary and secondary electrical effects is demonstrated in Fig. 10, which presents the dependences of the Soret coefficient

$$S_T = \frac{D_T}{D},$$

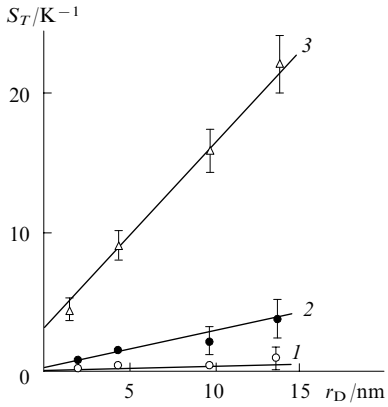


Figure 10. Soret coefficient plotted *vs.* Debye radius for particles of radius 0.1 (*1*), 0.25 (*2*) and 0.55 μm (*3*).[263]

(D is the diffusion coefficient of particles) on the Debye radius (r_D). As can be seen, the plots are linear, which indicates the main role of the electrical double layer. A large increase in the effect with increasing particle size points to a significant role of polarization effects. An explanation[263] is incomplete because consideration of the thermodynamic properties of particles in homogeneous media does not include all possible effects.

The aforesaid also concerns earlier studies on this effect (see, *e.g.*, Refs 264–267). More reliable are the models[203, 268, 269] with inclusion of changes in the local (surface) pressure near colloidal particles, which corresponds to the mechanism of thermophoresis of particles in fluids proposed by Derjaguin. Computational details are of secondary importance, *viz.*, the boundary pressure was expressed through the intermolecular interaction potential;[268] the structure of the electrical double layer near particles was simply studied;[203] or the boundary layer on the surface of particles was described within the framework of the Cahn–Hillard theory.[269] The use of the purely thermodynamic approach was to some extent inspired by the study[270] whose authors reported that an ensemble of particles placed in the temperature gradient field obeys the Boltzmann distribution, *i.e.*, the local equilibrium condition is apparently met. However, the proof seems not to be reliably substantiated because the authors simply measured the distribution of the ensemble of particles in the temperature gradient field when the gradient was directed horizontally and no external forces were assumed. There was a simple balance between diffusion and thermal diffusion of particles.

The dependence of the thermophoretic mobility on the particle size is significant. Expression (128) does not include this dependence, but this is valid for large particles only. If the particle size is smaller than the thickness of the boundary layers, such a dependence clearly does occur; however, similarly to the case for electrophoresis, it should not be too strong. One can agree with the assumption[265, 266] that the Soret coefficient for small particles should be proportional to their size. Indeed, in this case the 'driving force' depends only on the structure of the boundary layer which remains almost unchanged for small particles, and the diffusion coefficient is inversely proportional to the particle size. It follows that the Soret coefficient should increase with a decrease in the particle size, as is observed in the experiments.

However, one should keep in mind that the dependence of the mobility on the particle size is determined by the nature of the system under study. For instance, no dependence of the Soret coefficient on the diameter of particles was revealed.[271] Experiments were carried out with 'water in oil' microemulsions stabilized by 'Aerosol OT'. In this case, the mechanism (provided the key role of the boundary layers) should be different from that described above because the particles are also stabilized by steric forces. Here we deal with a kind of analogue of thermocapillary motion whose velocity is independent of the particle size (see below), although usually the thermocapillary motion is essentially suppressed by the surfactant adsorption layers.

A theoretical study[272] based on the Fokker–Planck equation concerned the co-operative behaviour of colloidal particles in nonuniform temperature fields taking into account Brownian motion and hydrodynamic interaction between particles. The Fokker–Planck equation was formally used in a study[273] of co-operative effects in nonuniformly heated colloidal dispersions. Particles can move towards both cold and hot regions; therefore, they can be either displaced from or move towards the zone being heated. Conditions for stability loss by a laser-heated colloidal dispersion owing to thermophoretic interaction between particles were established[273] based on the experimental data obtained elsewhere.[274]

The results[273] are practically important because it was proposed to use thermophoresis for high concentration of DNA molecules.[252] The experimental design was as follows. A DNA solution was pumped through a capillary. The central part of the capillary was heated by laser radiation (Fig. 11). As a result, a temperature gradient directed opposite to the direction of the solution flow was produced in the capillary. This gradient retarded the macromolecules present in the solution; they accumulated ahead of the heated zone as if near the potential barrier. It was shown[252] that if the temperature in the central zone of the heated region is 16 degrees higher than at the capillary inlet, the concentration of DNA molecules ahead of the heated region increases by a factor of 18 (theoretically, a 800-fold increase is attainable; however, it requires a rather long time). Not only the temporal, but also some other limitations on the possible effect of accumulation of particles were established.[273]

Mutual influence of particles on the velocity of thermophoretic motion is also significant. Experiments with various systems showed[275–279] that the thermophoretic mobility linearly depends on the change in the volume fraction of particles, but the magnitude and even the direction of these changes have not been theoretically substantiated as yet. This is due to the superposition of numerous co-operative effects, from the mutual influence of the moving particles to their co-operative influence on the average temperature gradient. The latter is due to the appearance of thermal dipole moments on particles in an external temperature gradient; summation of the thermal dipole moments provides the thermal polarization of the medium and its direction is determined by the ratio of the thermal conductivities of particles and the dispersion medium. This feature is usually ignored when considering thermophoretic motion of ensembles of particles. The difference between the thermal conductivities of particles and the medium is also often ignored. Probably, this factor is insignificant for small particles (particle size is smaller than the thickness of the boundary layer), but it should be taken into account when analyzing the co-operative behaviour of colloidal particles in nonuniform temperature fields.

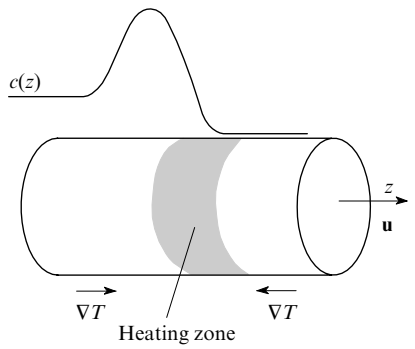


Figure 11. Concentration of nanoparticles in capillaries under the action of laser radiation.[252]

The cross effect, thermal polarization of particles moving in a homogeneous fluid, can hardly be measured experimentally because it is very weak. The mechanism of thermal polarization is obvious. A homogeneous fluid flow around a particle involves the boundary layers in which the enthalpy of the fluid is different from its bulk value. As a result, a heat flux due to the change in enthalpy in the boundary layers (see above) appears along the particle surface. A solution to the problem using conventional expressions for the flow velocity near the spherical particle gives for the thermal dipole moment

$$\mathbf{A} = -3\eta R \frac{\eta_f}{\rho} \frac{K_{ts}}{\lambda_i + 2\lambda_e} \mathbf{U}_0 , \qquad (129)$$

where $\mathbf{U}_0$ is the fluid velocity far from the particle and the thermal slip coefficient is expressed through the enthalpy of the boundary layers using relation (124). This confirms the fulfillment of the Onsager symmetry relations in Eqns (89).

2. Thermocapillary motion of droplets and bubbles and the cross effect

Thermocapillary motion of bubbles in a nonuniformly heated fluid is one of the most known manifestations of thermophoresis. This phenomenon was for the first time studied theoretically and experimentally by Young *et al.*[280] Various approaches to the description of thermocapillary motion of bubbles were analyzed in detail.[281, 282] Nonequilibrium thermodynamics of bubbles in nonuniform media including the temperature gradient field was constructed[283, 284] and the cross heat effect related to the flow of a homogeneous liquid around a bubble (or ensemble of bubbles) was predicted.

In spite of simplicity of thermocapillary motion of bubbles and droplets, interest in studies of this phenomenon is far from being ceased. This is first of all due to progress in microfluidics. The motion of droplets and bubbles caused by temperature gradients has been the subject of detailed studies.[285] Microfluidics also considers volatile fluids and studies the motion of fairly small bubbles at elevated temperatures where the effect of bubble evaporation on the motion cannot be ignored. An analysis of this effect is available.[286]

The effect of thermocapillary motion is determined by the temperature dependence of the surface tension

$$\sigma(T) = \sigma_0 + \frac{\partial\sigma}{\partial T}\left[T(\mathbf{R}) - T_0\right], \tag{130}$$

where σ_0 is the surface tension of the fluid at the temperature T_0; the $\partial\sigma/\partial T$ coefficient is negative.

If a bubble (or a droplet of another fluid) is placed in a nonuniformly heated liquid medium, an uncompensated stress is developed at the interface, *viz*., the surface will be 'shrinked' towards the colder region because of the higher surface tension. The motion of the interface will cause the motion of adjacent fluid layers, which eventually will manifest itself as the motion of the bubble at a constant velocity; here, the surface tension gradient will be compensated by the viscous stresses in the liquid moving around the bubble.

The aforesaid is formally reflected in the boundary conditions for stresses at the interface

$$\Pi^{\mathrm{l}}_{r\theta} = \Pi^{\mathrm{i}}_{r\theta} - \frac{\partial\sigma}{\partial T}\nabla_\theta T, \tag{131}$$

where $\mathbf{\Pi}^{\mathrm{i}}$ and $\mathbf{\Pi}^{\mathrm{l}}$ are the viscous stress tensors within the bubble (droplet) and in the carrier fluid. The second term on the right side determines the stresses developed on the bubble surface in the presence of temperature gradients. A solution to the hydrodynamic equations with this boundary condition leads to famous Young relation for the velocity of thermocapillary motion of a bubble (droplet)

$$\mathbf{U}_{\mathrm{tc}} = -\frac{2R}{2\eta_{\mathrm{f}} + 3\eta_{\mathrm{i}}}\frac{\lambda_{\mathrm{e}}}{\lambda_{\mathrm{i}} + 2\lambda_{\mathrm{e}}}\frac{\partial\sigma}{\partial T}\nabla T, \tag{132}$$

where η_{i} is the viscosity of the gas (or liquid droplet) and λ_{i} is the corresponding thermal conductivity. This equation shows that droplets (gas bubbles) in the liquid with temperature gradient begin to move towards the warmer region.

Consider the cross effect. Let a bubble (or an alien droplet) move in a homogeneous liquid at the velocity $\mathbf{U}_0$. The heat effect is due to the formation of new surface in the fore region of the bubble and its disappearance in the stern region. The surface energy of the liquid is $\sigma - T(\partial\sigma/\partial T)$. When the interface moves, the capillary forces execute the work (similarly to the work of pressure forces). The contribution of capillary forces to the energy flux is $-\sigma\mathbf{u}_{\mathrm{s}}$, where $\mathbf{u}_{\mathrm{s}}$ is the surface velocity (for the bulk case, the corresponding contribution is $p\mathbf{u}$). Here we take into account the fact that the surface tension equals minus the surface pressure applied to the liquid contour. By combining the surface energy flux and the work of surface tension forces during the motion of the interface one gets that a singular (localized in the thin surface layer) energy flux flows along the bubble/liquid interface

$$\hat{\mathbf{j}}^{\mathrm{e}} = -T\frac{\partial\sigma}{\partial T}\mathbf{u}_{\mathrm{s}}. \tag{133}$$

Substituting this expression into the equation of heat balance at the interface [*cf*. Eqn (34)]

$$-\lambda_{\mathrm{e}}\frac{\partial T}{\partial r} + \lambda_{\mathrm{i}}\frac{\partial T_{\mathrm{i}}}{\partial r} = -\mathrm{div}_\tau\hat{\mathbf{j}}^{\mathrm{e}}_\tau \tag{134}$$

gives, after solution of the heat problem, the following expression for the temperature drop at the bubble poles:

$$\Delta T = \frac{2T}{R}\frac{(\partial\sigma/\partial T)}{\lambda_{\mathrm{i}} + \lambda_{\mathrm{e}}}\frac{\eta_{\mathrm{f}}}{\eta_{\mathrm{f}} + \eta_{\mathrm{i}}}U_0, \tag{135}$$

One can show that the result obtained confirms fulfillment of the Onsager symmetry relations for Eqns (89).

The temperature drop is rather large. For a 3-mm bubble floating in water under the action of buoyancy force at a velocity of $3\ \mathrm{m\ s^{-1}}$, the temperature drop is $\Delta T \approx 0.5\,\mathrm{K}$ and can be measured with certainty.

3. Thermocrystallization flow of particles and the cross effect

If the temperature of a solid containing alien particles is close to the melting point, thin liquid layers can form near the particle (Fig. 12). The reason is the so-called surface melting[86] due to the change in the fluid structure near interfaces under the action of surface forces.[85] Non-freezing layers play an important role in technological and geophysical processes.[85,287] In particular, they are related to such phenomena as frost heave, dynamics of glaciers and slip on the surface of ice. An important role is also played by thermocapillary flow of non-freezing layers which recently has attracted considerable attention.[288–290]

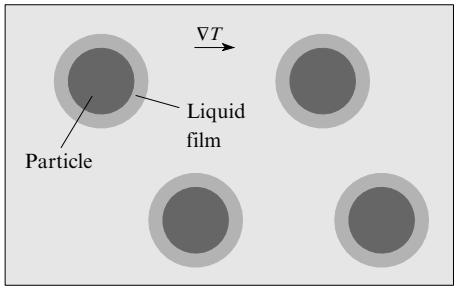


Figure 12. The structure of a dispersion of nanoparticles frozen in the solid (ice) and surrounded by liquid films.

We will consider migration of solid inclusions surrounded by non-freezing layers under the action of a temperature gradient using equations of nonequilibrium thermodynamics (89). We will also show fulfillment of the Onsager symmetry relations. This issue was discussed in a recent study[290] and it was shown that the symmetry relations are fulfilled for the equations

$$\mathbf{J}_{\mathrm{p}} = -D\nabla\varphi + (1-\varphi)\varphi D_T\nabla T, \tag{136}$$

$$\mathbf{q} = (1-\varphi)T_{\mathrm{m}}D_q\frac{\partial\pi_0}{\partial\varphi}\nabla\varphi - \lambda_{\mathrm{e}}\nabla T,$$

where

$$\mathbf{J}_{\mathrm{p}} = \varphi\mathbf{U}$$

is the inclusion flux density; φ is the volume fraction of inclusions; D and D_T are the diffusion and thermal diffusion coefficients of particles; T_{m} is the melting point; D_q is the Dufour coefficient; λ_{e} is the thermal conductivity of the solid; $\mathbf{q}$ is the heat flux density; and π_0 is the osmotic pressure of particles.

The thermal diffusion and Dufour coefficients were calculated and it was shown [290] that they coincide at small volume fraction of particles, as follows from the Onsager symmetry relations (see Ref. 3). However, it should be noted that not all arguments [290] can be accepted unconditionally. In particular, the authors assumed equal thermal conductivities for inclusions and for the surrounding medium. At different thermal conductivities, the Onsager symmetry violates. Since the proof of fulfillment of the Onsager symmetry relations for Eqns (136) is cumbersome, we will do it for Eqns (89). In principle, having proved the symmetry of kinetic coefficients in Eqns (89), one can readily pass to establishment of fulfillment of the symmetry relations in Eqns (136).

Consider the motion of particles in the presence of a temperature gradient in the solid (ice). With no temperature gradient, a thin liquid layer (film) is formed near the particle. Let, for simplicity, the particle be spherical. The film thickness H is determined by the pressure (p) and temperature (T); the external pressure is compensated by the disjoining pressure in the film, which depends on the film thickness and temperature. If the temperature gradient differs from zero, the particle–film–ice system deviates from the equilibrium state. The solid should to some extent melt at the warmer side because the higher temperature corresponds to the thicker liquid film which in turn corresponds to the lower disjoining pressure. Therefore, the force exerted on the particle from the thinner film side will cause it to move towards the warmer region.

The physical mechanism of thermocrystallization flow of fluids in thin channels was for the first time disclosed by Derjaguin and Churaev [291, 292] (see also Ref. 85). Clearly, the motion of particles is the same process which is considered in the coordinate system related to the liquid phase. As mentioned above, the pressure gradient in the film due to the temperature gradient is related to the excess enthalpy in the liquid film, which is determined by the heat of melting. As a result, one can write that an 'excess' pressure is produced in the film

$$\delta p = -\frac{L_{\mathrm{m}}\rho_{\mathrm{s}}\left[T(\mathbf{R}) - T_0\right]}{T_{\mathrm{m}}}, \tag{137}$$

where L_{m} is the latent heat of melting and ρ_{s} is the density of the solid. The particle moves under the action of the pressure drop specified by expression (137) (the pressure from the 'cold' side is higher). The velocity of the motion is determined using the solution to the problem of motion of a spherical particle in a liquid filling a spherical cavity,[202]

$$\mathbf{U}_{\mathrm{tc}} = \frac{L_{\mathrm{m}}\rho_{\mathrm{s}}H^3}{2\eta_{\mathrm{f}}R^2T_{\mathrm{m}}}\,\frac{\lambda_{\mathrm{e}}}{\lambda_{\mathrm{i}} + 2\lambda_{\mathrm{e}}}\nabla T. \tag{138}$$

As can be seen, the velocity vector is aligned to the temperature gradient, *i.e.*, particles move towards the warmer region.

Assume that a particle surrounded by a layer of a fluid is influenced by the force **F**. Under the action of **F**, this layer is compressed on the one side and expands on the other side. Compression causes the pressure within the layer to increase and thus leads to melting of the solid; expansion of the layer is accompanied by a decrease in the pressure and subsequent solidification of the fluid.

Melting of solids is characterized by absorption of heat while solidification of fluids is characterized by heat release, *i.e.*, a heat source and heat sink appear in the polar regions of the particle.

Assume that the process is limited only by transfer of the fluid in the thin layer from the 'fore' to 'stern' regions of the particle. Using the solution to the problem of motion of the fluid between concentric spheres (see above), the velocity of the particle under the action of the force **F** is

$$\mathbf{U} = \frac{H^3\mathbf{F}}{8\pi\eta_{\mathrm{f}}R^4}. \tag{139}$$

With this velocity one can easily calculate the quantity of heat released (absorbed) per unit time from (by) the unit surface of the cavity; it obeys a cosine distribution

$$I_q = \rho_{\mathrm{s}}L_{\mathrm{m}}U\cos\theta.$$

Using this expression for surface heat source, the temperature distributions inside the particle and in the solid are obtained readily. In the latter case, one has

$$T_{\mathrm{e}} = T_0 + \frac{\rho_{\mathrm{s}}L_{\mathrm{m}}V}{\lambda_{rmi} + 2\lambda_{\mathrm{e}}}\,\frac{R^2\cos\theta}{r^2}, \tag{140}$$

where r is the distance from the centre of the particle. It follows the expression for the combination (89) including the thermal dipole moment:

$$4\pi\lambda_{\mathrm{e}}\mathbf{A} = \frac{4\pi\lambda_{\mathrm{e}}\rho_{rms}L_{\mathrm{m}}\mathbf{U}}{\lambda_{\mathrm{i}} + 2\lambda_{\mathrm{e}}} = \frac{1}{2}\,\frac{\lambda_{\mathrm{e}}\rho_{\mathrm{s}}L_{\mathrm{m}}}{\lambda_{\mathrm{i}} + 2\lambda_{\mathrm{e}}}\,\frac{H^3}{\eta_{\mathrm{f}}R^2}\mathbf{F}. \tag{141}$$

A comparison of Eqns (138) and (141) illustrates fulfillment of the Onsager symmetry relations.

Experimental data on the velocity of particles are shown in Fig. 13. As can be seen, the resuts of measurements corrected for the thickness of non-freezing layers are in good agreement with theoretical predictions.

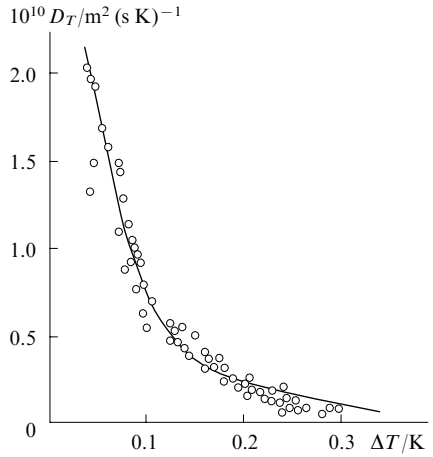


Figure 13. Experimental dependence of the thermal diffusion coefficient of 12.7 μm silica particles on the degree of supercooling of ice ΔT, which determines the thickness of the non-freezing film.[293] Solid line: calculations using relation (138).

4. Thermophoresis and thermal polarization in gases

The motion of aerosol particles under the action of a temperature gradient was studied in detail much earlier than thermophoretic motion of colloidal particles in the liquid phase. This is due to the fact that the velocities of particles in gases are a few orders of magnitude higher than the velocity of thermophoresis in fluids. Also, the thermophoretic force in gases can be measured using sensitive equipment developed for the electron charge measurements.

Numerous experiments showed that thermophoretic motion of aerosol particles occurs towards colder regions. This effect allows particles passing through a flat channel whose surfaces have different temperatures to be deposited on the cold wall; thus the gas is cleared of suspended particles. The reverse use is also possible, namely, if a heated body is placed in a cold gas, particles will repel from it due to the thermophoretic force; this prevents the solid surface from being covered with particles (dust). This phenomenon is used in fabrication of microelectronics devices whose operation is violated by dust deposition; the devices are assembled at elevated temperature to provide efficient repulsion of particles from the microelements. The steady interest of researchers in thermophoresis is due to great practical value of the technique.[12, 22, 294–304]

Thermophoretic motion in gases is strongly influenced by the thermal conductivity of particles which can be a few orders of magnitude higher than those of gases. For this reason, the velocity of particles depends strongly on their size (more exactly, on the ratio of the mean free path l_f of gas molecules to the particle radius R, which is called the Knudsen number)

$$\mathrm{Kn} = \frac{l_f}{R}.$$

At $R \ll l_f$, a body placed in a nonuniformly heated gas experiences the thermophoretic force due to the nonequilibrium state of the gas. In this case, thermophoresis can also be treated as thermal diffusion of giant molecules in a binary gas mixture.[12] Using the nonequilibrium distribution function and having calculated the momentum transferred to the sphere from the nonuniformly heated gas, the expression[12] for the velocity of thermophoresis of small particles is as follows:

$$\mathbf{U}_{tf} = -\frac{3}{4(1+\pi b/8)}\frac{\eta}{\rho}\frac{\nabla T}{T_0}, \qquad (142)$$

\where b is the accommodation coefficient of the tangential momentum of molecules on the surface of particles. As can be seen, the velocity is in fact independent of the nature of particles because the accommodation coefficient is close to unity for arbitrary surfaces in real systems.

For large particles with $R \gg l_f$, the velocity of thermophoresis is determined by expression (128) where

$$K_{ts} \simeq 0.75(1 + 0.5b).$$

However, the velocities calculated using relation (128) are much underestimated compared to experimental values even at $R > l_f$. This discrepancy was explained as follows. Since usually the thermal conductivity of particles much exceeds that of the gas, their combination is a small quantity, thus indicating a small temperature gradient on the particle surface. But the temperature of the gas can be different from the temperature of the particle due to the temperature jump on the surface (see Section III). As a result, the temperature gradients are also different and, as a consequence, the velocity of thermophoresis can be much higher than that predicted by relation (128). The simplified expression has the form

$$\mathbf{U}_{tf} = -K_{ts}\frac{\eta}{\rho T}\frac{2\lambda_e}{\lambda_i + 2\lambda_e}\nabla_\infty T\left[1 + \frac{\lambda_i}{\lambda_e}\mathrm{Kn}G\left(\frac{\lambda_i}{\lambda_e}, ...\right)\right], \qquad (143)$$

where $G(\lambda_i/\lambda_e, ...)$ is a function dependent on the ratio of the thermal conductivities and on some kinetic coefficients appearing in the boundary conditions (141); its magnitude is of the order of unity.

From relation (143) it follows that even at very large λ_i/λ_e ratios and finite Knudsen numbers, the velocity of thermophoresis does not tend to zero, as observed in the experiment. For aerosol particles, the velocity of thermophoresis can hardly be calculated using expression (128) because of the large λ_i/λ_e ratio.

At particular values of kinetic parameters, the function $G(\lambda_i/\lambda_e, ...)$ can take negative values, *i.e.*, negative thermophoresis is possible. Note that negative thermophoresis is not a consequence of the approximate character of calculations. The thermophoresis velocity calculations within the framework of the kinetic theory of gases for the whole range of Knudsen numbers[305–309] also suggest the possibility of negative thermophoresis.

To date, there is no reasonable agreement between theory and experiment (see a review[298]). At small Knudsen numbers, experimental data differ by several times, being strongly different from the theoretical predictions (Fig. 14). The results of rigorous theoretical calculations were also different from experimental data[310, 311] obtained at zero gravity (no gravitational convection). The experimental values of the velocity of thermophoresis are also higher

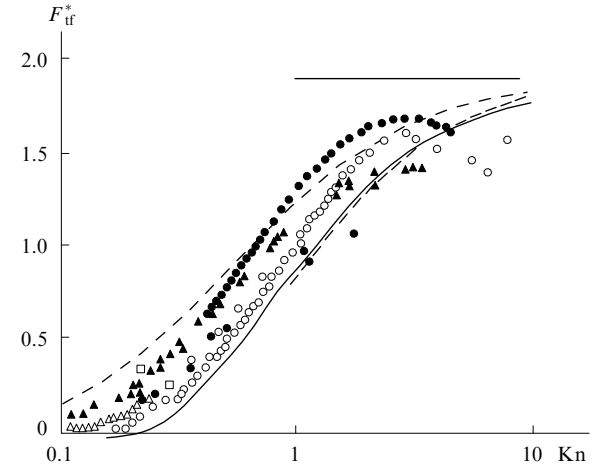


Figure 14. Dimensionless thermophoretic force plotted *vs.* Knudsen number using various experimental data.[298]
The solid and dashed lines, the open and solid circles, open squares and solid triangles span the Knudsen number ranges according to the corresponding models.
The horizontal line: results of calculations using expression (142).

than the predicted values. Thus, the old problem is still to be solved both experimentally and theoretically. It should be noted that the thermophoresis velocity (thermophoretic force) is usually measured for charged aerosol particles. The charge on the surface of particles can influence,[312] in particular, the slip velocity and, correspondingly, other kinetic effects, so the theoretical description of thermophoresis of aerosol particles should be carried out for some realistic conditions.

The cross effect, namely, thermal polarization of particles, is more pronounced in gases than in fluids; it was observed experimentally (see below).

This effect was predicted theoretically [12] and then observed experimentally in a study on the motion of particles in gases.[188] Recently, thermal polarization of particles has again attracted the attention.[190–193] The effect is due to the isothermal heat fluxes in the boundary layers. The flow of a gas around a solid particle is accompanied by the appearance of a nonuniform pressure field and subsequent production of bulk isothermal heat flux proportional to the pressure gradient (see Section II) and the heat flux in the boundary layer due to the action of tangential stresses near the surface of the particle (see Section III). The equation for the thermal dipole moment formed in the gas can be derived using methods of nonequilibrium thermodynamics from expression (89)

$$\mathbf{A} = -3\eta R\,\frac{\eta}{\rho}\,\frac{K_{\mathrm{ts}}}{\lambda_{\mathrm{i}}+2\lambda_{\mathrm{e}}}\left[1+\frac{\lambda_{\mathrm{i}}}{\lambda_{\mathrm{e}}}\mathrm{Kn}G\left(\frac{\lambda_{\mathrm{i}}}{\lambda_{\mathrm{e}}},\ldots\right)\right]\mathbf{U}_0\,. \tag{144}$$

Since the particle and gas temperatures differ because of the temperature jump (see above), the temperature drop in the polar regions of the particle ΔT_i will be somewhat different. The expression for calculations corrected for the Knudsen number has the form [189]

$$\Delta T_i = \sqrt{\frac{\pi c_p}{2c_v}}\,\frac{\mathrm{KnM}K_{\mathrm{ts}}}{1+0.5\lambda_{\mathrm{i}}/\lambda_{\mathrm{e}}}\left[1+\mathrm{Kn}G_1\left(\frac{\lambda_{\mathrm{i}}}{\lambda_{\mathrm{e}}}\right)\right], \tag{145}$$

where c_p and c_v are the heat capacities of gas at constant pressure and volume, respectively;

$$\mathrm{M} = \frac{U_0}{v_T}$$

is the Mach number; v_T is the thermal velocity of molecules and G_1 is some function of kinetic parameters. Thermal polarization calculations for arbitrary Knudsen numbers were carried out.[313] The results obtained were compared with experimental data for a wider range of Knudsen numbers.

The temperature drop between the ends of the diameter passing through the centre of sphere is given by

$$\Delta T_i^p = \Delta T_i \cos\theta_0, \tag{146}$$

where θ_0 is the angle between the vector $\mathbf{U}_0$ and the direction of the diameter connecting two points on the sphere.

This dependence of the temperature drop on the angle of rotation of the diameter relative to the incident flux was indeed reproduced experimentally, as well as the linear dependence of the temperature drop on the incident flux velocity (Fig. 15), *i.e.*, the measured effect is not due to viscous energy dissipation which causes heating proportional to the squared velocity.

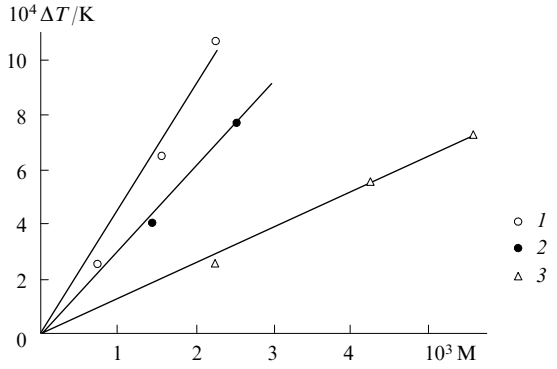


Figure 15. Temperature drop at the poles of a sphere placed in argon flow plotted *vs.* Mach number at different Knudsen number values.[188]
Kn: 0.081 (*1*), 0.037 (*2*) and 0.0137 (*3*).

The dependence of the temperature drop on the Knudsen number appeared to be more informative. The plots $\Delta T^*(\mathrm{Kn})$

$$\Delta T^* = \frac{\Delta T_i(1+0.5\lambda_{\mathrm{i}}/\lambda_{\mathrm{e}})}{T_0\mathrm{KnM}\sqrt{\pi c_p/2c_v}} \tag{147}$$

for a number of systems are shown in Fig. 16.

Note that at $\mathrm{Kn}\to 0$, the $\Delta T^*(\mathrm{Kn})$ function tends to K_{ts} — the thermal slip coefficient, *i.e.*, there is good agreement between theory and experiment.

Since the quantity K_{ts} depends on the momentum accommodation coefficient and the G_1 function additionally depends on the energy accommodation coefficient of gas molecules on the particle surface, both these parameters can be determined in a single experiment from the intercept of the experimental curve with the ordinate axis and the slope. The momentum and energy accommodation coefficients determined in the thermal polarization experiments agree well with the data obtained in other experiments.[189]

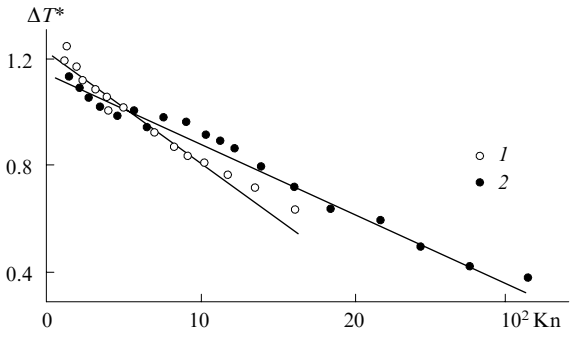


Figure 16. Reduced temperature drop on a glassy sphere covered with an oil film plotted *vs.* Knudsen number in argon (*1*) and helium (*2*).[188]

VII. Membrane processes

Main relations for transport processes in membranes were derived long ago in studies of so-called discontinuous systems.[3] It is appropriate to consider them for the following reasons. In essence, membranes are typical disperse systems because their behaviour and properties are governed by the boundary layers. Therefore, it is not accidental that membranes are often modelled by ensembles of colloidal particles (cell models, dusty-gas model). Nonequilibrium thermodynamics of membrane processes can be derived from the equations for colloidal systems, *viz*., transmembrane transport can be considered as the motion of an ensemble of membrane-forming (probably, complex-structure) colloidal particles in a fluid. This interpretation of membrane processes is not always clear owing to a rather complicated structure of many membranes,[98] but, formally, it is based on transition from a coordinate system related to the membrane to a coordinate system related to the fluid being filtered.

A typical example of a discontinuous system shown in Fig. 17 is provided by two large vessels separated by a

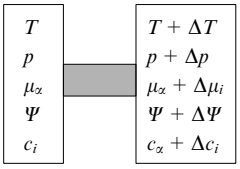


Figure 17. Nonequilibrium discontinuous system used to describe transport in capillary-porous bodies: a schematic.

porous wall (capillaries, membrane). Imagine that such a system is out of equilibrium, *i.e*., there exist a pressure drop (Δp), component concentration drops (Δc_i), a temperature drop (ΔT) between the vessels, as well as an electrostatic potential drop ($\Delta\Psi$). If no external factors act on the nonequilibrium system, it relaxes to the equilibrium state and the corresponding entropy production per unit surface area of the capillary connecting the vessels can be written in the form [3]

$$\Delta S = \frac{u_v \Delta p}{T} + \frac{J_q \Delta T}{T^2} + \frac{I_e \Delta\Psi}{T} + \sum_{i=1}^{N-1} J_i \frac{\Delta(\mu_i - \mu_N)}{T}, \qquad (148)$$

where

$$u_v = \frac{1}{n}\sum_i n_i u_i = \sum_i c_i u_i$$

is the average volume (molar) flow velocity of the mixture through the capillaries; J_q is the heat flux; I_e is the electric current;

$$J_i = n_i(u_i - u_v)$$

is the diffusion flux of particles of the ith component; and u_i and n_i are respectively the average velocity and numerical density. All fluxes are assumed to be averaged over the cross section of the capillary or channel connecting the reservoirs.

The change in the chemical potentials in Eqn (148) is taken at constant temperature and pressure. Also, one has $\sum_i J_i = 0$ because the diffusion fluxes are determined relative to the average molar velocity of the components; this condition made it possible to exclude the flux J_N; therefore, summation in the last term is performed over $N-1$ components of the system.

Having chosen u_v, J_q, I_e, J_i as thermodynamic fluxes and the Δp, ΔT, $\Delta\Psi$, $\Delta(\mu_i - \mu_N)$ drops as thermodynamic forces, one can write the overall system of transport equations analogously to system (10) which includes all nonequilibrium processes accompanying the flow of mixtures through capillary-porous bodies. Generally, this system of equations is cumbersome, namely, it includes $N+2$ equations and $(N+2)(N+2)$ kinetic coefficients. Therefore, we will restrict ourselves to a number of practically interesting cases which can be completely described by systems including two or three equations.

Note that representation of the entropy production by expression (148) is not a dogma. Some cases may require the inclusion of new forces or transition to other variables. In particular, the formulation with the entropy gradient as driving force is more convenient for studying filtration of near-critical fluids.[314]

Based on the entropy production (148), one can derive a system of integral phenomenological equations of nonequilibrium thermodynamics. The kinetic coefficients appearing in these equations are determined by specific features of transport of molecules through membrane channels. Transfer through channels is described by specific local equations whose form depends on the nature of the transferred medium, channel geometry, type of processes, *etc*. Derivation of local equations is a particular task which is usually solved using local conservation equations. Non-trivial character of this problem is illustrated by, *e.g*., the results of a study [315] on the flow of two immiscible fluids in a porous medium. Even the derivation of equations, apart from their solution, is a rather complicated procedure and can be done only under certain admissions. Gray [315] considered an inert porous medium and used not only the laws of conservation, but also elements of nonequilibrium thermodynamics that make it possible to correlate data obtained using various approximations. The situation becomes much more complicated if the porous body changes its thermal or elastic properties. An analysis of transport of two immiscible fluids through a thermoplastic porous body using elements of nonequilibrium thermodynamics was reported.[316, 317]

1. Thermoosmosis and the mechanocaloric effect

If a single- or multicomponent system is characterized by a constant concentration of components and no electrical phenomena occur, the expression for the entropy production is reduced to

$$\Delta S = \frac{u_v \Delta p}{T} + \frac{J_q \Delta T}{T^2}, \qquad (149)$$

and the system (10) is simplified and includes two equations:

$$u_v = \Lambda_{vv}\frac{\Delta p}{T} + \Lambda_{vq}\frac{\Delta T}{T^2}, \qquad (150a)$$

$$J_q = \Lambda_{qv}\frac{\Delta p}{T} + \Lambda_{qq}\frac{\Delta T}{T^2}. \qquad (150b)$$

The Λ_{vv} coefficient characterizes transport of a fluid (gas) through a capillary under the action of the pressure drop (filtration gas or fluid), it is determined by the geometry of channels and by the phase state of the medium being filtered. The Λ_{vq} coefficient describes the motion of a fluid or gas through a capillary-porous body, which is caused by the temperature drop, *i.e.*, thermoosmotic flow. The form of the Λ_{vq} coefficient depends not only on the phase state of the medium (fluid or gas) being transferred, but also on its more subtle molecular-kinetic characteristics. For thermoosmosis, the cross effect is the heat (mechanocaloric) effect characterized by the Λ_{qv} coefficient and manifesting itself in the flow of a fluid (or gas) under the action of the pressure drop. Namely, the flow of a fluid (gas) with no temperature gradient through a capillary-porous body is accompanied by heat transfer. The appearance of a heat flux in the isothermal system is due to the presence of boundary layers where the values of thermodynamic parameters differ from corresponding bulk values.

The Λ_{qq} coefficient characterizes heat transfer through a capillary-porous body and is related to the thermal conductivity of the fluid (gas). Emphasize that it is determined by just the thermal conductivity of the liquid (gas) in thin channels, which can be different from the thermal conductivities of unlimited media.

Formal application of methods of nonequilibrium thermodynamics made it possible to predict two not quite obvious effects, *viz.*, the flow of a liquid (gas) under the action of temperature drop and heat transfer in the presence of a pressure drop provided no temperature drop. The flow under the action of a temperature drop leads to an important consequence. Keeping two vessels connected by a capillary-porous body at different temperatures will cause mass transfer from one vessel to the other. This will lead to an increase in the pressure in the vessel to which mass is transferred. An excess pressure will induce the counter-flux compensating transfer under the action of the temperature gradient. A steady state will be established when mass transfer under the action of the temperature drop will be exactly compensated by mass transfer under the action of the pressure drop induced by the primary flux, *i.e.*, when the average velocity of the fluid flow in the capillary u_v vanishes.

The pressure drop corresponding to the steady state can be found from Eqs (150a) and the condition $u_v = 0$:

$$\Delta p = -\frac{\Lambda_{vq}}{\Lambda_{vv}} \frac{\Delta T}{T}. \tag{151}$$

The appearance of the pressure drop is called the thermomechanical effect, or the thermomolecular pressure drop. For liquids, this effect is not too strong but can be measured experimentally.[94] It is most pronounced for liquid helium,[318] being related to the spouting of superfluid helium in thin capillaries with different end temperatures. The thermomechanical effect is also noticeable for gases where the pressure drop coincides with the pressure in order of magnitude.[21, 22, 102]

Non-trivial character of this effect consists in that, at first glance, it contradicts the Pascal law, *i.e.*, equality of the pressures in the connected vessels. But it should be remembered that the Pascal law is applicable to equilibrium systems where all physicochemical parameters of the gas or fluid in the connected vessels are maintained equal. Thus, generally, the thermomechanical effect does not contradict the fundamental laws provided that they are interpreted correctly.

For thermomolecular pressure drop, the cross effect is the mechanocaloric effect, *i.e.*, heat transfer during isothermal fluid flow through narrow channels. The transferred heat is called the heat of transfer, thus indicating no relation to the conventional thermal conductivity. The mechanocaloric effect (J_q^*) is defined as the ratio of the heat flux to the bulk fluid flow

$$J_q^* = \frac{J_q}{vu_v} = \frac{L_{qv}}{vL_{vv}}, \tag{152}$$

where v is the specific volume.

Using the definition (152), the thermomolecular pressure drop is represented in the form

$$\frac{\Delta p}{\Delta T} = -\frac{J_q^*}{vT}. \tag{153}$$

This expression was for the first time obtained by Derjaguin and Sidorenkov.[319] It shows with certainty that the thermomolecular pressure drop (and, correspondingly, thermoosmosis) is due to processes occurring within the boundary layers. In wide capillaries, where bulk transport processes dominate, the heat of transfer is zero. From the same relation it follows that for systems with thermoosmosis, which plays an important role in membrane processes, should also manifest itself the cross effect related to thermal polarization of the membrane during filtration of fluids.

A system described by Eqns (150) was tested using methods of statistical mechanics and molecular dynamics.[320] The system included two vessels separated by a thin wall with a small orifice. Direct calculations of fluctuations in the system were performed, the fulfillment of some fluctuation theorems was checked and the particle and energy fluxes (heat of transfer) were calculated for various cases. The fulfillment of the Onsager symmetry relations was demonstrated for the conditions when purely thermodynamic parameters are insufficient to completely describe the state of the system.

2. The diffusion osmosis and reverse osmosis

Consider a non-isothermal binary mixture (a solute and a solvent) at a constant potential with no electric charges. Changes in the chemical potentials of components (at constant pressure and temperature) are related by the Gibbs–Duhem equation [3]

$$\sum_i c_i \Delta\mu_i = 0. \tag{154}$$

The entropy production equation (148) for this system can be written as follows:

$$\Delta S = \frac{u_v \Delta p}{T} + \frac{\left(J_q - \sum_i h_i J_i\right)\Delta T}{T^2} + \tag{155}$$

$$+ (u_1 - u_2)\,\frac{\Delta c_1 (\partial \ln a_{c1}/\partial c_1)_{T,p} c_1 nkT}{T},$$

where the chemical potential of the first component is expressed through its activity a_{c1},

$$\mu_1 = kT \ln a_{c1} + \mu_{01}(T, p).$$

The phenomenological equations of nonequilibrium thermodynamics take the form

$$u_v = \Lambda_{mm}\frac{\Delta p}{T} + \Lambda_{mq}\frac{\Delta T}{T^2} + \Lambda_{md}\frac{\Delta c_1}{T}\left(\frac{\partial \ln a_{c1}}{\partial c_1}\right)_{T,p} c_1 , \qquad (156)$$

$$J_q - \sum_\alpha h_\alpha J_\alpha = \Lambda_{qm}\frac{\Delta p}{T} + \Lambda_{qq}\frac{\Delta T}{T^2} + \Lambda_{qd}\frac{\Delta c_1}{T}\left(\frac{\partial \ln a_{c1}}{\partial c_1}\right)_{T,p} c_1,$$

$$(u_1 - u_2)nkT = \Lambda_{dm}\frac{\Delta p}{T} + \Lambda_{dq}\frac{\Delta T}{T^2} + \Lambda_{dd}\frac{\Delta c_1}{T}\left(\frac{\partial \ln a_{c1}}{\partial c_1}\right)_{T,p} c_1.$$

Note that for gases and ideal solutions one has

$$\left(\frac{\partial \ln a_{c1}}{\partial c_1}\right)_{T,p} c_1 = 1.$$

In Eqns (156), the Λ_{mm} coefficient describes the flow of the mixture under the action of the pressure drop. The Λ_{dd} coefficient describes interdiffusion of the mixture components in the presence of component concentration drops (gradients) (recall that for a binary mixture one has $\Delta c_1 = -\Delta c_2$ because $c_1 + c_2 = 1$). The Λ_{md} coefficient characterizes the flow of the mixture under the action of a concentration drop, *i.e.*, the diffusion osmosis. The $\Lambda_{dm} = \Lambda_{md}$ cross coefficient describes the effect of reverse osmosis, *i.e.*, the relative motion of components under the action of the pressure drop. For gas mixtures, this effect is usually called the pressure diffusion.

The reverse osmosis effect is of crucial importance to modern membrane technologies. It is used for separation of mixture components, fluid clarification, desalting of solutions, *etc*. One of the main goals of membrane technologies is to design systems with large Λ_{dm} coefficient.

Consider a system including two vessels with an initially specified concentration drop. As time passes, a quasi-steady state ($u_v = 0$) is established, characterized by a pressure drop between the vessels

$$\Delta p = -\frac{\Lambda_{md}}{\Lambda_{dd}}\Delta c_1 \left(\frac{\partial \ln a_{c1}}{\partial c_1}\right)_{T,p} c_1 = \pi_0. \qquad (157)$$

For gas mixtures, this effect is called the diffusion pressure effect; it can be measured with ease.[21, 22] In the case of liquid media and semi-permeable membranes maintaining the concentration drop for a particular component, this quantity is the osmotic pressure (π_0).

In studying membrane processes one should keep in mind that if during membrane separation the solute concentrations ahead of and behind the membrane are different, the molar flow velocity of the mixture is determined by two terms in the first equation (156). This equation can be re-written in the form

$$u_v = \Lambda_{mm}\frac{\Delta p}{T} + \Lambda_{md}\frac{\Delta c_1}{T} = \qquad (158)$$

$$= \frac{\Lambda_{mm}}{T}\left[\Delta p + \frac{\Lambda_{md}}{\Lambda_{mm}}\Delta c_1 \left(\frac{\partial \ln a_{c1}}{\partial c_1}\right)_{T,p} c_1\right] = \frac{\Lambda_{mm}}{T}(\Delta p - \pi_0).$$

Thus, in the presence of a concentration drop on the membrane, the transport equations should include the pressure drop minus the osmotic component rather than the simply pressure drop.

This conclusion is of fundamental importance and should be taken into account in considering the reverse osmosis, or ultra-filtration separation of components, because the solute can accumulate ahead of the membrane (so-called concentration polarization). As a result, operation of a membrane will be accompanied by changes in the conditions for the solution flow through the membrane (osmotic pressure changes). This effect manifests itself not only in the membrane processes, but also in, *e.g.*, transport of Langmuir – Blodgett films.[321] Nonequilibrium thermodynamics of membrane processes with allowance for the concentration polarization effect has been considered in detail.[322, 323] Note that transmembrane transport can be accompanied by not only the concentration polarization, but also thermal polarization. Sorption/desorption of the transferred component and heat transfer favour the appearance of temperature drops on membranes, which can significantly affect the efficiency of membrane operation.[324]

Capillary osmosis in wide pores is governed by the diffusion slip [see Eqn (46)]. In this case, the velocity of diffusion osmosis coincides with the slip velocity. If the boundary layers overlap, calculations of transport involving osmotic pressure should be carried out with the true component concentrations in thin pores. Here, the role of the real pore structure becomes more important. The diffusion osmosis was calculated for flat capillaries,[90, 325] cylindrical capillaries [326] and for porous media of complex structure.[327, 328] Diffusion osmosis for electrolytes in flat channel of arbitrary width was studied [329] with the emphasis placed on the effect of lateral ion distribution and diffusion-osmotic flow on the strength of tangential electric field created in the channel. Great changes in the velocity of diffusion-osmotic flow in the electrical double layer were revealed.

A theory of reverse-osmotic separation [330] was modified in more recent studies.[331, 332] The selectivity of reverse-osmotic membranes is quite reliably determined from the expression

$$1 - \frac{c_f}{c_0} = 1 - \frac{1}{1 + (\gamma_e/\upsilon - 1)} \times \qquad (159)$$

$$\times \frac{1}{[1 - \exp(-\upsilon u_0 H_m/D_m)]\exp(-\upsilon\delta_c/D_0)},$$

where c_0 and c_f are the concentrations ahead of and behind the membrane; γ_e is the equilibrium distribution coefficient of the solute between the bulk phase and pores; υ is the parameter characterizing the 'delay' of solute relative to the solvent for the flow in pores; u_0 is the filtration velocity; δ_c is the thickness of the layer due to the diffusion polarization; H_m is the membrane thickness; D_0 and D_m are the diffusion coefficients of the solute in the bulk solution and in the membrane pores.

Examples of application of nonequilibrium thermodynamics to various membrane processes are provided by the membrane distillation studies [333, 334] completed by establishment of optimum conditions of the process. It was emphasized that calculations should be performed taking account of the mutual influence of heat and mass transfer; other-

wise, incorrect signs of the heat fluxes can be obtained.[334] Mass transfer is only slightly affected by the cross effect.

The medium transferred through the membrane can change the membrane parameters; this especially concerns polymeric membranes (swelling of polymeric matrix occurs, heat effects are manifested on evaporation and sorption of solvent, *etc.*). There is a detailed study of transport phenomena in polymeric membranes taking into account the effects predicted by classical nonequilibrium thermodynamics for the bulk phase and for interfaces.[335] Also, a large array of experimental data on transport of organic solvents through acetate membranes was reported.[335] Modified equations of nonequilibrium thermodynamics were proposed.[336, 337] They include new variables responsible for changes in the properties of the membrane matrix and take into account temperature-induced deformations of membranes, electrostatic stresses appeared on transport of electrolytes and the influence of deformations not only on the pore size, but also on the pore tortuosity.

Transport of gases through porous bodies was studied in detail.[22, 111, 112, 338] This case, as well as transport of fluids, is often described using the Stefan – Maxwell equations representing the equations of force balance in the system. Usually, the mutual 'friction' of components is introduced

$$\sum_j c_j\zeta_{ij}(u_i - u_j) + u_i\zeta_{i\mathrm{m}} = -\frac{1}{kT}(\nabla_T\mu_i - F_i) - \sum_\beta \frac{c_i}{D_{ij}} D_{ij}^T \nabla \ln T, \tag{160}$$

where ζ_{ij} is the interdiffusion friction coefficient, $\zeta_{i\mathrm{m}}$ is the diffusion friction coefficient of the ith component with the membrane,

$$\zeta_{ij} = \frac{1}{D_{ij}} + \frac{KkT}{\eta D_{\mathrm{m}j}}\zeta_{j\mathrm{m}}, \tag{161}$$

where K is the membrane permeability and D_{ij}^T is the thermal diffusion coefficient. The chemical potential gradient at constant temperature is given by

$$\nabla_T\mu_i = kT\nabla_T \ln a_{c_i} + v_i\nabla p, \tag{162}$$

where a_{c_i} is the activity of the ith component, v_i is the molecular volume of the ith component and F_i is the external force acting on the ith component.

The Stefan – Maxwell equations are in reasonable agreement with the transport equations following from nonequilibrium thermodynamics.[339]

When considering transport through membranes, nonequilibrium processes on the membrane surfaces should be taken into account. As mentioned above (see Section III), jumpwise changes in thermodynamic parameters may occur on the surface. The form of corresponding equations describing such jumps is independent of the surface nature which determines only the kinetic coefficients. The corresponding equations and kinetic coefficients for Silicalite-1 membranes were analyzed [340] using methods of nonequilibrium thermodynamics and molecular dynamics. The emphasis was placed on the mutual influence of heat and mass transfer processes. It was shown that the near-surface region on the gas side strongly resists heat transfer, whereas the near-surface region on the membrane side strongly resists mass transfer. The mutual influence of these processes is to a great extent determined by the fine structure of the surface layer.

The role of surface processes becomes particularly important is sorption/desorption of components is accompanied by high heat effects. This case was analyzed taking transport of hydrogen through palladium membranes as an example.[341] The system is characterized by dissociative sorption of hydrogen and its transport as hydrogen atoms in the palladium. The equations of nonequilibrium thermodynamics, which take into account chemical reactions in the surface layers, include additional fluxes and forces; the expression for the entropy production has the form

$$\Delta S = J_{\mathrm{H}_2}\left(2\frac{\mu_{\mathrm{H}}}{T_{\mathrm{w}}} - \frac{\mu_{\mathrm{H}_2}}{T_{\mathrm{f}}}\right), \tag{163}$$

where J_{H_2} is the molecular hydrogen flux through the membrane, μ_{H_2} is the chemical potential of molecular hydrogen, μ_{H} is the chemical potential of hydrogen atoms in the membrane, T_{w} is the temperature of the membrane surface and T_{f} is the temperature of molecular hydrogen on the feed side.

In this case, violation of the Curie principle is possible because the system under study is anisotropic and the fluxes and forces of different tensor dimensionality can be coupled, as for the surface entropy production.

The results obtained are quite interesting. For instance, heating of the membrane on the permeate side causes the hydrogen flux to increase; as the temperature decreases, transport of hydrogen is suppressed. Also, there exists a transmembrane temperature difference at which transport of hydrogen through the membrane stops.

3. Electro-osmosis and the flow current

Let the liquid medium be an electrolyte in which the chemical potentials of the mixture components and the temperature are maintained constant. Introduce a pressure drop and an electrostatic potential drop. Then, the entropy production is given by

$$\Delta S = \frac{u_v\Delta p}{T} + \frac{I_{\mathrm{e}}\Delta\Psi}{T}, \tag{164}$$

and the system of phenomenological equations takes the form

$$u_v = \Lambda_{vv}\frac{\Delta p}{T} + \Lambda_{vc}\frac{\Delta\Psi}{T}, \tag{165a}$$

$$I_{\mathrm{e}} = \Lambda_{cv}\frac{\Delta p}{T} + \Lambda_{cc}\frac{\Delta\Psi}{T}. \tag{165b}$$

This system describes some effects in addition to those discussed above. The Λ_{vc} coefficient characterizes the flow caused by the electrostatic potential drop, *i.e.*, electro-osmosis. Equation (165b) shows the possibility for a current due to the pressure drop to appear in the system at zero potential drop. Since the pressure drop induces the electrolyte flow in capillary-porous bodies, it is called the flow current. The flow current is related to ion transport in the diffuse region of the electrical double layer by hydrodynamic flow. The flow current is determined by the coefficient

$$\Lambda_{cv} = \Lambda_{vc},$$

which depends on the structure of the porous body or capillary. For sufficiently wide pores, the velocity of electro-osmosis will be equal to the slip velocity [see Eqn (102)]. Various aspects of electrokinetic phenomena for this case have been considered in quite detail in a monograph.[90] Overlap of the electrical double layers complicates the situation. An analysis of the kinetic coefficients was reported in Ref. 342. Note that exact solution can be obtained by numerical methods; analytical approaches give only approximate solutions.

If a system of two connected vessels is characterized by a preset pressure drop and no charge transfer through the capillary-porous body occurs ($I_e = 0$), a potential drop called the flow potential should appear between the vessels in the steady-state case:

$$\Delta\Psi = -\frac{\Lambda_{cv}}{\Lambda_{cc}}\Delta p. \tag{166}$$

The Λ_{cc} coefficient is determined by the conductivity of the fluid in the capillary and by the length of the capillary. Experiments showed that the flow potential can be as high as a few tens of Volts.[94]

Electrokinetic phenomena have been studied in detail; however, transport of electrolytes through thin channels still attracts the attention of researchers, first of all in connection with the development of microfluidics.[343] Since a single review is too short to cover all practical applications of electrokinetic phenomena, here mention may be made only of original attempts to design specific kinds of nanodiodes and transistors.[344–347]

An electrolyte solution contains at least two types of ions. The multicomponent character of the system is taken into account by simply adding the last term from Eqns (148) to the expression for the entropy production (164). This gives obvious transport equations of nonequilibrium thermodynamics.

Transmembrane transport of electrolytes can also be described using the Stefan–Maxwell equations written with allowance for electrostatic forces. These equations combined with principles of nonequilibrium thermodynamics are often used to describe transmembrane transport of electrolytes including an analysis of processes in fuel cells.[348, 349] In particular, methods of nonequilibrium thermodynamics were used to describe the electrochemical cell (lithium ion battery) degradation due to the cross effects.[349] Here, by the cross effect the situation is meant when the ionic and electronic currents flow in the same direction; this is usually ignored. A thorough analysis showed that this effect may cause a local increase in the chemical potential of lithium that exceeds the limiting equilibrium value. As a consequence, lithium precipitation becomes possible and appreciable degradation of the operating characteristics of the Li-ion battery.

4. The Knudsen compressor

Recently, the effect discovered by Knudsen in 1910[350, 351] again has attracted the attention of researchers. Knudsen connected two vessels by two capillaries with different diameters. If the temperature of the contact zone was 500 °C higher than that of the vessels, a pressure drop appeared in the vessels, the pressure in one vessel being almost ten times higher that in the other. The phenomenon observed by Knudsen is analogous to the Peltier effect[318] and can be considered as a kind of asymmetrical flow in the same direction, due to antiparallel temperature gradients (Fig. 18) provided that no temperature drop occurs at the channel ends.

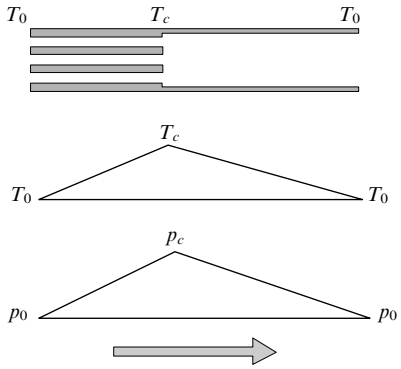


Figure 18. Main element of Knudsen compressor.
The pressure drop at the ends of thin capillaries is higher than at the ends of the wide capillary due to thermoosmosis; this causes unidirectional motion of gas.

The interest in the Knudsen effect was inspired by studies[352–354] on the gas flow in complex-shape capillaries in the absence of pressure and temperature drops at the capillary ends. In particular, a periodic system of narrow and wide channels was considered. The temperature at the junction points was different from the temperature at the channel ends (Fig. 19).[354] According to numerical calculations, the gas moves in one direction. One-way motion of gas in the absence of temperature and pressure drops at channel ends was also demonstrated[355] by heating the junction point of two capillaries with different diameters.

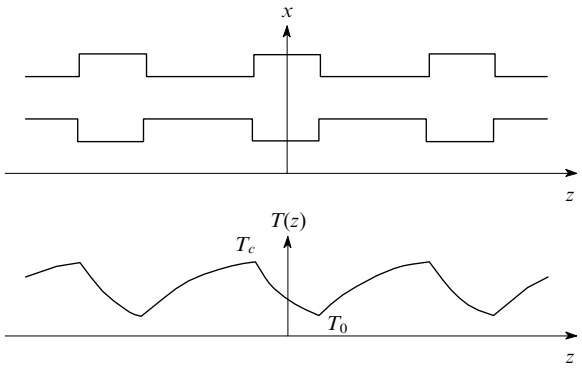


Figure 19. Chain of alternating thin and wide capillaries used in calculations of the performance of a Knudsen compressor.

Consider a channel formed by two consecutively connected capillaries with different diameters and the same length. Assume the possibility of heat transfer through capillary walls (all equations considered above were derived assuming no such kind of heat transfer). The entropy production calculations give[356]

$$\Delta S_s = J_q^s \frac{\Delta_s T}{T^2} + \langle u \rangle \frac{\Delta p}{T}. \tag{167}$$

where J_q^s is the total heat flux through the lateral surface normalized to the capillary cross section;

$$\Delta_s T = T_c - \frac{T_I + T_{II}}{2};$$

T_c is the channel wall temperature at the junction point; T_I and T_{II} are the temperatures in the vessels connected by the channel; and Δp is the pressure drop between the vessels.

The corresponding phenomenological equations have the form

$$J_q^s = \tilde{\lambda}_{qq}\frac{\Delta_s T}{T^2} + \tilde{\lambda}_{qp}\frac{\Delta p}{T}, \qquad (168)$$

$$\langle u\rangle = \tilde{\lambda}_{pq}\frac{\Delta_s T}{T^2} + \tilde{\lambda}_{pp}\frac{\Delta p}{T}.$$

It follows that mass transfer is also possible in the absence of pressure or temperature drops at the channel ends. This can be due to heating or cooling the middle region of the channel. In addition, transport of gas through the channel under isothermal conditions is accompanied by heat transfer through the lateral walls of the capillaries. As a result, the temperature at the junction point can be different from the average temperature of gas. Calculations[356] of the $\tilde{\lambda}_{pq} = \tilde{\lambda}_{qp}$ coefficients for small Knudsen numbers gave

$$\tilde{\lambda}_{pq} = \Delta K_{ts}\frac{\eta_f T}{2L\rho}, \qquad (169)$$

where ΔK_{ts} is the thermal slip coefficient difference between the surfaces of different capillaries, L is the total length of the capillaries. As can be seen, the effect occurs if the thermal slip velocities of gas in the contacting capillaries are different. This difference can be due to either modification of the capillary surfaces or different capillary diameters (the velocity of gas flow in the capillary under the action of temperature gradient depends on the diameter of the capillary).

The effects described by Eqns (168) were studied experimentally.[355,357,358] Different surface characteristics of capillaries were provided by abrasive treatment of their inner surfaces.[357,358] The dependence of the heat effect on the Knudsen number for 26-cm long glassy capillaries of radius 1.59 mm is shown in Fig. 20. The experiments were carried out with helium and xenon for the Knudsen number range from 0.005 to 0.2. The results obtained show that the change in the direction of gas flow influences the sign of the temperature drop in accordance with Eqns (168).

Gas flow in the absence of temperature and pressure drops at channel ends (one-way flow) is the cross effect to the heat effect. It is sometimes called the Hobson accommodation pumping.[359] At present, the system operating on this principle is called the Knudsen compressor. In the experiments, two connected tubes with different diameters were heated at the contact zone and flow through the tubes was observed.[355] The tube radii varied from 5 to 12 mm and the tube length was 60 mm. Experiments were carried out with air for the Knudsen number range from 0.005 to 0.05. It was established that the flow does occur only if the tubes have different diameters and that the flow velocity is inversely proportional to the gas pressure; this agrees with relations (168) and (169).

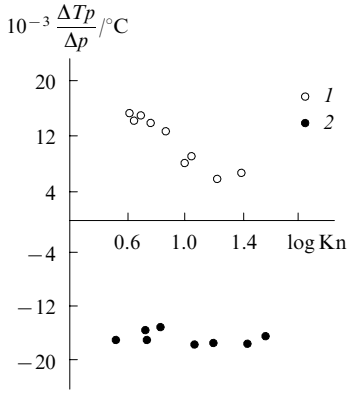


Figure 20. Thermal effect plotted *vs.* Knudsen number for the flow from the left to the right (*1*) and from the right to the left (*2*).[358]

Recently, there has been a new tide of interest in Knudsen compressors due to the design of various nano- and microdevices. A large number of studies on calculations of operating regimes of Knudsen compressors with different geometry were reported.[360–366] As an example, consider the results obtained in a study[367] based on solution of the Boltzmann equations for the system shown in Fig. 19. The pressure distributions along the channel for a temperature drop of 1.5 at channel ends and a narrow-to-wide channel length ratio of 2 are shown in Fig. 21. The channel diameters also differed by two times. As can be seen, the pressure increases along the channel, the effect observed being macroscopic, *i.e.*, the pressures at different channel ends differ by almost an order of magnitude. It is the high effect that is the reason for interest in Knudsen compressors. It should be noted that the dependence on the Knudsen number is not strong, although being noticeable.

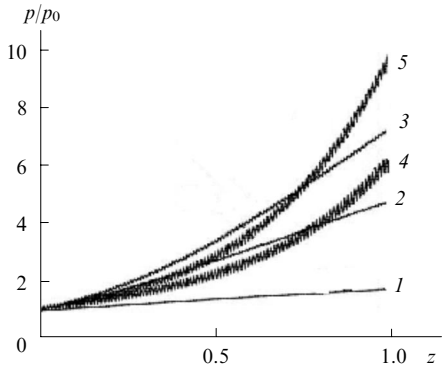


Figure 21. Pressure plotted *vs.* running coordinate z for the system including 100 Knudsen elements for different Knudsen numbers.[367] Kn: 0.1 (*1*), 0.5 (*2*), 1 (*3*), 5 (*4*) and 10 (*5*).

* * *

From the aforesaid it follows that recently, nonequilibrium thermodynamics again has become an actual tool in studies of colloidal systems. As in the early stage of development, it allows one to predict new phenomena and find original

methods to solution of traditional problems in physical chemistry of colloids.

Presently, there is a rising tide of interest in the surface phenomena that underlie the genesis and progress in microfluidics that serves a basis for the design of new mini-devices and for setting original experiments and discovery of unusual effects. The aforesaid clearly demonstrates great prospects for application of nonequilibrium thermodynamics to the description of processes in microfluidics.

The review has been written with the financial support from the Russian Foundation for Basic Research (Project No. 12-03-00589).

References

1. L Onsager *Phys. Rev.* **37** 405 (1931)
2. L Onsager *Phys. Rev.* **38** 2265 (1931)
3. S de Groot, P Mazur *Non-Equilibrium Thermodynamics* (Amsterdam: North-Holland,1962)
4. H B G Casimir *Rev. Mod. Phys.* **17** 343 (1945)
5. I Prigogine *Physica* **15** 271 (1949)
6. S Chapman, T G Cowling *The Mathematical Theory of Non-uniform Gases* (Cambridge: Cambridge University Press, 1939)
7. M N Kogan *Dinamika Razrezhennogo Gaza* (Dynamics of Rarefied Gas) (Moscow: Nauka, 1967)
8. Y Dimerel, S I Sandler *J. Chem. Phys. B* **108** 31 (2004)
9. J R Brock *J. Colloid Sci.* **20** 570 (1965)
10. Yu I Yalamov, I N Ivchenko *Zh. Fiz. Khim.* **43** 2622 (1969) [a]
11. S P Bakanov, V I Roldugin *Kolloid. Zh.* **39** 1027 (1977) [b]
12. S P Bakanov, B V Deryagin, V I Roldugin *Usp. Fiz. Nauk* **129** 255 (1979) [c]
13. S P Bakanov, V I Roldugin *Kolloid. Zh.* **42** 1043 (1980) [b]
14. S P Bakanov, V I Roldughin *J. Colloid Interface Sci.* **72** 428 (1979)
15. S P Bakanov, V I Roldughin *Aerosol Sci. Technol.* **7** 249 (1987)
16. J A MacLennan *Phys. Rev. A* **10** 1272 (1974)
17. S P Bakanov, V I Roldugin *Prikl. Matem. Mekh.* **41** 651 (1977) [d]
18. V I Roldugin *Dokl. Akad. Nauk SSSR* **263** 606 (1982) [e]
19. V I Roldughin *J. Non-Equilib. Thermodyn.* **9** 71 (1984)
20. I Kuscer *Physica A* **133** 397 (1985)
21. V M Zhdanov, V I Roldugin *Usp. Fiz. Nauk* **168** 407 (1998) [c]
22. V I Roldughin, V M Zhdanov *Adv. Colloid Interface Sci.* **98** 121 (2002)
23. F Sharipov, D Kalempa *J. Stat. Phys.* **125** 661 (2006)
24. F Sharipov *Phys. Rev. E* **73** 026110 (2006)
25. P-H Chavanis *Physica A* **332** 89 (2004)
26. U Gegenmüller, U M Titulaer, B U Felderhof *Physica A* **119** 53 (1983)
27. U Gegenmüller, U M Titulaer, B U Felderhof *Physica A* **120** 635 (1983)
28. L F Cugliandolo, J Kurchan, L Peliti *Phys. Rev. E* **55** 3898 (1997)
29. A Perez-Madrid, D Reguera, J M Rubi *Physica A* **329** 357 (2003)
30. V I Roldugin *Zh. Fiz. Khim.* **79** 594 (2005) [a]
31. D Jou, J Casas-Vázquez, G Lebon *Extended Irreversible Thermodynamics* (Second Ed.) (New York: Springer, 1996)
32. S I Serdyukov *Zh. Fiz. Khim.* **71** 1572 (1997) [a]
33. S I Serdukov *Phys. Lett. A* **324** 262 (2004)
34. S I Serdukov *C.R. Physique* **8** 93 (2007)
35. V M Zhdanov, V I Roldugin *Zh. Eksp. Teor. Fiz.* **122** 789(2002) [f]
36. D Jou, J Casas-Vázquez, G Lebon *Extended Irreversible Thermodynamics* (Fourth Ed.) (Berlin: Springer, 2010)
37. G P Beretta *Entropy* **10** 160 (2008)
38. B C Eu *Non-Equilibrium Statistical Mechanics: Ensemble Method* (Dordrecht: Kluwer, 1995)
39. B C Eu *J. Phys. Chem. B* **103** 8583 (1999)
40. J Vollmer *Phys. Rep.* **372** 131 (2002)
41. J P S Bizarro *J. Appl. Phys.* **108** 054907 (2010)
42. P Mazur *Physica A* **261** 451 (1998)
43. P Mazur *Physica A* **274** 491 (1999)
44. J M Rubi, P Mazur *Physica A* **276** 477 (2000)
45. A S Pleshakov *Dokl. Akad. Nauk* **381** 37 (2001) [e]
46. *Non-equilibrium Thermodynamics and the Production of Entropy in Life, Earth and Deyond* (Eds A Kleidon, R Lorenz) (Heidelberg: Springer, 2004)
47. R Dewar *J. Phys.* **38** L371 (2005)
48. L M Martushev, V D Seleznev *Phys. Rep.* **426** 1 (2006)
49. L M Martushev, A S Nazarova, V D Seleznev *J. Phys. A* **40** 371 (2007)
50. A Moroz, D I Wimpenny *Chem. Phys.* **380** 77 (2011)
51. P Attard *Phys. Chem. Chem. Phys.* **8** 3585 (2006)
52. V N Parmon *Catal. Today* **51** 435 (1999)
53. A P Gerasev *Usp. Fiz. Nauk* **174** 1061 (2004) [c]
54. V N Parmon *Thermodynamics of Non-Equilibrium Processes for Chemists with a Particular Application to Catalysis* (Amsterdam: Elsevier, 2010)
55. B R La Cour, W C Dchieve *Physica A* **331** 109 (2004)
56. H Ziegler *Some Extremum Principles in Irreversible Thermodynamics with Application to Continuum Mechanics* (Zurich: Swiss Federal Institute of Technology, 1962)
57. L D Landau, E M Lifshits *Gidrodinamika* (Hydrodynamics) (Moscow: Nauka, 1986)
58. G A Pavlov *Zh. Tekh. Fiz.* **80** 152 (2010) [g]
59. H Brenner *Physica A* **349** 60 (2005)
60. H Brenner *Physica A* **370** 190 (2006)
61. R Datta, S A Vilekar *Chem. Eng. Sci.* **65** 5976 (2010)
62. J M Rubi, D Reguera *Chem. Phys.* **375** 518 (2010)
63. V M Zhdanov *Tainy Razdeleniya Izotopov* (Secrets of Isotope Separation) (Moscow: MIFI, 2011)
64. S N Semenov, M E Shimpf *Usp. Fiz. Nauk* **179** 1105 (2009) [c]
65. G D Rabinovich, R Ya Gurevich, G I Bobrov *Termodiffuzionnoe Razdelenie Zhidkikh Smesei* (Thermodiffusion Separation of Liquid Mixtures) (Minsk: Nauka i Tekhnika, 1971)
66. J C Legos, P Goemaere, J K Platten *Phys. Rev. A* **32** 1903 (1985)
67. M G Bagnoli, A A Shapiro, E H Stenby *Philos. Mag.* **83** 2171 (2003)
68. L J T M Kempes, in *Lecture Notes in Physics* Vol. 584 (Eds W Köller, S Wiegand) (Berlin: Springer, 2002) p. 74
69. A A Shapiro *Physica A* **332** 151 (2004)
70. H Brenner *Phys. Rev. E* **74** 036306 (2006)
71. E Mason, A Malinauskas *Gas Transport in Porous Media: The Dusty Gas Model* (New York: Elsevier, 1983)
72. V M Zhdanov *Adv. Colloid Interface Sci.* **66** 1 (1996)
73. V Ya Rudyak, A A Belkin, S I Krasnolutskii *Thermophys. Aeromech.* **12** 89 (2005)
74. R Mauri *Non-Equilibrium Thermodynamics. Applications to the Rheology of Multiphase Systems* (Pisa: University of Pisa, 2011)
75. D Lhuillier *J. Non-Newtonian Fluid Mech.* **96** 19 (2001)
76. N J Wagner *J. Non-Newtonian Fluid Mech.* **96** 177 (2001)
77. D Bedeaux, J M Rubi *Physica A* **305** 360 (2002)
78. D Vlassopoulos, E Stiakakis, M Kapnistos *Rheol. Rev.* 179 (2007)
79. H Hijar, J G Mendez-Bermudez, I Santamaria-Holek *J. Chem. Phys.* **132** 084502 (2010)
80. P Ramirez-Gonzalez, M Medina-Noyola *Phys. Rev. E* **82** 061503 (2010)
81. A Perez-Madrid, D Reguera, J M Rubi *J. Phys.: Condens. Matter* **14** 1651 (2002)

82. J M Rubi, I Santamaria-Holek, A Perez-Madrid *J. Phys.: Condens. Matter* **16** S2047 (2004)
83. S Zhao, J Wu *J. Chem. Phys.* **134** 054514 (2011)
84. I Santamaria-Holek, A Perez-Madrid *J. Phys. Chem. B* **115** 9439 (2011)
85. B V Derjaguin, N V Churaev, V M Muller *Surface Forces* (New York: Springer, 1987)
86. V I Roldughin *Fizikokhimiya Poverkhnosti* (Physical Chemistry of Surface) (Dolgoprudnyi: ID 'Intellekt', 2008)
87. H Brenner *Phys. Fluids* **21** 053602 (2009)
88. Y Sone *Annu Rev. Fluid Mech.* **32** 779 (2000)
89. E D Shchukin, A V Pertsov, E A Amelina *Kolloidnaya Khimiya* (Colloidal Chemistry) (Moscow: Vysshaya Shkola, 2004)
90. S S Dukhin, B V Derjaguin *Elektroforez* (Electrophoresis) (Moscow: Nauka, 1976)
91. C Neto, D R Evans, E Bonaccurso, H-J Butt, V S J Craig *Rep. Prog. Phys.* **68** 2859 (2005)
92. P Tsai, A M Peters, C Pirat, M Wessling, R G H Lammertink, D Lohse *Phys. Fluids* **21** 112002 (2009)
93. M Chinappi, C M Casciola *Phys. Fluids* **22** 042003 (2010)
94. N V Churaev *Fizikokhimiya Protsessov Massoperenosa v Poristykh Telakh* (Physical Chemistry of Mass Transfer Processes in Porous Bodies) (Moscow: Khimiya, 1990)
95. H C Öttinger *J. Non-Newtonian Fluid Mech.* **152** 66 (2008)
96. A A Ovchinnikov, S F Timashev, A A Belyi *Kinetika Diffuzionno-Kontroliruemykh Khimicheskikh Protsessov* (Kinetics of Diffusion Controlled Chemical Processes) (Moscow: Khimiya, 1986)
97. S F Timashev, Y S Polyakov, P I Misurkin, S G Lakeev *Phys. Rev. E* **81** 041128 (2010)
98. S F Timashev *Fizikokhimiya Membrannykh Protsessov* (Physical Chemistry of Membranous Processes) (Moscow: Khimiya, 1988)
99. B V Derjaguin, S P Bakanov *Dokl. Akad. Nauk SSSR* **141** 384 (1961) [e]
100. B V Derjaguin, S P Bakanov *Dokl. Akad. Nauk SSSR* **144** 535 (1962) [e]
101. B V Derjaguin, Yu I Yalamov *J. Colloid Sci.* **20** 555 (1965)
102. V I Roldughin *Adv. Colloid Interface Sci.* **65** 1 (1996)
103. L Waldmann *Z. Naturforsch., A* **22** 1269 (1967)
104. E M Lifshits, L P Pitaevskii *Fizicheskaya Kinetika* (Physical Kinetics) (Moscow: Nauka, 2007)
105. D Bedeaux *Adv. Chem. Phys.* **64** 1027 (1977)
106. V I Roldughin *J. Non-Equilib. Thermodyn.* **16** 13 (1991)
107. V I Roldughin *J. Non-Equilib. Thermodyn.* **16** 285 (1991)
108. S P Bakanov, V I Roldugin *Prikl. Matem. Mekh.* **60** 761 (1996) [d]
109. V I Roldughin *Kolloid. Zh.* **58** 381 (1996) [b]
110. V M Zhdanov, V I Roldugin *Zh. Eksp. Teor. Fiz.* **109** 1267 (1996) [f]
111. V M Zhdanov, V I Roldughin *Int. J. Nanomech. Sci. Technol.* **1** 49 (2010)
112. V M Zhdanov, V I Roldughin *Int. J. Nanomech. Sci. Technol.* **1** 99 (2010)
113. L M C Sagis *Physica A* **260** 261 (1998)
114. L M C Sagis *J. Phys. Chem. B* **112** 13503 (2008)
115. L M C Sagis *Physica A* **389** 673 (2010)
116. L M C Sagis *Adv. Colloid Interface Sci.* **153** 58 (2010)
117. L M C Sagis, D Bedeaux *Physica A* **230** 437 (1996)
118. K Rah, B C Eu *Physica A* **292** 102 (2001)
119. A D Rey *J. Non-Newtonian Fluid Mech.* **96** 45 (2001)
120. D Jou, G Lebon, M S Mongiovi, R A Peruzza *Physica A* **338** 445 (2004)
121. A F Mills *Int. J. Heat Mass Transfer* **50** 5087 (2007)
122. Y P Pao *Phys. Fluids* **14** 306 (1971)
123. K Aoki, C Cercignani *Phys. Fluids* **26** 1163 (1983)
124. Y Sone, T Ohwada, K Aoki *Phys. Fluids A* **1** 1398 (1985)
125. L J F Hermans, J J M Beenakker *Phys. Fluids* **29** 4231 (1985)
126. D Bedeaux, L J F Hermans, T Ytrehus *Physica A* **169** 263 (1990)
127. D Bedeaux, J A M Smit, L J F Hermans, T Ytrehus *Physica A* **182** 388 (1992)
128. L F Phillips *Chem. Phys. Lett.* **228** 533 (1994)
129. J Xu, S Kjelstrup, D Bedeaux, A Rosjorde, L Rekvig *J. Colloid Interface Sci.* **299** 452 (2006)
130. E Johannessen, J Gross, D Bedeaus *J. Chem. Phys.* **129** 184703 (2008)
131. J Ge, S Kjelstrup, D Bedeaus, J M Simon, B Roussean *Phys. Rev. E* **75** 061604 (2007)
132. J W Cipolla, H Lang, S K Loyalka, *J. Chem. Phys.* **61** 69 (1974)
133. C T Mills, L F Phillips *Chem. Phys. Lett.* **366** 279 (2002)
134. L F Phillips *Chem. Phys. Lett.* **458** 388 (2008)
135. R A James, L F Phillips *Chem. Phys. Lett.* **407** 358 (2005)
136. C J Pursell, L F Phillips *Phys. Chem. Chem. Phys.* **8** 4694 (2006)
137. D M Packwood, L F Phillips *J. Non-Equilib. Thermodyn.* **35** 75 (2010)
138. L F Phillips *Chem. Phys. Lett.* **495** 1 (2010)
139. C Fang, C A Ward *Phys. Rev. E* **59** 417 (1999)
140. C Fang, C A Ward *Phys. Rev. E* **59** 441 (1999)
141. C A Ward, D Stanga *Phys. Rev. E* **64** 051509 (2001)
142. A Aoki, S Takata, S Kosuge *Phys. Fluids A* **10** 1519 (1998)
143. V A Kaminskii, S F Timashev *Zh. Fiz. Khim.* **85** 384 (2011) [a]
144. A Røsjorde, D W Fossmo, D Bedeaux, S Kjelstrup, B Hafskjold *J. Colloid Interface Sci.* **232** 178(2000)
145. M Bond, H Struchtrup *Phys. Rev. E* **70** 061605 (2004)
146. J P Caputa, H Struchtrup *Physica A* **390** 31 (2011)
147. D Bedeaux, S Kjelstrup, J M Rubi *J. Chem. Phys.* **119** 9163 (2003)
148. R B Currie, L F Phillips *J. Non-Equilib. Thermodyn.* **34** 265 (2010)
149. I Inzoli, S Kjelstrup, D Bedeaux, J M Simon *Chem. Eng. Sci.* **66** 4533 (2011)
150. Y D Shikhmurzaev *J. Multiphase Flow* **19** 589 (1993)
151. D Bedeaux *J. Chem. Phys.* **120** 3744 (2004)
152. T O Ogurtani *J. Chem. Phys.* **124** 144706 (2006)
153. L Xu, H Fan, C Yang, W M Huang *J. Colloid Interface Sci.* **323** 126 (2008)
154. K Sefiane, J Skilling, J MacGillivray *Adv. Colloid Interface Sci.* **138** 101 (2008))
155. Y D Shikhmurzaev *Physica D* **217** 121 (2006)
156. V S Nikolayev *Phys. Fluids* **22** 082105 (2010)
157. V I Roldugin *Russ. J. Phys. Chem.* **74** S522 (2000)
158. V A Shneidman, P Hänggi *J. Stat. Phys.* **78** 431 (1995)
159. B V Derjaguin *J. Chem. Phys.* **61** 3665 (1974)
160. V I Roldugin *Teor. Eksp. Khim.* **20** 595 (1984) [h]
161. D Reguera, J M Rubi, A Perez-Madrid *Physica A* **227** 205 (1997)
162. D Reguera, J M Rubi, A Perez-Madrid *Physica A* **259** 10 (1998)
163. E Smith *Rep. Prog. Phys.* **74** 046601 (2011)
164. C Valeriani, R J Allen, M J Morelli, D Frenkel, P R ten Wolde *J. Chem. Phys.* **127** 114109 (2007)
165. M Pagonabarraga, A Perez-Madrid, J M Rubi *Physica A* **237** 205 (1997)
166. J F Lutsko *J. Chem. Phys.* **136** 034509 (2012)
167. H Feng, J Wang *J. Chem. Phys.* **135** 234511 (2011)
168. J M Rubi, A Gadomski *Physica A* **326** 333 (2003)
169. P A Mulheran *Acta Metall. Mater.* **40** 1827 (1992)
170. F D Fischer, J Svoboda *Scr. Mater.* **58** 93 (2008)
171. H Emmerich *Adv. Phys.* **57** 1 (2008)
172. A Gadomski, J M Rubi *Chem. Phys.* **293** 169 (2003)
173. J S Langer *Rev. Mod. Phys.* **52** 1 (1980)
174. L M Martyushev, V D Seleznev, I E Kuznetsova *Zh. Eksp. Teor. Fiz.* **118** 149 (2000) [f]

175. L M Martushev, E M Sal'nikova *J. Phys.: Condens. Matter* **15** 1137 (2003)
176. V I Roldughin *Russ. Chem. Rev.* **72** 823 (2003) [*Usp. Khim.* **72** 931 (2003)]
177. V I Roldughin *Russ. Chem. Rev.* **72** 913 (2003) [*Usp. Khim.* **72** 1027 (2003)]
178. E Brener, H Müller-Krumbhaar, D Temkin, T Abel *Physica A* **249** 73 (1998)
179. M Kohmoto *Phys. Rev. A* **37** 1345 (1988)
180. M A Lopez-Quintela, M C Bujan-Nunez *Mol. Phys.* **77** 857 (1992)
181. A Bershadskii *Physica A* **25**3 23 (1998)
182. R Pastor-Satorras, J Wagensberg *Physica A* **224** 436 (1996)
183. R Pastor-Satorras, J Wagensberg *Physica A* **251** 291 (1998)
184. S R de Groot, P Mazur, J T J Overbeck *J. Chem. Phys.* **20** 1825 (1952)
185. B V Deryagin, S P Bakanov *Dokl. Akad. Nauk SSSR* **147** 139 (1962) [e]
186. V I Roldughin *Kolloid. Zh.* **44** 927 (1982) [b]
187. V I Roldughin *J. Non-Equilib. Thermodyn.* **16** 241 (1991)
188. S P Bakanov, V V Vysotski, B V Derjaguin, V I Roldughin *J. Non-Equilib. Thermodyn.* **8** 75 (1983)
189. V I Roldughin *J. Non-Equilib. Thermodyn.* **19** 349 (1994)
190. S Takata *Phys. Fluids* **21** 112001 (2009)
191. F Sharipov *Phys. Fluids* **22** 049101 (2010)
192. S Takata *Phys. Fluids* **22** 049102 (2010)
193. M Torrilhon *Phys. Fluids* **22** 072001 (2010)
194. V V Vysotskii, V I Roldughin *Physica A* **209** 25 (1994)
195. T Speck, U Seifert *Europhys. Lett.* **74** 391 (2006)
196. G M Wang, E M Sevick, E Mittag, D J Searles, D J Evans *Phys. Rev. Lett.* **89** 050601 (2002)
197. V Blickle, T Speck, L Helden, U Seifert, C Bechinger *Phys. Rev. Lett.* **96** 070603 (2006)
198. E H Trepagnier, C Jarzynski, F Ritort, G E Crooks, C J Bustamante, J Liphardt *Proc. Natl. Acad. Sci. USA* **101** 15038 (2004)
199. V Blickle, T Speck, C Lutz, U Seifert, C Bechinger *Phys. Rev. Lett.* **98** 210601 (2007)
200. L Y Chen *J. Chem. Phys.* **129** 144113 (2008)
201. L D Landau, E M Lifshits *Statisticheskaya Fizika* (Statistical Physics) (Moscow: Nauka, 1974)
202. J Happel, H Brenner *Low Reynolds Number Hydrodynamics* (Leyden: Noordhoff, 1965)
203. A Würger *Rep. Prog. Phys.* **73** 126601 (2010)
204. H Kramers, J Kistemaker *Physica* **10** 713 (1943)
205. S Beresnev, V Chernyak, S Starikov *J. Aerosol Sci.* **30** S761 (1999)
206. F Prodi, G Santachiara, C Cornetti *J. Aerosol Sci.* **33** 181 (2002)
207. X-C Luu, J-P Hsu, S Tseng *J. Chem. Phys.* **134** 064708 (2011)
208. H J Tu, H J Keh *J. Colloid Interface Sci.* **231** 265 (2000)
209. Y K Wei, H J Keh *J. Colloid Interface Sci.* **269** 240 (2004)
210. W Liu, R He, H Zhu, H Hu, M Li, X Zhao *Appl. Phys. Lett.* **96** 053114 (2010)
211. P Y Chen, H J Keh *J. Colloid Interface Sci.* **286** 744 (2005)
212. H J Keh, Y S Hsu *Chem. Eng. Sci.* **61** 3550 (2006)
213. J-P Hsu, W-L Hsu, M-H Ku, Z-S Chen, S Tseng *J. Colloid Interface Sci.* **342** 598 (2010)
214. S Y Bae, C H Jung, Y P Kim *J. Aerosol Sci.* **40** 621 (2009)
215. S Y Bae, C H Jung, Y P Kim *J. Aerosol Sci.* **41** 266 (2010)
216. G A Loosmore, R T Cederwall *Atmos. Environ.* **38** 993 (2004)
217. A Martin-Molinaa, M Quesada-Perez, F Galisteo-Gonzalez, R Hidalgo-Alvarez *Colloids Surf. A* **222** 155 (2003)
218. V M Muller, I P Sergeeva, V D Sobolev, N V Churaev *Kolloid. Zh.* **48** 718 (1986) [b]
219. L Joly, C Ybert, E Trizac, L Bocquet *Phys. Rev. Lett.* **93** 257805 (2004)
220. N V Churaev, J Ralston, I P Sergeeva, V D Sobolev *Adv. Colloid Interface Sci.* **96** 265 (2002)
221. C I Bouzigues, P Tabeling, L Bocquet *Phys. Rev. Lett.* **101** 114503 (2008)
222. J Morthomas A Würger *J. Phys.: Condens. Matter* **21** 035103 (2009)
223. A S Khair, T M Squires *Phys. Fluids* **21** 042001 (2009)
224. O A Kiseleva, V D Sobolev, D A Semenov, A P Ershov, I P Sergeeva, N V Churaev *Kolloid. Zh.*. **71** 72 (2009) [b]
225. Z Adamczyk, K Sadlej, E Wajnryb, M Nattich, M L Ekiel-Jeżewska, J Bławzdziewicz *Adv. Colloid Interface Sci.* **153** 1 (2010)
226. E Yariv, T Miloh *J. Fluid Mech.* **595** 163 (2008)
227. T Miloh *Phys. Fluids* **20** 063303 (2008)
228. T Miloh *Phys. Fluids* **20** 107105 (2008)
229. S C Wang, H P Chen, C Y Lee, C C Yu, H C Chang *Biosens. Bioelectron.* **22** 563 (2006)
230. C K Harnett, J Templeton, K A Dunphy-Guzman, Y M Senousy, M P Kanouff *Lab. Chip* **8** 565 (2008)
231. E Yariv *J. Fluid Mech.* **613** 85 (2008)
232. G Yossifon, I Frankel, T Miloh *J. Fluid Mech.* **620** 241 (2009)
233. M Z Bazant, M S Kilic, B D Storey, A Ajdar *Adv. Colloid Interface Sci.* **152** 48 (2009)
234. E Yariv, A M J Davis *Phys. Fluids* **22** 052006 (2010)
235. H Ohshima *J. Colloid Interface Sci.* **188** 481 (1997)
236. H Ohshima *J. Colloid Interface Sci.* **208** 295 (1998)
237. H Ohshima *Adv. Colloid Interface Sci.* **88** 1 (2000)
238. H Zhao *Phys. Fluids* **22** 072004 (2010)
239. W B Zimmerman *Chem. Eng. Sci.* **66** 1412 (2011)
240. F Schönfeld, G Goet, T Baier, S Hardt *Phys. Fluids* **21** 092002 (2009)
241. Y Jian, L Yang, Q Liu *Phys. Fluids* **22** 042001 (2010)
242. J H Yun, M-S Chun, H W Jung *Phys. Fluids* **22** 052004 (2010)
243. Y C Shu, C C Chang, Y S Chen, C Y Wang *Phys. Fluids* **22** 082001 (2010)
244. P J Stiles, H M Regan *J. Colloid Interface Sci.* **202** 562 (1998)
245. O A Tarasov *Kolloid. Zh.* **67** 259 (2005) [b]
246. V Blickle, C Bechinger *Nature Physics* **8** 143 (2012)
247. A R Vasconcellos, J Fort, D Jou, R Luzzi *Physica A* **300** 386 (2001)
248. A R Vasconcellos, J Fort, D Jou, R Luzzi *Physica A* **300** 503 (2001)
249. J Fort, P Roura *J. Stat. Phys.* 97 941 (1999)
250. V I Roldughin *Kolloid. Zh.* **68** 86 (2006) [b]
251. E Blum, A Mezulis, M Maiorov, G Kronkals *J. Magn. Magn. Mater.* **169** 220 (1997)
252. S Duhr, D Broun *Phys. Rev. Lett.* **97** 038103 (2006)
253. S Duhr, D Braun *Appl. Phys. Lett.* **86** 131921 (2005)
254. H-R Jiang, H Wada, N Yoshinaga, M Sano *Phys. Rev. Lett.* **102** 208301 (2009)
255. D Di Leonardo, F Ianni, G Ruocco *Langmuir* **25** 4247 (2009)
256. T Squiers, S Quake *Rev. Mod. Phys.* **77** 977 (2005)
257. Z Jiao, X Huang, N-T Nguyen, P Abgral *Microfluid. Nanofluid.* **5** 205(2008)
258. J-P Delville, M R de Saint-Vincent, R D Schroll, H Chraibi, B Issenmann, R Wunenburger, D Lasseux, W Zhang, E Brasselet *J. Opt. A: Pure Appl. Opt.* **11** 034015 (2009)
259. K I Morozov *Zh. Eksp. Teor. Fiz.* **115** 1721 (1999) [f]
260. A Würger *Phys. Rev. Lett.* **101** 108302 (2008)
261. F M Weinert, D Braun *Phys. Rev. Lett.* **101** 168301 (2008)
262. S A Putnam, D G Cahill *Langmuir* **21** 5317 (2005)
263. J K G Dhont, S Wiegand, S Duhr, D Braun *Langmuir* **23** 1674 (2007)
264. E Bringuier, A Bourdon *Phys. Rev. E* **67** 011404 (2003)
265. J K G Dhont *J. Chem. Phys.* **120** 1632 (2004)
266. J K G Dhont *J. Chem. Phys.* **120** 1642 (2004)
267. S Duhr, S Arduini, D Braun *Eur. Phys. J. E* **15** 277 (2004)
268. S N Semenov, M E Schimpf *C. R. Mech.* **339** 280 (2011)
269. D Lhuillier *Physica A* **390** 1221 (2011)
270. S Duhr, D Braun *Phys. Rev. Lett.* **96** 168301 (2006)

271. D Vigolo, G Brambilla, R Piazza *Phys. Rev. E* **75** 040401(R) (2007)
272. J M Rubi, P Mazur *Physica A* **250** 253 (1998)
273. R Golestanian *Phys. Rev. Lett.* **108** 038303 (2012)
274. H-R Jiang, N Yoshinaga, M Sano *Phys. Rev. Lett.* **105** 268302 (2010)
275. R Piazza, A Guarino *Phys. Rev. Lett.* **88** 2083021 (2002)
276. S Fayole, T Bickel, S Le Boiteux, A Wurger *Phys. Rev. Lett.* **95** 208301 (2005)
277. H Ning, J K J Dhont, S Wiegand *Langmuir* **24** 2426 (2008)
278. R Rusconi, L Isa, R Piazza *J. Opt. Soc. Am. B* **21** 605 (2004)
279. N Ghofraniha, G Ruocco, C Conti *Langmuir* **25** 12495 (2009)
280. N O Young, J S Goldstein, M J Block *J. Fluid Mech.* **6** 350 (1959)
281. G Wozniak, J Siekmann, J Srulijes *Z. Flugwiss. Weltraumforsch.* **12** 137 (1988)
282. R S Subramanian, in *Transport Processes in Bubbles, Drops and Particles* (Hemisphere, NY: RCR Press, 1992)
283. V I Roldughin *Kolloid. Zh.* **58** 839 (1996) [b]
284. V I Roldughin *Colloids Surf. A* **239** 101 (2004)
285. H-B Nguyen, J-C Chen *Phys. Fluids* **22** 062102 (2010)
286. V I Roldughin *Kolloid. Zh.* **68** 362 (2006) [b]
287. J G Dash, A W Rempel, J S Wettlaufer *Rev. Mod. Phys.* **78** 695 (2006)
288. A W Rempel, J S Wettlaufer, M G Worster *Phys. Rev. Lett.* **87** 088501 (2001)
289. J S Wettlaufer, M G Worster *Ann. Rev. Fluid Mech.* **38** 427 (2006)
290. S S I Peppin, M J Spannuth, J S Wettlaufer *J. Stat. Phys.* **134** 701 (2009)
291. B V Derjaguin, N V Churaev *J. Colloid Interface Sci.* **67** 391 (1979)
292. B V Deryagin, N V Churaev *Kolloid. Zh.* **42** 842 (1980) [b]
293. M J Romkens, R D Miller *J. Colloid Interface Sci.* **42** 103 (1973)
294. S P Bakanov *Aerosol Sci. Technol.* **15** 77 (1991)
295. H J Keh, N Y Ho *J. Colloid Interface Sci.* **216** 167 (1999)
296. X Chen *J. Colloid Interface Sci.* **213** 1488 (1999)
297. A V Filippov *J. Colloid Interface Sci.* **241** 479 (2001)
298. F Zheng *Adv. Colloid Interface Sci.* **97** 255 (2002)
299. Y Sone *Kinetic Theory and Fluid Dynamics* (Boston: Birkhauser, 2002)
300. M Hütter, M Kröger *J. Chem. Phys.* **124** 044511 (2006)
301. A Messerer, R Niessner, U Poschl *Aerosol Sci. Technol.* **38** 456 (2004)
302. H Brenner, J R Bielenberg *Physica A* **355** 252 (2005)
303. H J Keh, Y C Chang *Phys. Fluids* **21** 062001 (2009)
304. S I Grashchenkov *Kolloid. Zh.* **74** 41 (2012) [b]
305. S A Beresnev, V G Chernyak *Teplofiz. Vys. Temp.* **24** 317 (1986) [i]
306. S A Beresnev, V G Chernyak *Teplofiz. Vys. Temp.* **24** 549 (1986) [i]
307. K Yamamoto, Y Isshihara *Phys. Fluids* **31** 3618 (1988)
308. S K Loyalka *J. Aerosol Sci.* **23** 292(1992)
309. S Takata, K Aoki, Y Sone, in *Progress in Astronautics and Aeronautics. Rarefied Gas Dynamics: Theory and Simulations* (Eds B D Shizgal, D P Weaver) (New York: AIAA, 1994) Vol. 159, p. 626
310. A Toda, Y Ohi, R Dobashi, T Hirano, T Sakurava *J. Chem. Phys.* **105** 7083 (1996)
311. W Oostra, J C M Marijnissen, B Scarlett *Spase Forum* **3** 251 (1998)
312. V I Roldughin, V M Zhdanov *Kolloid. Zh.* **66** 376 (2004) [b]
313. S A Beresnev, V G Chernyak, G A Fomyagin *J. Fluid Mech.* **219** 405 (1990)
314. K M Magomedov *Dokl. Akad. Nauk* **361** 768 (1998) [e]
315. W G Gray *Adv. Water Res.* **22** 521 (1999)
316. V I Kondaurov *J. Appl. Math. Mech.* **73** 88 (2009)
317. X H Chen, M A Hicks *Comput. Geotech.* **38** 925 (2011)
318. R S de Groot *Thermodynamics of Irreversible Processes* (Amsterdam: North-Holland, 1951)
319. B V Deryagin, G P Sidorenkov *Dokl. Akad. Nauk SSSR* **32** 622 (1941) [e]
320. B Cleuren, C Van den Broeck *Phys. Rev. E* **74** 021117 (2006)
321. V I Kovalchuk, E K Zholkovskiy, M P Bondarenko, V M Starov, D Vollhardt *Adv. Colloid Interface Sci.* **168** 114 (2011)
322. S S L Peppin, J A W Elliott *Adv. Colloid Interface Sci.* **92** 1 (2001)
323. S S L Peppin, J A W Elliot, M G Worster *Phys. Fluids* **17** 053301 (2005)
324. B Ravindra Babu, N K Rastogi, K S M S Raghavarao *J. Membr. Sci.* **322** 146 (2008)
325. D C Prieve, J L Anderson, J Ebel, M E Lowell *J. Fluid Mech.* **148** 247 (1984)
326. V Sasidhar, E Ruckenstein *J. Colloid Interface Sci.* **85** 332 (1982)
327. H J Keh, J H Wu *Langmuir* **17** 4216 (2001)
328. Y K Wei, H J Keh *Colloids Surf. A* **211** 175 (2003)
329. H C Ma, H J Keh *J. Colloid Interface Sci.* **298** 476 (2006)
330. G A Martynov, V M Starov, N V Churaev *Kolloid. Zh.* **42** 489 (1980) [b]
331. N V Churaev, R G Holdich, P P Prokopovich, V M Starov, S I Vasin *J. Colloid Interface Sci.* **288** 205 (2005)
332. E Nagy, E Kulsar, A Nagy *J. Membr. Sci.* **368** 215 (2011)
333. L N Wang, J C Min *J. Membr. Sci.* **378** 462 (2011)
334. D F Mendoza, S Kjelstrup *Chem. Eng. Sci.* **66** 2713 (2011)
335. G D Verros *J. Membr. Sci.* **328** 31 (2009)
336. A Revil, N Linde *J. Colloid Interface Sci.* **302** 682 (2006)
337. A Revil *J. Colloid Interface Sci.* **307** 254 (2007)
338. V I Roldughin, V M Zhdanov *Adv. Colloid Interface Sci.* **168** 223 (2011)
339. J Kuhna, R Stemmera, F Kapteijn, S Kjelstrup, J Grossa *J. Membr. Sci.* **330** 388 (2009)
340. I Inzoli, S Kjelstrup, D Bedeaux, J M Simon *Micropor. Mesopor. Mater.* **125** 112 (2009)
341. R Skorpa, M Voldsund, M Takla, S K Schnell, D Bedeaux, S Kjelstrup *J. Membr. Sci.* **394 – 395** 131 (2012)
342. A E Yaroshchuk *Adv Colloid Interface Sci.* **183 – 185** 68 (2011)
343. H Chang, L Y Yeo *Electrokinetically-Driven Microfluidics and Nanofluidics* (Cambridge: Cambridge University Press, 2010)
344. H Daiguji, Y Oka, K Shirono *Nano Lett.* **5** 2274 (2005)
345. H Daiguji *Chem. Soc. Rev.* **39** 901 (2010)
346. I Vlassiouk, T R Kozel, Z S Siwy *J. Am. Chem. Soc.* **131** 8211 (2009)
347. S Z Siwy, S Howorka *Chem. Soc. Rev.* **39** 1115 (2010)
348. J J Baschuk, X Li *Int. J. Hydrogen Energy* **35** 5095 (2010)
349. A V Virkar *J. Power Sources* **196** 5970 (2011)
350. M Knudsen *Ann. Phys.* **31** 205 (1910)
351. M Knudsen *Ann. Phys.* **33** 1435 (1910)
352. G Pham-Van-Diep, P Keeley, E P Muntz, D P Weaver, in *Rarefied Gas Dynamics* Vol. 1 (Eds J Harvey, G Lord) (Oxford: Oxford University Press, 1995) p. 144
353. M L Hudson, T J Bartel, in *Rarefied Gas Dynamics* Vol. 1 (Eds R Brun, R Campargue, R Gatignol, J-C Lengrand) (Toulouse: CEPADUES, 1999) p. 719
354. Y Sone, Y Waniguchi, K Aoki *Phys. Fluids* **8** 2227 (1996)
355. Y Sone, K Sato *Phys Fluids* **12** 1864 2000
356. O E Aleksandrov, S P Obraz, B T Porodnov, V D Seleznev *Inzh.-Fiz. Zh.* **55** 566 (1988) [j]
357. O E Alexandrov, S P Obraz, B T Porodnov, V D Seleznev, A G Flyagin, in *Rarefied Gas Dynamics* (Ed. A E Beylich) (Weinheim: VCH, 1991) p. 618
358. O E Aleksandrov, S P Obraz, B T Porodnov, V D Seleznev *Inzh.-Fiz. Zh.* **59** 466 (1990) [j]
359. J P Hobson *J. Vac. Sci. Technol.* **7** 351 (1970)

360. M Young, Y L Han, E P Muntz, S Shiflett, A Ketsdever, A Green, in *The 23rd International Symposium on Rarefied Gas Dynamics, AIP Conference Proceedings 663, Melville, NY, 2003* (Eds A D Ketsdever, E P Muntz) p. 743
361. Y-H Han, E P Muntz, A Alexeenko, V Young *Nanoscale Microscale Thermophys. Eng.* **11** 151 (2007)
362. Y-L Han, E P Muntz *J. Vac. Sci. Technol.* **25** 703 (2007)
363. K Aoki, P Degond, L Mieussens, S Takata, H Yoshida *Multiscale Model. Simul.* **6** 1281 (2008)
364. K Aoki, P Degond, L Mieussens *Comput. Phys. Commun.* **6** 919 (2009)
365. H Sugimoto *J. Vac. Soc. Jpn.* **49** 481 (2006)
366. S Taguchi *Phys. Fluids* **22** 102001 (2010)
367. K Aoki, P Degond, S Takata, H Yoshida *Phys. Fluids* **19** 117103 (2007)

[a] — *Russ. J. Phys. Chem., Ser. A (Engl. Transl.)*
[b] — *Colloid. J. (Engl. Transl.)*
[c] — *Physics-Uspekhi (Engl. Transl.)*
[d] — *J. Appl. Math. Mech. (Engl. Transl.)*
[e] — *Dokl. Phys. Chem. (Engl. Transl.)*
[f] — *J. Exp. Theor. Phys. (Engl. Transl.)*
[g] — *Tech. Phys. (Engl. Transl.)*
[h] — *Theor. Exp. Chem. (Engl. Transl.)*
[i] — *High Temp. (Engl. Transl.)*
[j] — *J. Eng. Phys. Thermophys. (Engl. Transl.)*